

Arbeitsbericht NAB 13-27

Hydrogeological model Jura Südfuss

May 2014

J. Luo, B. Monnikhoff, J. K. Becker

Nationale Genossenschaft
für die Lagerung
radioaktiver Abfälle

Hardstrasse 73
CH-5430 Wettingen
Telefon 056-437 11 11

www.nagra.ch

Arbeitsbericht NAB 13-27

Hydrogeological model Jura Südfuss

May 2014

J. Luo¹, B. Monnikhoff¹, J.K. Becker²

¹DHI-WASY

²NAGRA, Wettingen

KEYWORDS

Local scale hydrogeological model, Jura-Südfuss,
hydraulic heads, path lines, groundwater flow

Nationale Genossenschaft
für die Lagerung
radioaktiver Abfälle

Hardstrasse 73
CH-5430 Wettingen
Telefon 056-437 11 11

www.nagra.ch

Nagra Working Reports concern work in progress that may have had limited review. They are intended to provide rapid dissemination of information.

"Copyright © 2014 by Nagra, Wettingen (Switzerland) / All rights reserved.

All parts of this work are protected by copyright. Any utilisation outwith the remit of the copyright law is unlawful and liable to prosecution. This applies in particular to translations, storage and processing in electronic systems and programs, microfilms, reproductions, etc."

Zusammenfassung

Der vorliegende Bericht dokumentiert Simulationen zu den lokalen Grundwasserzirkulationsverhältnissen im potenziellen Standortgebiet Jura-Südfuss mittels eines dreidimensionalen hydrogeologischen Modells. Das hier beschriebene Modell umfasst eine Grundfläche von ca. 19×16 km um das potenzielle Standortgebiet von der Geländeoberfläche bis zu einer Tiefe von 1400 m. Das Modell umfasst 20 hydrogeologische Einheiten vom Quartär bis zu den Gesteinen der Anhydritgruppe. Störungen von regionaler Bedeutung (insbesondere Teile der Jura Überschiebungen und die Born-Engelberg Antiklinale) sind ebenfalls im Modell abgebildet. Der Schichtverlauf der hydrogeologischen Einheiten und die Geometrie der tektonischen Strukturen sind aus einem regionalen geologischen Modell entnommen, das in Gmünder et al. (2013a) dokumentiert ist. Die für das lokale Modell erforderlichen lateralen Randbedingungen werden aus einem regionalen, die gesamte Nordwestschweiz umfassenden, hydrogeologischen 3-D Modell abgeleitet (siehe Gmünder et al. 2013b).

Die lokalen hydrogeologischen Verhältnisse im Standortgebiet werden massgeblich von der Topographie und den hydraulischen Eigenschaften der regionalen Störungssysteme geprägt. Um deren Einfluss auf die Grundwasserzirkulation systematisch zu analysieren, wurde eine Sensitivitätsstudie mit 4 verschiedenen Basisfällen und umfangreichen Parametervarianten durchgeführt. In den 4 Basisfällen wurden die regionalen Störungen als geringmächtige vertikale Strukturen mit komplementären hydraulischen Eigenschaften ("permeable fault – along flow/cross flow", "sealing fault", "throw only") implementiert, welche die sedimentären Schichtpakete fragmentieren. Zusätzlich wurde im Rahmen von weiteren Parametervarianten die Bedeutung einzelner hydrogeologischer Einheiten als potenziell wasserführende Systeme untersucht.

Zusammenfassend kann festgehalten werden, dass die hydrogeologischen Verhältnisse stark an die Topographie, vor allem entlang der Jura Überschiebungen, gekoppelt sind. Alle im Modell berücksichtigten Einheiten haben entlang dieser Störung Aufschlüsse, die als Infiltrationsorte massgeblich den Grundwasserfluss bestimmen. Zusätzlich haben die hydraulischen Eigenschaften der Störungen, vor allem der Eppenbergs Flexur, einen grossen Einfluss auf das Grundwasserfließsystem. Lassen die hydraulischen Eigenschaften der Störungen einen vertikalen Fluss zu, ist in allen Simulationen die Eppenbergs Flexur, zumindest teilweise, bevorzugtes Exfiltrationsgebiet. Zusätzlich führt die Lage der Infiltrationsgebiete (entlang der Jura Überschiebungen) und die Orientierung der Eppenbergs Flexur und der Born-Engelberg Antiklinale dazu, dass im Falle von undurchlässigen Störungen (C2, teilweise auch C3) der Grundwasserfluss zwischen diesen beiden Strukturen Richtung Osten geleitet wird. Dabei bilden sich meist auf der Nordseite der Eppenbergs Flexure höhere hydraulische Potenziale als auf der Südseite (vor allem im Fall C2), da die Infiltrationsgebiete im Norden von der undurchlässigen Störung abgeschirmt werden.

Ein Vergleich der errechneten Grundwasserpotenziale mit den vorhandenen gemessenen Potenzialen zeigt, dass aufgrund der Simulationen keiner der Basisfälle ausgeschlossen bzw. als weniger wahrscheinlich bewertet werden kann.

Table of Contents

Zusammenfassung.....	I
Table of Contents	III
List of Tables.....	V
List of Figures	VI
1 Introduction	1
1.1 Project Background	1
1.2 Objectives for the local scale model Jura-Südfuss	3
2 Regional and local (hydro)geological setting	5
2.1 Regional setting	5
2.1.1 Regional geological setting	5
2.1.2 Regional hydrogeological setting	8
2.2 Local setting	9
2.2.1 Local scale geology	10
2.2.2 Local hydrogeological setting	11
3 Model Implementation	13
3.1 Overview	13
3.1.1 Regional scale hydrogeological model.....	13
3.1.2 Local scale hydrogeological model	14
3.1.3 Used Software.....	16
3.2 Model geometry.....	17
3.2.1 General aspects.....	17
3.2.2 Horizontal discretization.....	17
3.2.3 Vertical discretization.....	19
3.2.4 Regional faults.....	21
3.2.5 Composite mesh	23
3.3 Property assignment	25
3.3.1 General aspects.....	25
3.3.2 Hydraulic/Hydrogeological units.....	26
3.3.3 Faults	29
3.4 Boundary conditions.....	30
3.4.1 Top/surface boundary	30
3.4.2 Lateral boundaries	32
3.4.3 Bottom	32
4 Modelling results.....	33
4.1 Modelling strategy.....	33
4.1.1 Nested modelling.....	34
4.1.2 Working hypotheses and base cases.....	34

4.1.3	Sensitivity analyses.....	35
4.1.4	Modelling products and analysis	36
4.1.5	Model calibration and consistency checks	37
4.2	Base case C1 ("throw only").....	38
4.2.1	Hydraulic heads	38
4.2.2	Recharge and discharge paths.....	43
4.2.3	Sensitivity Runs.....	47
4.3	Base case C2 ("sealing faults").....	52
4.3.1	Hydraulic heads	52
4.3.2	Recharge and discharge paths.....	57
4.3.3	Sensitivity Runs.....	60
4.4	Base case C3 ("connecting faults").....	64
4.4.1	Hydraulic heads	64
4.4.2	Recharge and discharge paths.....	69
4.4.3	Sensitivity Runs.....	72
4.5	Base case C3a ("fully connecting faults")	76
4.5.1	Hydraulic heads	76
4.5.2	Recharge and discharge paths.....	81
4.5.3	Comparison of results C3a and C3	84
5	Discussion of results	89
6	Conclusions	93
7	References	97
Appendix 1: Vertical gradients		A-1

List of Tables

Tab. 3-1:	Implemented layers of the 3D Model JS.	20
Tab. 3-2:	Hydraulic conductivities according the Regional Model (Gmünder et al 2013b). Note that in case of the Keuper aquifer, the whole local model is located in the same zone.	28
Tab. 3-3:	Hydraulic conductivities of the hydrogeologically refined formations Passwang, Keuper-Lias and Effingen Member	28
Tab. 4-1:	Overview on sensitivity cases performed with the local model JS.....	36
Tab. 6-1:	Hydrogeological characteristics of the Opalinus Clay and the Effingen Member in the siting region Jura-Südfuss. Note that since the orientation of the vertical gradient changes in most simulations within the siting region, the expected minimum and maximum gradients are given instead of reference values. POI means the point of interest.	94
Tab. 6-2:	Hydrogeological characteristics of the regional and local aquifer systems/ potentially transmissive units in the siting region Jura-Südfuss. Note that only the most prominent discharge areas are given in the table. In case that no clear preferred value can be deduced for a certain parameter, only alternative values are given.	96

List of Figures

Fig. 1-1:	Potential siting regions and host rocks for geological disposal of low- and intermediate-level (L/ILW) and high-level (HLW) radioactive waste in Switzerland (Nagra 2008).....	2
Fig. 2-1:	Tectonic sketch map of the wider study area illustrating the main tectonic units of the region and the major fault structures; see Madritsch et al. (2012) for a detailed discussion (modified from Madritsch et al. 2012).....	5
Fig. 2-2:	Geological setting of the area of interest. A) Map of the regionally most important lithostratigraphic units. Note that the Quaternary cover is not shown here. B) Idealized sedimentary sequence of the area in the siting region Jura-Südfuss including possible aquifers and locally transmissive units indicated by blue arrows. Solid blue arrows indicate regionally important aquifers, hollow blue arrows mark possible local aquifers and stippled blue arrows mark potential locally important water conducting units (modified from Nagra 2010).....	8
Fig. 2-3:	Model boundaries, topography and local scale geology of the local model JS. As the boundaries of the local scale model domain in all subsequent figures is clearly visible the scale bar has been omitted in most figures. 2x vertical exaggeration, modified from Isler et al. 1984.....	10
Fig. 2-4:	Overview of hydrogeological tests in the borehole Schafisheim (modified from NTB 88-11, Beilage 8.15).....	11
Fig. 3-1:	3D hydrogeological model including all relevant horizons and layers. Black lines delineate the area of the local scale models, green polygons resemble possible siting regions, white lines are trace lines of regional faults implemented in the model. Only the major rivers and lakes (blue) are shown. 2x vertical exaggeration, Quaternary cover not shown. Black lines delineate the boundaries of the four local-scale hydrogeological models JS, JO, NL and ZNO-SR.	13
Fig. 3-2:	Local model Jura-Südfuss (shown without Quaternary cover). 2x vertical exaggeration. Black bars in cross-sections depict location of the siting region.	15
Fig. 3-3:	Simplification/changes of faults within the model area. Note that due to the dip of the hydrogeological units, fault planes are not always (fully) visible. The fault traces are shown in Fig. 3-2. a) Original shape of regional faults in the 3D geological model. b) Implemented faults in the hydrogeological model. Note that the Trimbach Olten Fault has been connected to the northernmost fault plane of the Born-Engelberg Anticline while the Eppenbergl Flexure and the southernmost fault plane of the Jura Thrusts have also been connected.	16
Fig. 3-4:	Horizontal Discretisation. Top: Black lines represent borders of the super-polygons or trace lines where faults cut the respective regional faults. Bottom: Finite-Element mesh generated from meshing the super-polygons. The length of the triangles varies between 80 and 300 m in general and 8 and 15 m in zones of mesh refinement, e.g. near outcrops or along traces of faults (red lines indicate locations where the faults intersect the geological formations considered).	18

Fig. 3-5:	Illustration of fault implementation in the local scale FEFLOW-Model.....	21
Fig. 3-6:	Intersection between a fault trace and geological horizons (situation/surface mesh): Black lines indicate polygons of the super-mesh (i.e. surface projection of intersection lines), red indicates a reference line with numbered intersection points (to be compared with Fig. 3-7).....	22
Fig. 3-7:	Intersection between a fault and geological horizons (vertical section through reference line in Fig. 3-6).	22
Fig. 3-8:	3D view from the west of the regional faults implemented as inclined and vertical faults. 2x vertical exaggeration.....	23
Fig. 3-9:	3D-View of the JS model from E. Lateral boundaries with geological layering, implemented faults and basic 2D-mesh along bottom of the domain. 2x vertical exaggeration.....	24
Fig. 3-10:	3D-View of the JS model. Lateral boundaries with geological layering, surface mesh with elevations. 2x vertical exaggeration.....	24
Fig. 3-11:	3D-View of the JS model from SE. Lateral boundaries with geological layering, surface mesh with fault traces. 2x vertical exaggeration.	25
Fig. 3-12:	Cross-section through the model domain indicating the layered stratigraphy of the model domain. Where the regular layering is “broken” at fault planes, discontinued layers are “reused” by assigning them to new hydrogeological units. 2x vertical exaggeration.....	26
Fig. 3-13:	Zones of Different Conductivities Implemented in the Local Model Jura-Südfuss (see Gmünder et al. (2013b) for a detailed discussion).....	27
Fig. 3-14:	3D view of the implemented hydrogeological units without covering Quaternary. 2x vertical exaggeration.....	29
Fig. 3-15:	Groundwater heads considered as fixed head boundary conditions at the top of the model domain in the Regional Model (Gmünder et al. 2013b).....	30
Fig. 3-16:	Distribution of the groundwater recharge (precipitation) as considered in the regional model (Gmünder et al. 2013b).....	31
Fig. 3-17:	Groundwater recharge as implemented in the model JS (compare with Fig. 3-16).....	31
Fig. 4-1:	Modelling strategy adopted for the hydrogeological simulations.....	33
Fig. 4-2:	Parameter assignment of the different elements of the faults for the different cases. Faults in the base cases are represented by 3 layers of elements. By assigning different hydraulic properties to the layers, the hydraulic behaviour of the fault can be changed. A) Base case C1: Fault elements are assigned with the same conductivities as the surrounding rocks. This effectively means that the fault does not exist and flow is governed by offset only. B) Base case C2: All fault elements are assigned very low conductivities. C) Base case C3: Fault elements on the outside are permeable, the central row of fault elements are assigned with very low conductivities. D) Base case C3a: All fault elements are assigned with high conductivities.	35
Fig. 4-3:	Location of cross-sections in the model area.....	37
Fig. 4-4:	Base case C1 - Overall 3D View of the simulated groundwater flow system. The Opalinus Clay is indicated by brown colors, 2x vertical exaggeration.	38

Fig. 4-5: Base case C1 – Simulated head fields along aquifers above the Opalinus Clay..... 39

Fig. 4-6: Base case C1 – Simulated head field along aquifers below the Opalinus Clay..... 41

Fig. 4-7: Base case C1 – Simulated head field along vertical sections (location see Fig. 4-3). 2x vertical exaggeration..... 42

Fig. 4-8: Base case C1 – Vertical gradients in the Opalinus Clay..... 43

Fig. 4-9: Location of starting points for the path line computations in the Malm aquifer..... 44

Fig. 4-10: Location of starting points for the path line computations in the Muschelkalk aquifer..... 44

Fig. 4-11: Base case C1 – Calculated path lines starting in the Malm aquifer. (Blue: recharge path; red: discharge paths, green polygon depicts the siting region, strong colors indicate pathlines reaching the top of the model, pale colors indicate pathlines leaving the model along the lateral boundaries). 45

Fig. 4-12: Base case C1 – Calculated path lines starting from the Hauptrogenstein aquifer. (Blue: recharge path; red: discharge paths, green polygon depicts the siting region, strong colors indicate pathlines reaching the top of the model, pale colors indicate pathlines leaving the model along the lateral boundaries)..... 46

Fig. 4-13: Base case C1 – Calculated path lines starting from the Muschelkalk aquifer. (Blue: recharge path; red: discharge paths, green polygon depicts the siting region, strong colors indicate pathlines reaching the top of the model, pale colors indicate pathlines leaving the model along the lateral boundaries) 46

Fig. 4-14: Sensitivity case C1-RD4 – Simulated head differences in RD4 (Sissach Member) compared to base case C1..... 48

Fig. 4-15: Sensitivity case C1-RD4– Simulated head field in RD4 (Sissach Member) compared to base case C1..... 49

Fig. 4-16: Sensitivity case C1-AKA – Simulated head differences in the Arietenkalk compared to the base case C1..... 50

Fig. 4-17: Sensitivity case C1-AKA – Simulated head field in the Arietenkalk compared to the base case C1..... 51

Fig. 4-18: Base case C2 – Simulated head field along aquifers above the Opalinus Clay..... 53

Fig. 4-19: Base case C2 – Simulated head field in aquifers below the Opalinus Clay..... 55

Fig. 4-20: Base case C2 – Simulated head field along vertical sections (location see Fig. 4-3). 2x vertical exaggeration..... 56

Fig. 4-21: Base case C2 – Vertical gradients in the Opalinus Clay..... 57

Fig. 4-22: Base case C2 – Calculated path lines starting in the Malm aquifer. (Blue: recharge path; red: discharge paths, green polygon depicts the siting region, strong colors indicate pathlines reaching the top of the model, pale colors indicate pathlines leaving the model along the lateral boundaries) 58

Fig. 4-23:	Base case C2 – Calculated path lines starting from the Hauptrogenstein aquifer. (Blue: recharge path; red: discharge paths, green polygon depicts the siting region, strong colors indicate pathlines reaching the top of the model, pale colors indicate pathlines leaving the model along the lateral boundaries).....	59
Fig. 4-24:	Base case C2 – Calculated path lines starting from the Muschelkalk aquifer. (Blue: recharge path; red: discharge paths, green polygon depicts the siting region, strong colors indicate pathlines reaching the top of the model, pale colors indicate pathlines leaving the model along the lateral boundaries)	59
Fig. 4-25:	Sensitivity case C2-RD4 – Simulated head field differences in RD4 (Sissach Member) compared to the base case C2.	60
Fig. 4-26:	Sensitivity case C2-RD4 – Simulated head field in RD4 (Sissach Member) compared to the base case C2.	61
Fig. 4-27:	Sensitivity case C2-AKA – Simulated head differences in the Arietenkalk compared to the base case C2.	62
Fig. 4-28:	Sensitivity case C2-AKA – Simulated head field in the Arietenkalk compared to the base case C2.	63
Fig. 4-29:	Base case C3 – Simulated head field along aquifers above the Opalinus Clay.....	65
Fig. 4-30:	Base case C3 – Simulated head field along aquifers below the Opalinus Clay.....	67
Fig. 4-31:	Base case C3 – Simulated head field along vertical sections (location see Fig. 4-3). 2x vertical exaggeration.....	68
Fig. 4-32:	Base case C3 – Evaluation of head differences in the Opalinus Clay.	69
Fig. 4-33:	Base case C3 – Calculated path lines starting from the Malm aquifer. (Blue: recharge path; red: discharge paths, green polygon depicts the siting region, strong colors indicate pathlines reaching the top of the model, pale colors indicate pathlines leaving the model along the lateral boundaries)	70
Fig. 4-34:	Base case C3 – Calculated path lines starting in the Hauptrogenstein aquifer. (Blue: recharge path; red: discharge paths, green polygon depicts the siting region, strong colors indicate pathlines reaching the top of the model, pale colors indicate pathlines leaving the model along the lateral boundaries)	71
Fig. 4-35:	Base case C3 – Calculated path lines starting in the Muschelkalk aquifer. (Blue: recharge path; red: discharge paths, green polygon depicts the siting region, strong colors indicate pathlines reaching the top of the model, pale colors indicate pathlines leaving the model along the lateral boundaries)	71
Fig. 4-36:	Sensitivity case C3-RD4 – Simulated head field differences in RD4 (Sissach Member) compared to base case C3.	72
Fig. 4-37:	Sensitivity case C3-RD4 – Simulated head field in RD4 (Sissach Member) compared to base case C3.....	73
Fig. 4-38:	Sensitivity case C3-AKA – Simulated head field differences in the Arietenkalk compared to base case C3.....	74
Fig. 4-39:	Sensitivity case C3-AKA – Simulated head field in the Arietenkalk compared to base case C3.....	75
Fig. 4-40:	Base case C3a – Simulated head field along aquifers above the Opalinus Clay.....	77

Fig. 4-41:	Base case C3a – Simulated head field along aquifers below the Opalinus Clay.....	79
Fig. 4-42:	Base case C3a – Simulated head field along vertical sections (Location see Fig. 4-1). 2x vertical exaggeration.....	80
Fig. 4-43:	Base case C3a – Vertical gradients in the Opalinus Clay.....	81
Fig. 4-44:	Base case C3a – Calculated path lines starting from the Malm aquifer. (Blue: recharge path; red: discharge paths, green polygon depicts the siting region, strong colors indicate pathlines reaching the top of the model, pale colors indicate pathlines leaving the model along the lateral boundaries)	82
Fig. 4-45:	Base case C3a – Calculated path lines starting from the Hauptrogenstein aquifer. (Blue: recharge path; red: discharge paths, green polygon depicts the siting region, strong colors indicate pathlines reaching the top of the model, pale colors indicate pathlines leaving the model along the lateral boundaries).....	83
Fig. 4-46:	Base case C3a – Calculated path lines starting from the Muschelkalk aquifer. (Blue: recharge path; red: discharge paths, green polygon depicts the siting region, strong colors indicate pathlines reaching the top of the model, pale colors indicate pathlines leaving the model along the lateral boundaries)	83
Fig. 4-47:	Base case C3a – Simulated head field in the Malm aquifer compared to base case C3.....	85
Fig. 4-48:	Base case C3a – Simulated head field in RD2 (Hauptrogenstein) compared to base case C3.	86
Fig. 4-49:	Base case C3a – Simulated head field in the Keuper aquifer compared to base case C3.....	87
Fig. 4-50:	Base case C3a – Simulated head field in the Muschelkalk aquifer compared to base case C3.	88
Fig. 5-1:	Comparison of measured and simulated values for different aquifers and boreholes within the model domain.....	90

1 Introduction

1.1 Project Background

The Sectoral Plan Deep Geological Repositories / SGT (SFOE 2008) is the Swiss road map to establish repositories for radioactive waste. SGT / Stage 1 with focus on the selection of geologically suitable regions (Nagra 2008) led to the proposal of the six geological siting regions for the L/ILW repository (Südranden, Zürich Nordost, Nördlich Lägern, Jura Ost, Jura-Südfuss, Wellenberg) and the three geological siting regions for the HLW repository (Zürich Nordost, Nördlich Lägern, Jura Ost). Four different host rock formations are assessed as part of the L/ILW program (Opalinus Clay, 'Brown Dogger', Effingen Member, Helvetic Marls). The Opalinus Clay is the proposed host rock formation for the SF/HLW/ILW program.

SGT / Stage 2 requires the selection of at least two siting regions for each repository type (L/ILW and HLW). As a quantitative decision basis for the site selection process, provisional safety analyses studies are to be performed for all relevant repository configurations.

Comprehensive geoscientific data bases have to be prepared for the comparison with respect to, the so-called geodata sets for safety assessment. In this context, conceptual and numerical models of the groundwater flow conditions are elaborated on different scales of interest, ranging from the regional scale to the immediate vicinity of the proposed repository. The proposed numerical analyses of groundwater flow are divided into two work packages:

- WP 1 / Regional scale modelling, aimed at evaluating the regional groundwater flow and therewith possible recharge and discharge areas of the regional aquifer systems and at specifying the hydraulic boundary conditions for the local scale models;
- WP 2 / Local scale modelling, aimed at evaluating the local groundwater flow conditions in the different siting regions, including the identification of possible local recharge and discharge areas and path lengths.

For the local scale models, four hydrogeological local models, based on a three dimensional geological model, were built. Fig. 1-1 shows the location of the geological sites Jura-Südfuss (local model JS), Jura Ost (local model JO), Nördlich Lägern (local model NL), Zürich Nordost combined with Südranden (local model ZNO-SR) and the Wellenberg. For the site Wellenberg, a local scale hydrogeological model has previously been established (see e.g. Nagra 1997).

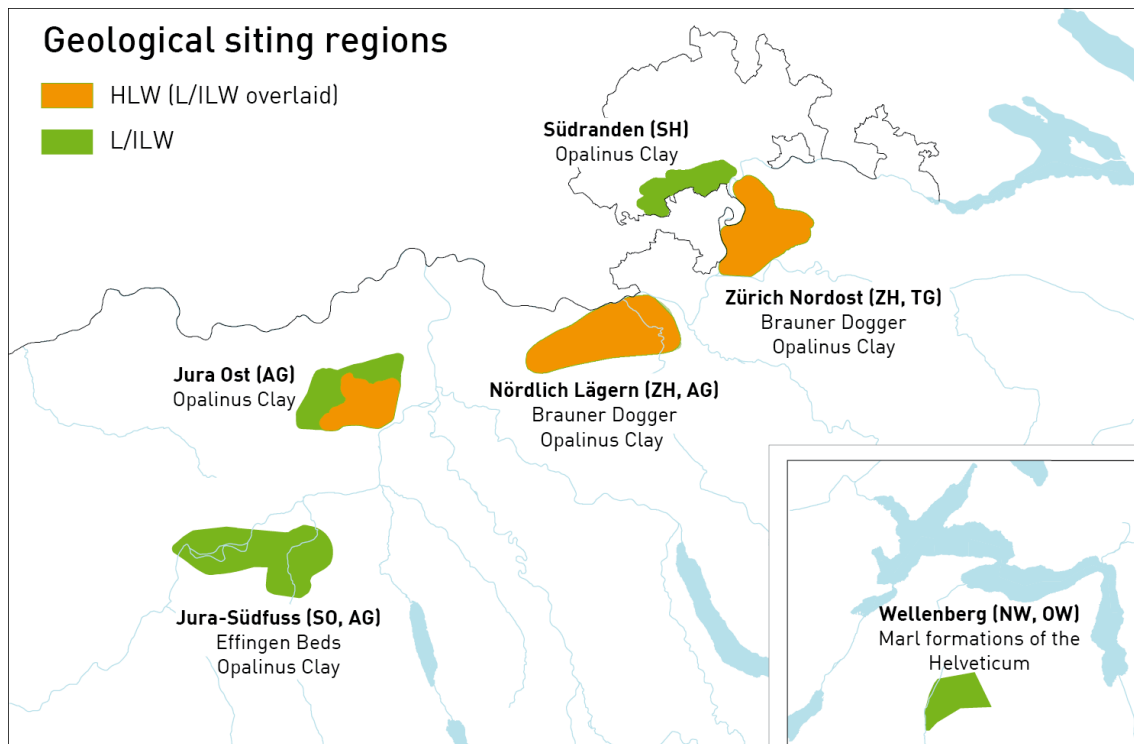


Fig. 1-1: Potential siting regions and host rocks for geological disposal of low- and intermediate-level (L/ILW) and high-level (HLW) radioactive waste in Switzerland (Nagra 2008).

The general objectives of the hydrogeological local scale models (WP 2) are aimed at characterizing the local groundwater flow conditions in the different siting regions:

- **Evaluation of host rock performance as a flow barrier** (incl. adjacent confining units): Assessment of conceptual and parametric uncertainties with respect to the role of water conducting features and the confining units (
- **Evaluation of local / regional aquifer systems**: Assessment of hydraulic interactions between regional and local aquifer systems and identification of potential discharge paths. Estimation of effective hydraulic properties
- Visualizations of the hydrogeological conditions in support of communication of systems understanding
- Supply of input for site specific hydraulic gradients and fluxes in the host rock

The general objectives marked in bold are subdivided into site specific issues addressing the key questions to be solved for the individual siting regions (see next chapter).

1.2 Objectives for the local scale model Jura-Südfuss

For the hydrogeological local scale model Jura-Südfuss (JS) described in this report a set of objectives has been defined prior to modelling. The main interest lies in the main regional aquifers and to some extent also in the local aquifers and their flow field and transport paths, including possible recharge and discharge areas and in the lower and upper confining units of the host rock formations and their role as flow barriers. For the aforementioned characterizations, the regional Jura Thrusts, the Born-Engelberg Anticline and its related faults and to some extent the Eppenbergr Flexure and Trimbach Olten Fault may play an important role (see Fig. 2-2). Depending on the properties of the faults (e.g. as impermeable barriers or as regions with low or medium transmissivities), they can have large effects on the overall flow field.

The site specific objectives can therefore be divided into related groups:

- The impact of regional faults on the local hydrogeological situation needs to be characterized. The regional fault zones have been implemented in the local scale model domain cross cutting and offsetting the proposed host rocks and confining units. Depending on the hydrogeologic properties of the faults, they influence local gradients as well as flow paths and therewith discharge and recharge areas/locations.
- The hydraulic interaction between locally important, transmissive units and the regional aquifer systems and potential discharge and recharge areas needs to be characterized and identified. In addition, vertical gradients within the host rocks itself and/or horizontal gradients within the regional and local groundwater systems are important for a full characterization and safety assessment of the siting region. Since the aforementioned interaction may depend to a large degree on the hydraulics of the fault zones, they cannot be assessed independently.

Since the role of the local, potentially transmissive units for the local hydrogeology and/or the conductivities of the regional scale faults in the model domain are largely unknown, sensitivity analyses with respect to the transmissivity of the local units and the fault systems have been performed.

2 Regional and local (hydro)geological setting

2.1 Regional setting

2.1.1 Regional geological setting

The area of investigation (here the area of the siting region Jura-Südfuss, see Fig. 2-2A) is located within the northern Alpine foreland of Northern Switzerland. The tectonic setting is of interest for hydrogeological simulations because faults that have developed during the different tectonic stages may influence the regional and local hydrogeological setting, depending on their conductivity. In the following, the main fault systems of the different tectonic units (see Fig. 2-1) are shortly described. An extensive review of the tectonic setting is given in e.g. Madritsch et al. (2012) and will not be repeated here.

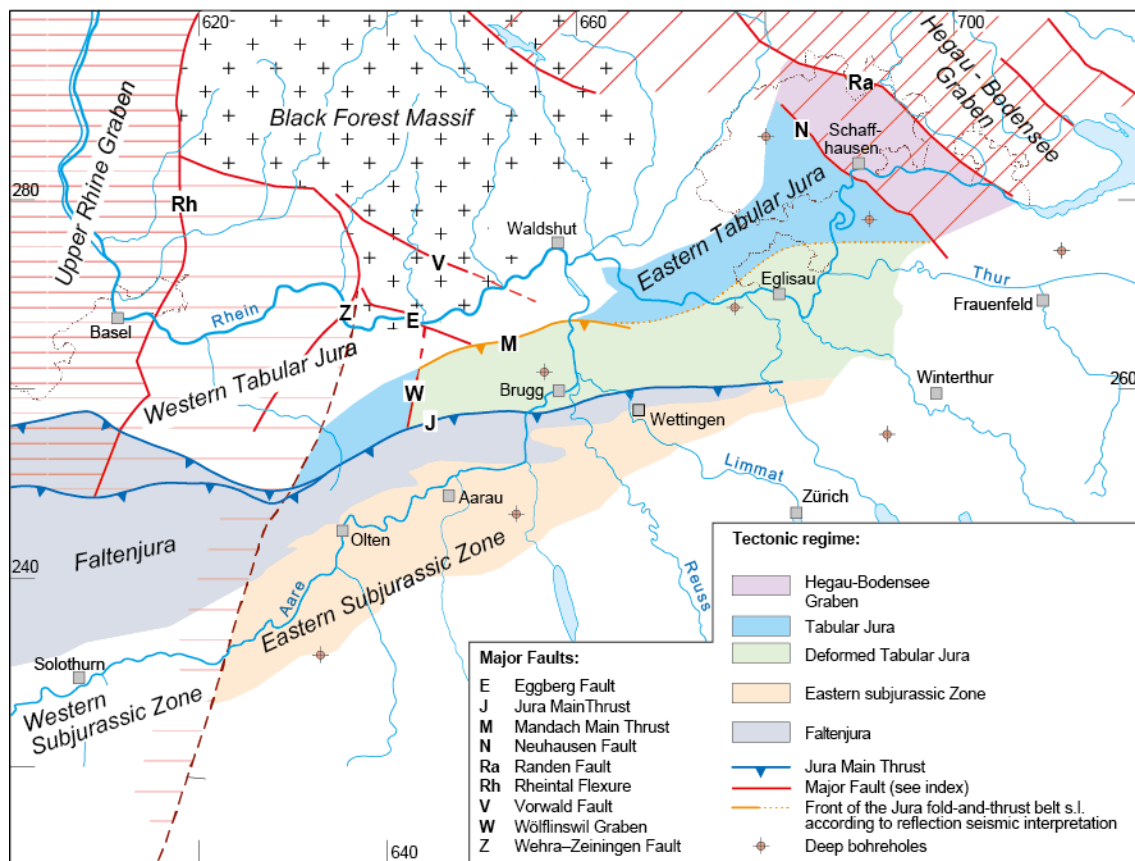


Fig. 2-1: Tectonic sketch map of the wider study area illustrating the main tectonic units of the region and the major fault structures; see Madritsch et al. (2012) for a detailed discussion (modified from Madritsch et al. 2012).

The Folded Jura, also called Jura Fold-and-Thrust Belt, is characterized by dominantly ENE-WSW striking folds and thrusts that are occasionally cut by N-S striking faults. The frequency of these structures increases towards the Upper Rhine Graben. Moreover, NW-SE striking faults, such as the Trimbach Olten Fault (see Fig. 2-2), occur. The roughly E-W striking Jura Thrusts form the transition to the Deformed Tabular Jura in the north.

The Deformed Tabular Jura is less intensely deformed than the Folded Jura. The lower Aare Valley separates this tectonic unit into a western and eastern part. The western is separated from the northward adjacent Tabular Jura by the ENE-WSW striking Mandach Thrust. The eastern part of the Deformed Tabular Jura is characterized by blind thrusts, the transition towards the Tabular Jura is ill-defined.

The Tabular Jura is characterized by horizontally layered to slightly SSE dipping Mesozoic sediments that run out at the south-eastern edge of the Black Forest Massif. Compared to the Deformed Tabular Jura, the Tabular Jura is less deformed and does not feature regional-scale compressive structures with the exception of the Mettau Fault (cf. Laubscher 1986). To the east and west, the Tabular Jura is influenced by the Hegau-Bodensee-Graben and the Upper Rhine Graben, respectively.

As this report is mostly concerned with the hydrogeological situation within the siting area Jura-Südfuss, only a very broad description of the regionally important lithostratigraphic units in the regional area of interest (see Fig. 2-2A) is given below. A lithostratigraphic geological profile of the siting region JS is given in Fig. 2-2B. The regional and local stratigraphy has recently been revised (see e.g. Bläsi et al. 2013; Deplazes et al. 2013; Bitterli-Dreher 2012 or Reisdorf et al. 2011 for a recent stratigraphy). In this report, the stratigraphy according to the regional geological model of Gmünder et al. (2013a) is used which is mainly based on the stratigraphy as defined in Nagra (2010).

- **Molasse:** The Molasse usually is divided into the Upper Freshwater Molasse (OSM), the Upper Marine Molasse (OMM), the Lower Freshwater Molasse (USM) and the Lower Marine Molasse (UMM). The OSM is a succession of fine sandstones and silt to clay rich rocks as well as marl and freshwater carbonates intercalated with coarse sandstones and conglomerates - the so called Jura Nagelfluh. A significant part of the OMM is comprised of homogeneous, marine sandstones which locally can be regarded as aquifers. The USM is a heterogeneous succession of mainly fluvial clays, marls, siltstones and fine sandstones that frequently show channels of coarser sandstones. The UMM is absent in northern Switzerland.
- **Malm:** The final phase of Jurassic sedimentation in the region is marked by an increased occurrence of calcareous rocks. The lithostratigraphic group of "Malm" in general is divided into Felsenkalke / Massenkalk, Schwarzbach Formation, Villigen Formation and Wildeggen Formation. The upper units are comprised of layered, homogenous limestones (Felsenkalke) and more massive limestones (Massenkalk). The Schwarzbach Formation consists of partly fossil-rich, calcareous-rich marls. The Villigen Member consists of mainly limestones with intercalations of clay- and calcareous-rich marls. The Wildeggen Formation includes the Effingen Member and the Birmenstorf Member. The Effingen Member is characterized by layered successions of calcareous-rich marls and mostly clay-rich limestones (Deplazes et al. 2013). The often fossil-rich Birmenstorf Member is comprised of limestones and calcareous-rich marls.
- **Dogger:** The Dogger sediments in the area of interest are comprised of a thick succession of clay-rich rocks with local intercalations of siltstones, marls, sandstones, iron oolites and limestones. At the base of the Dogger, the Opalinus Clay is a regionally homogeneous clay. Above the Opalinus Clay, the Passwang Formation comprises of a number of unconformity-bounded coarsening-upwards successions. The coarsening-upward successions start typically with siliciclastic mudstones grading into micritic limestones. In the west the Passwang Formation incorporates thicker limestone-successions than in the east. On a regional scale shown in Fig. 2-2 two different types of facies were deposited above the Passwang Formation: the Hauptrogenstein Formation and the Klingnau Formation. In the western part, a broad oolitic belt, the Hauptrogenstein Formation, was deposited on a

carbonate platform. In the eastern part, the Hauptrogenstein Formation is replaced by a marl to clay-dominant facies, the so called Klingnau Formation that was deposited in a more distal setting. The Klingnau-Formation is overlain by claystones and iron oolites, which are called Upper Dogger.

- Lias: The Staffelegg Formation (the stratigraphic unit comprising all Lias sediments) is characterized by heterogenous clay-rich rocks with some limestones and subordinately sandstones. A detailed description of the Staffelegg Formation of northern Switzerland can be found in Reisdorf (2011). A notable calcareous rich layer is formed by the Arietenkalk (Beggingen Member).
- Keuper: The sediments of the Keuper, the upper lithostratigraphic group of the Trias, can be separated into the Upper Middlekeuper and Gipskeuper. The Upper Middlekeuper consist in general of marls and clays with intercalations of sandstones and dolomites (Traber 2013). Sandstone layers occur mostly in the otherwise clay-rich sediments of the Stubensandstein and Schilfsandstein Formations. These fluvial sediments show a locally varying composition depending on the depositional setting (flood plain, river channel, delta). Another notable unit is the Gansinger Dolomit, which often consists of marly dolomite. The Gipskeuper mainly consists of clays, dolomitic marls and anhydrite.
- Muschelkalk: The Muschelkalk is the middle of three lithostratigraphic groups within the Trias. In the area of interest, the Muschelkalk is divided into the upper Muschelkalk (top), the Anhydritgruppe (middle) and the Wellengebirge (lowermost unit of the Muschelkalk, not specifically part of the model domain). The upper Muschelkalk is mainly comprised of dolomites (Trigonodus Dolomite) and limestones/micrites, sometimes separated by thin layers of marl. The limestones are often micrites with partly biotrital banks. The Anhydritgruppe is a layered succession of evaporites (mainly anhydrite) or anhydrite breccia with thin clay and/or dolomite layers. Within the area of interest, thin salt layers are common. Generally, the Muschelkalk shows a remarkable uniformity with only very little variability, though thicknesses of the different lithostratigraphic units may vary on a regional scale.

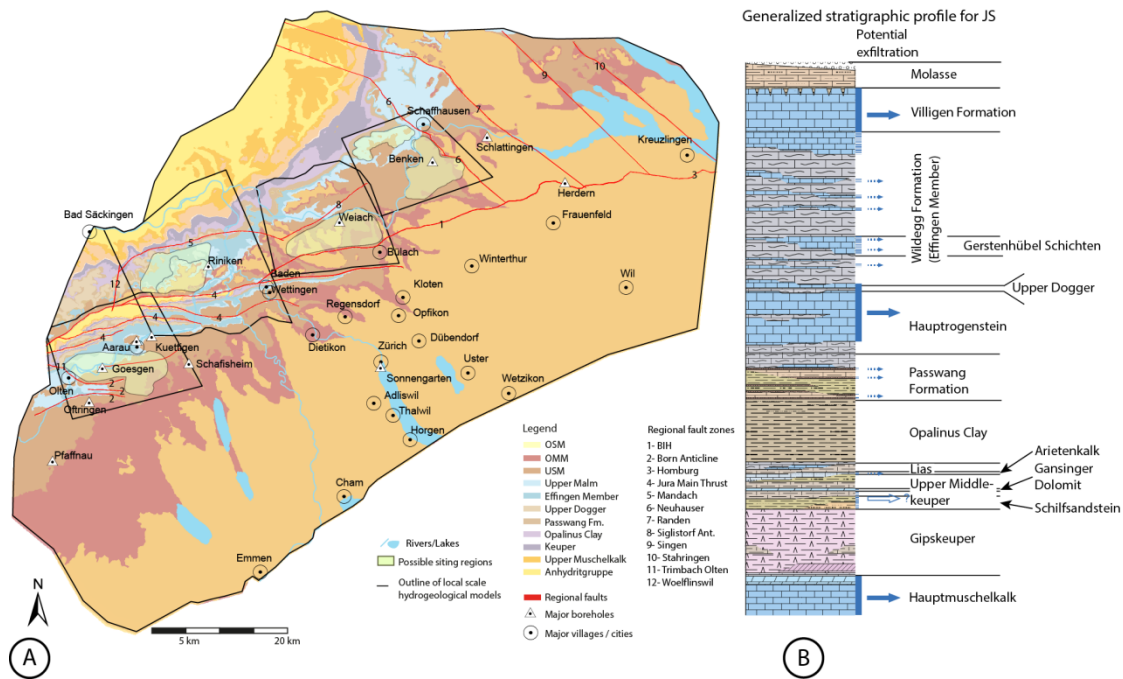


Fig. 2-2: Geological setting of the area of interest. A) Map of the regionally most important lithostratigraphic units. Note that the Quaternary cover is not shown here. B) Idealized sedimentary sequence of the area in the siting region Jura-Südfuss including possible aquifers and locally transmissive units indicated by blue arrows. Solid blue arrows indicate regionally important aquifers, hollow blue arrows mark possible local aquifers and stippled blue arrows mark potential locally important water conducting units (modified from Nagra 2010).

2.1.2 Regional hydrogeological setting

The regional hydrogeological situation is further described in several reports (e.g. Nagra 2002, Nusch et al. 2013) and is currently investigated using a regional hydrogeological model (Gmünder et al. 2013b) based on the sedimentary stack shortly described above and shown in Fig. 2-2B. The hydrology of the area is characterized by the Lake Constance and the rivers Rhine, Aare, Reuss, Limmat, Thur, Töss and Wutach and their respective tributaries. These rivers and the lake constitute the main discharge systems for the aquifers in the area. The area of interest includes parts of the Molasse basin and the most important discharge and recharge locations for the main regional aquifers. These aquifers belong to three main stratigraphic groups, namely the Quaternary deposits, the Tertiary to Permo-Carboniferous bedrock sediments, and the crystalline basement.

- The Quaternary mostly consists of unconsolidated sediments, is present over much of northern Switzerland and contains groundwater. Several activities, including pumping for water supplies, have modified the original groundwater flow systems. The Quaternary aquifer has been included in the model as groundwater discharging from lower aquifers may discharge into this aquifer.

- The bedrock Tertiary to Permo-Carboniferous sediments contain several important aquifers. The main aquifer groups are:
 - Tertiary-Malm group with important aquifers in the sandstones of the Upper Marine Molasse and in the limestones of the Malm
 - Upper Muschelkalk (limestones and dolomites)
 - Lower Triassic-Permian group with aquifers consisting of clastic sediments

These main aquifer groups are generally separated by hydraulic barriers consisting of clays, marls, anhydrites or rock salt. Aquifers within these regional hydraulic barriers include the Hauptrogenstein Formation limestone in the western facies of the Middle Dogger and some limestones, dolomites and sandstones of the Lias and the upper part of the Keuper.

- The first few hundred meters of the crystalline basement may exhibit a high hydraulic conductivity similar to that of some of the sedimentary aquifers. The groundwater of the crystalline basement presumably circulates along tectonic fracture zones and/or a "weathered" zone at the top. In parts of northern Switzerland, they are connected with the Lower Triassic-Permian aquifer group. In other parts of the region, they are separated from the overlying sedimentary aquifers by a hydraulic barrier of sediments of the Permo-Carboniferous Trough. This group is not included in the present hydrogeological models and will not be discussed here in further detail.

The dominantly horizontal or only slightly dipping bedding of the sediments and the frequent occurrence of hydraulic barriers in the form of clay-rich rocks generally prohibits upflow or downflow of groundwater through the hydrogeological units. Therefore, the deep groundwater of the different aquifer groups exhibit individual characters. However, tectonic faults may represent hydraulic connections between individual aquifers. To estimate the current hydrological situation in the area, hydraulic head and conductivity data for various formations have been gathered in various boreholes throughout the region. These are reported in further detail in Nusch et al. (2013).

2.2 Local setting

The local scale model Jura-Südfuss (JS) described here and in subsequent chapters covers an area of 292 km² and mainly lies within the area of the Eastern Subjurassic Zone (in the south) and Folded Jura (in the north). The Aare crosses the model area from east to west (see Fig. 2-3). Several seismic lines, outcrops and deep boreholes within the model domain document its local geological and hydrogeological situation (see Fig. 2-2 and 2-3). The boundaries of the local scale model JS were chosen so that the model domain includes all relevant outcrops and geologic structures as well as the major boreholes relevant for the siting region.

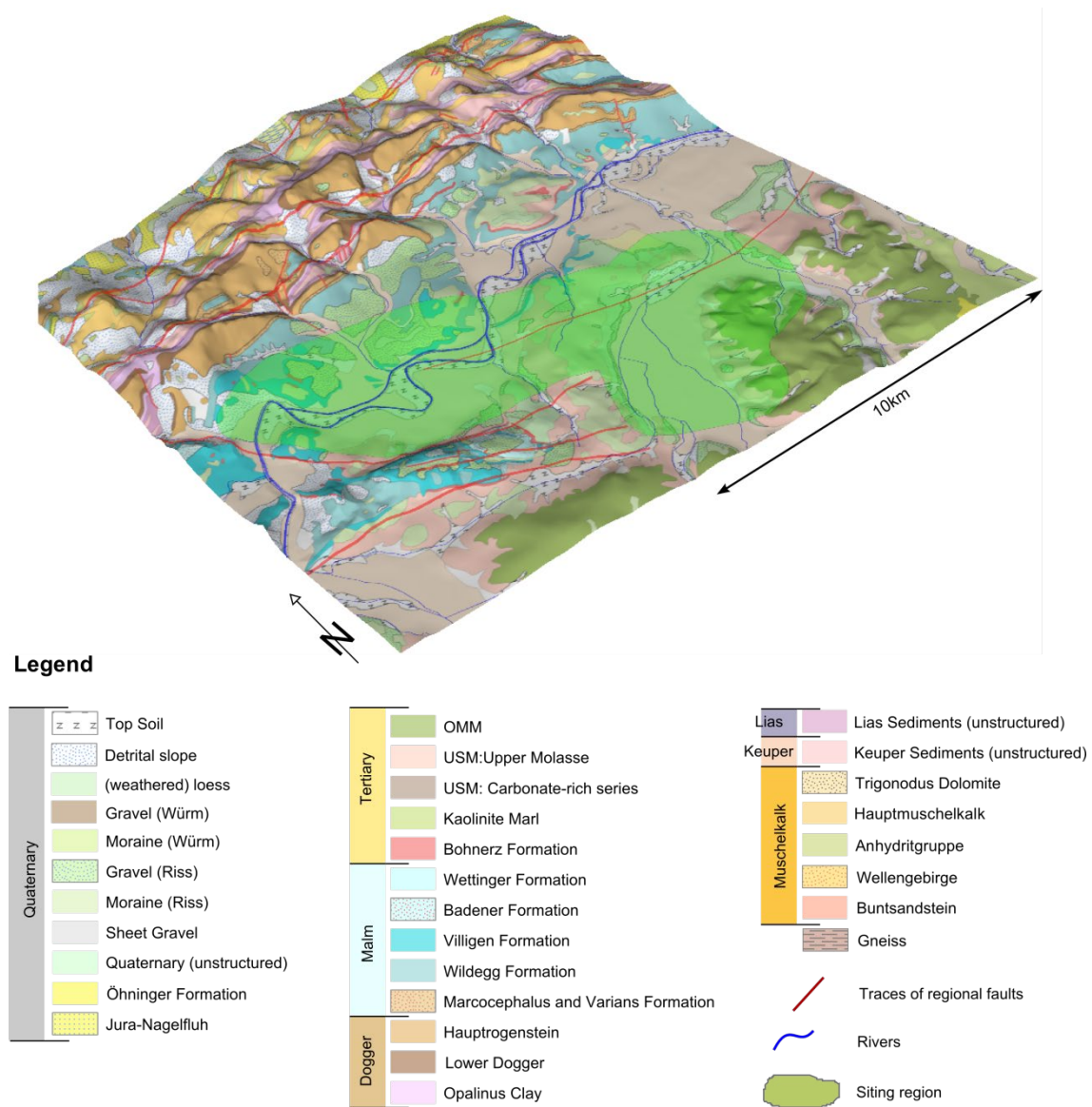


Fig. 2-3: Model boundaries, topography and local scale geology of the local model JS. As the boundaries of the local scale model domain in all subsequent figures is clearly visible the scale bar has been omitted in most figures. 2x vertical exaggeration, modified from Isler et al. 1984.

2.2.1 Local scale geology

The topography of the area is controlled by the south-dipping sedimentary units, the regional faults (the Jura Thrusts in the north, the Born-Engelberg Anticline in the south and the Eppenbergs Flexure in between these two) and the Aare and its tributaries (see Fig. 2-3). The regionally important fault systems run roughly E-W through the model domain (see Fig. 3-2). Disregarding the Quaternary cover, topographic heights in the north of the model domain (along the Jura Thrusts) show outcrops of all hydrogeological units considered in the model. The central and southern part of the model domain is covered with Molasse sediments (OMM and USM) while along the Born-Engelberg Anticline and in the south, towards the Jura Thrusts, outcrops of Malm sediments are frequent. Within the model area, smaller rivers (and valleys

incised by them) are oriented roughly NW-SE with the exception of the Aare. The Aare, as the locally most important discharge system, runs roughly E-W.

2.2.2 Local hydrogeological setting

The hydrogeological units considered in this model crop out along the Jura Thrusts (close to the NW boundary of the model domain), including the Anhydritgruppe. Therefore, the northern part of the model domain is hydraulically decoupled from the rest of the model. Potential discharge and recharge locations of interest are located between the southernmost part of the Folded Jura and the Aare valley. Depending on the hydrogeological properties of the fault systems, the Born-Engelberg Anticline also hydraulically decouples the southern from the central part of the model domain. However, the fault systems must be viewed in a regional context so that, even if they are impermeable, groundwater may still flow from north to south outside of the model domain. Locally however, the fault zones effectively prohibit groundwater flow between the blocks as they may decouple recharge/discharge zones of the aquifers in the northwest from the rest of the area, only allowing an NE-SW (or vice versa) directed flow.

Measurements of hydraulic heads and/or transmissivities in the model domain have been performed in several boreholes (Gösgen, exploration boreholes for the Wisenbergtunnel, Lostorf, Oftringen and Schafisheim). Fig. 2-4 shows the example of measurements performed in the borehole Schafisheim. However, most of the tests in this borehole have been performed aiming at the crystalline basement rocks and therefore are of limited use for the modelling described in this report.

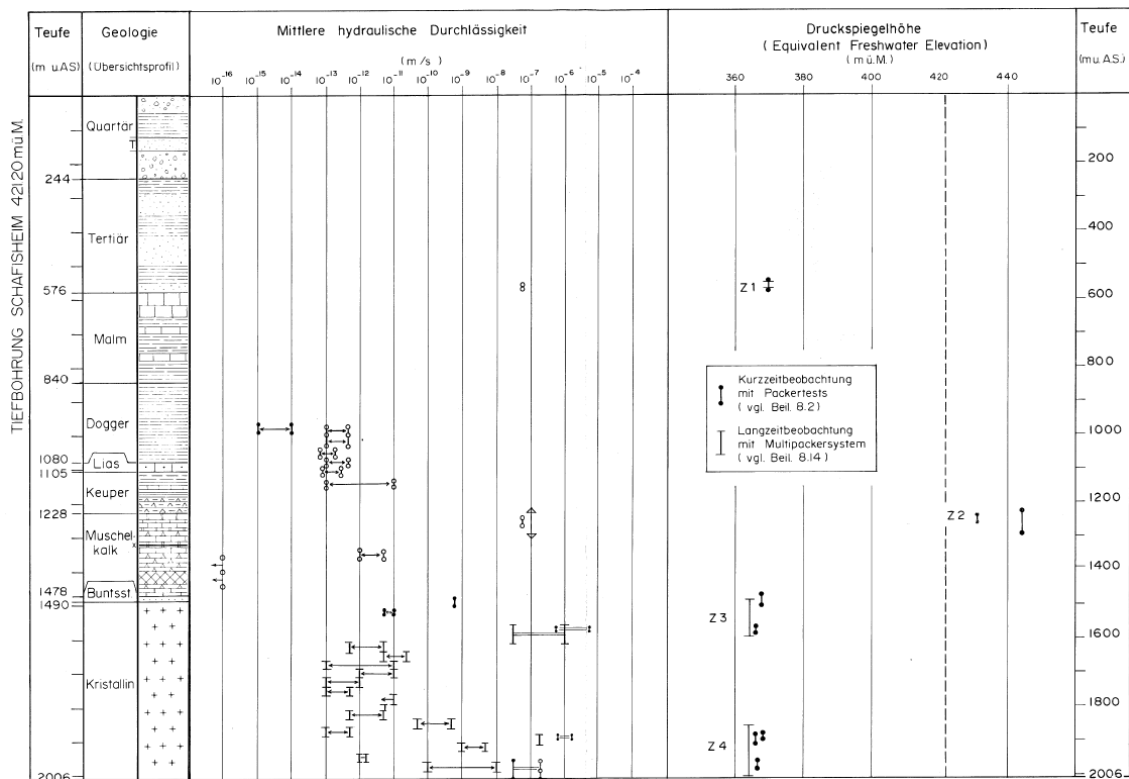


Fig. 2-4: Overview of hydrogeological tests in the borehole Schafisheim (modified from NTB 88-11, Beilage 8.15).

Since the crystalline basement rocks are not part of the hydrogeological model (as they are separated by the Anhydritegruppe from aquifers above), only boreholes using water from aquifers down to the Muschelkalk (including all aquifers and potentially transmissive units above) are of relevance. A detailed overview of all available (and reliable) data is given in Nusch et al. (2013).

3 Model Implementation

3.1 Overview

3.1.1 Regional scale hydrogeological model

Based on the information shortly summarized in Chapter 2, a geological model (GeoMod 2012.1, see Gmünder et al. 2013a) using all available sources such as seismic lines, boreholes, outcrops etc. has been compiled (see Fig. 3-1). Based on this geological model, a regional hydrogeological model was established. The layers included in the regional hydrogeological model are (from top to bottom): the Quaternary, OSM, OMM, USM, the Malm aquifer, the Effingen Member, the "upper" Dogger, the Hauptrogenstein, the "lower" Dogger, the Opalinus Clay, the clay-rich Lias and Keuper, the Keuper aquifer, the Gipskeuper, the Muschelkalk aquifer and the basal Anhydritgruppe. The Keuper aquifer was not part of the geological model but was constructed using simple thickness rules in the hydrogeological model. The regional fault system implemented in the geological model had to be simplified in the regional hydrogeological model to limit the complexity of the mesh generation process and simulations. For this purpose, the faults were rotated vertically with the center of rotation being at the top surface.

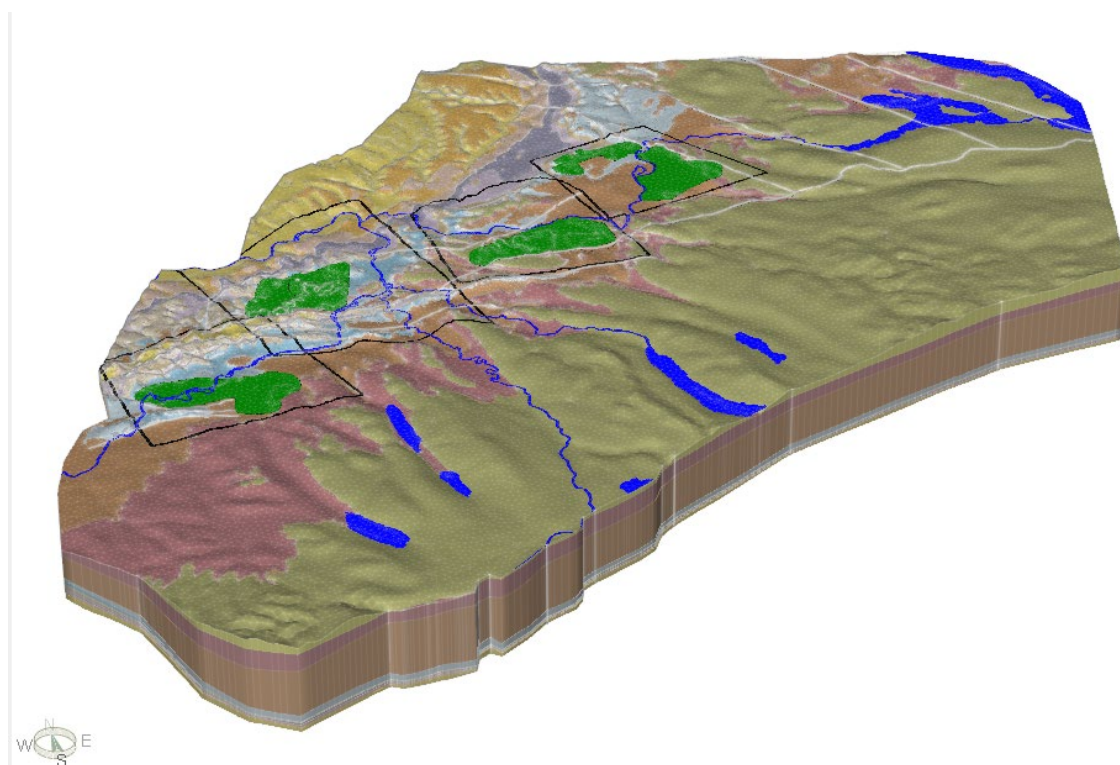


Fig. 3-1: 3D hydrogeological model including all relevant horizons and layers. Black lines delineate the area of the local scale models, green polygons resemble possible siting regions, white lines are trace lines of regional faults implemented in the model. Only the major rivers and lakes (blue) are shown. 2x vertical exaggeration, Quaternary cover not shown. Black lines delineate the boundaries of the four local-scale hydrogeological models JS, JO, NL and ZNO-SR.

3.1.2 Local scale hydrogeological model

In order to construct the local-scale hydrogeological models, the different local models were cut out of the regional geological model according to the predefined boundaries (see Fig. 3-1) and the same hydrogeological units as in the regional model were constructed. In addition, several hydrogeological units were added to ensure an adequate representation of the local groundwater flow conditions. Thus, local potentially transmissive units were implemented within the Dogger, Lias and Keuper units. These units have all been included using thickness rules (usually the minimum and maximum thickness of the layer and the distance to the next layer already existing in the geological model). The added hydrogeological units in the local model JS were the Keuper aquifer (constant thickness of 25 m), the Arietenkalk (constant thickness of 15 m) and the so called "Rest Dogger 4" (RD4), a thin layer of constant thickness (8 m) just above the Opalinus Clay representing the potential water conducting parts of the Sissach Member in the sensitivity analyses (see Chapter 4.1.3). The thicknesses of these layers were estimated from the thicknesses of the respective units in the borehole Schafisheim. The resulting model is shown in Fig. 3-2, the resulting stack of hydrogeological units is shown in Table 3-1.

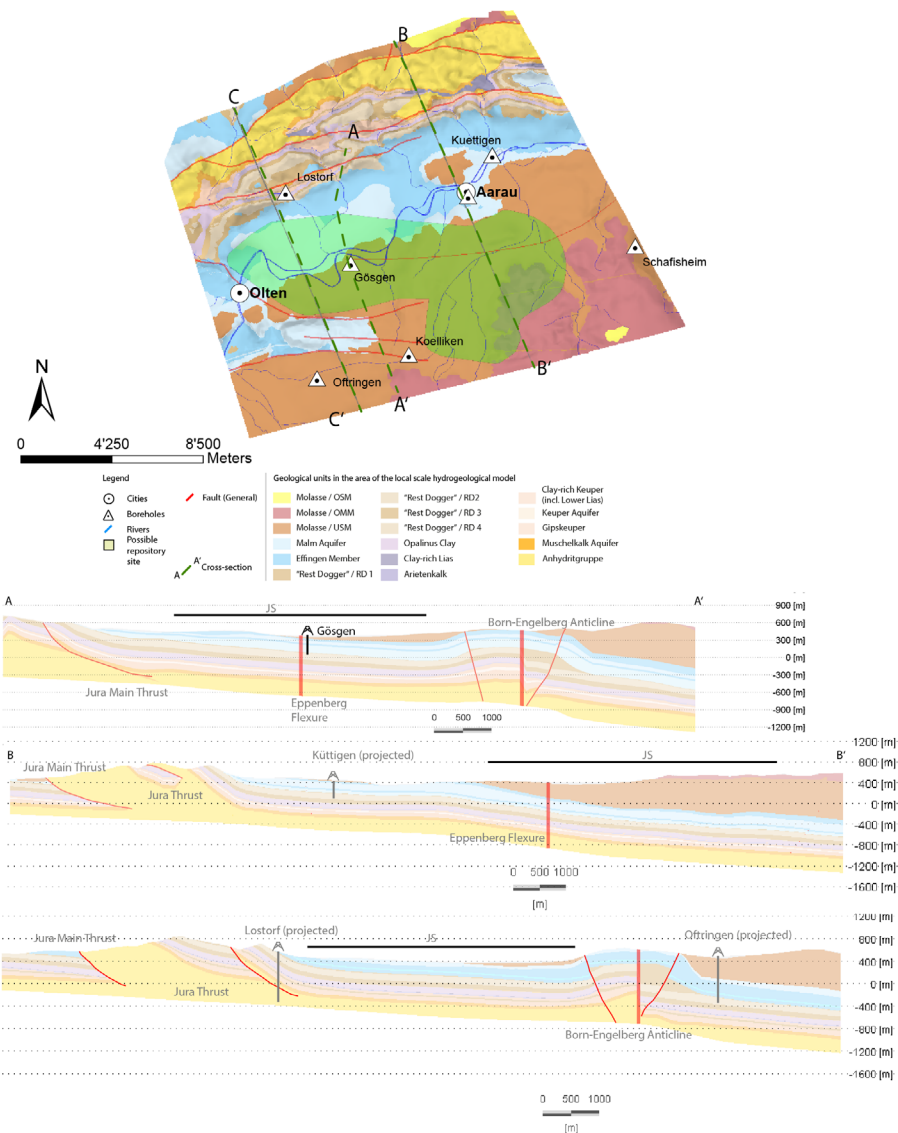


Fig. 3-2: Local model Jura-Südfuss (shown without Quaternary cover). 2x vertical exaggeration. Black bars in cross-sections depict location of the siting region.

Since the spatial resolution of the local model is much higher than in the regional model it was possible to represent the faults in greater detail using the actual dip as specified in the geological model. To simplify terminology and avoid confusion, in this report the area including the 3 fault planes associated with the Born-Engelberg Anticline are referred to simply as Born-Engelberg Anticline though actually these fault planes are only associated with it (see Fig. 3-3). The Eppenbergl Flexure was not covered in the regional scale geological model. As this fault has the potential to direct and channel flow on a local scale, it was added as a vertical fault but without offset of the hydrogeological units. Since a prerequisite of the used modelling software FEFLOW is that all layers cover the whole model domain, some faults have been connected to decrease the number of used elements/layers. This includes a connection of the Eppenbergl Flexure with a Jura Thrust and of the Trimbach Olten Fault with the northernmost fault plane of the Born-Engelberg Anticline. The connecting parts are assigned the same material properties as the surrounding hydrogeological layers. These changes are visualized in Fig. 3-3.

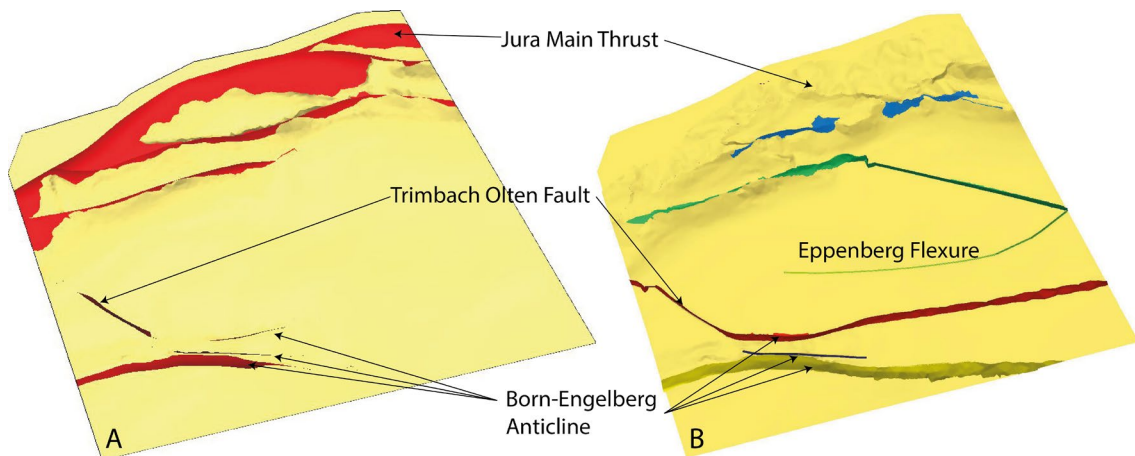


Fig. 3-3: Simplification/changes of faults within the model area. Note that due to the dip of the hydrogeological units, fault planes are not always (fully) visible. The fault traces are shown in Fig. 3-2. a) Original shape of regional faults in the 3D geological model. b) Implemented faults in the hydrogeological model. Note that the Trimbach Olten Fault has been connected to the northernmost fault plane of the Born-Engelberg Anticline while the Eppenberg Flexure and the southernmost fault plane of the Jura Thrusts have also been connected.

Due to constraints of the used modelling software, the planes representing the different faults all need to be present throughout the model domain. This is reflected by the fault planes crossing the whole model from roughly east to west. However, during the modelling only the necessary elements of the planes have been assigned as faults, the rest (e.g. the connection of the northernmost Jura Thrust plane in the model with the Eppenberg Flexure) represent hydrogeological units (see also Chapter 3.2).

In the subsequent chapters, a detailed overview of the model setup in terms of mesh generation (Chapter 3.2), property assignment (Chapter 3.3) and boundary conditions (Chapter 3.4) is given.

3.1.3 Used Software

For numerical implementations and simulation runs of the hydrogeological local models, the latest FEFLOW® Version 6.1 (DHI-WASY 2012) is used. FEFLOW is a professional software package for modelling fluid flow and transport of dissolved constituents and/or heat transport processes in the subsurface.

FEFLOW is a completely integrated system from simulation engine to graphical user interface, containing pre- and post-processing functionality and an efficient simulation engine, featuring user-friendly modern graphical interface, providing easy access to the extensive modeling options. FEFLOW also includes a public programming interface for user code.

FEFLOW is used by leading consulting firms, research institutes, universities and government organizations all over the world. Its scope of application ranges from simple local-scale to complex large-scale simulations.

3.2 Model geometry

3.2.1 General aspects

Based on the finite element method, FEFLOW allows using arbitrary triangulated grids representing the top boundary of the model (e.g. top ground surface). In the vertical direction, however, the mesh must follow the triangulation of the surface grid. This means that all the element layers representing the hydrogeological units must be present throughout the whole model domain. If, for instance, a geological unit reaches the topography (i.e. crops out) then the corresponding numerical layer has to continue to the model boundary even where this formation is not present. A minimal thickness and the conductivity of the underlying geological unit are then allocated to that (dummy) part of the numerical layer.

Other restrictions to shape and size of the elements are mainly dictated by the required numerical accuracy and the available computer capacity. In order to avoid an influence of the element shape on the model results, the form factor of the elements, i.e. the ratio between maximum and minimum dimension of an element should not be too large. Therefore, a ratio lower than 10 was maintained for the model at hand. With respect to the size of the elements, a compromise should be found between numerical accuracy and computational speed. Considering present-day computer capacities it is possible to calculate models with up to 25 million elements in a steady state FEFLOW run. In general, the model setup consists of 3 main stages:

- Construction of the horizontal mesh
- 3D gridding according the geological structure
- Allocation of hydrogeological properties and boundary conditions

The different steps are described in more detail in the subsequent chapters.

3.2.2 Horizontal discretization

The choice of the model area to be discretized was described in Chap. 2. In a first step, a so-called super-element mesh of the top horizon was constructed. This super-mesh honours (1) outcrop lines of hydrogeological units, (2) lateral boundaries of discontinuous layers, and (3) intersections of horizons with fault zones which all could be derived from the geological (GOCAD-) model. In a similar way the traces/contours of significant rivers and lakes were incorporated. Finally, this super-element mesh consists of 142 super-polygons illustrated in Fig. 3-4 (top).

Based on the super-element mesh, a finite-element mesh was automatically triangulated using the Advancing Front Mesh Generator in FEFLOW. Near outcrops of the geological formations considered or close to the faults zones, where high head gradients are expected mesh refinements are introduced. The final surface mesh consists of 139,116 nodes and 277,733 elements. The original mesh, resulting from the triangulation of the so called super-polygons (see Fig. 3-4, top), was not sufficient to properly map e.g. outcrops of hydrogeological units on the surface. Therefore, these areas had to be refined (see Fig. 3-4, bottom). The resulting finite mesh therefore shows triangle lengths that vary between 80 to 300 m in areas with a smooth topography and no outcrops (of hydrogeological units or faults) and 8 to 15 m in refined regions showing a high topography contrast and/or outcrops of hydrogeological units or faults. The resulting surface mesh is shown in Fig. 3-4.

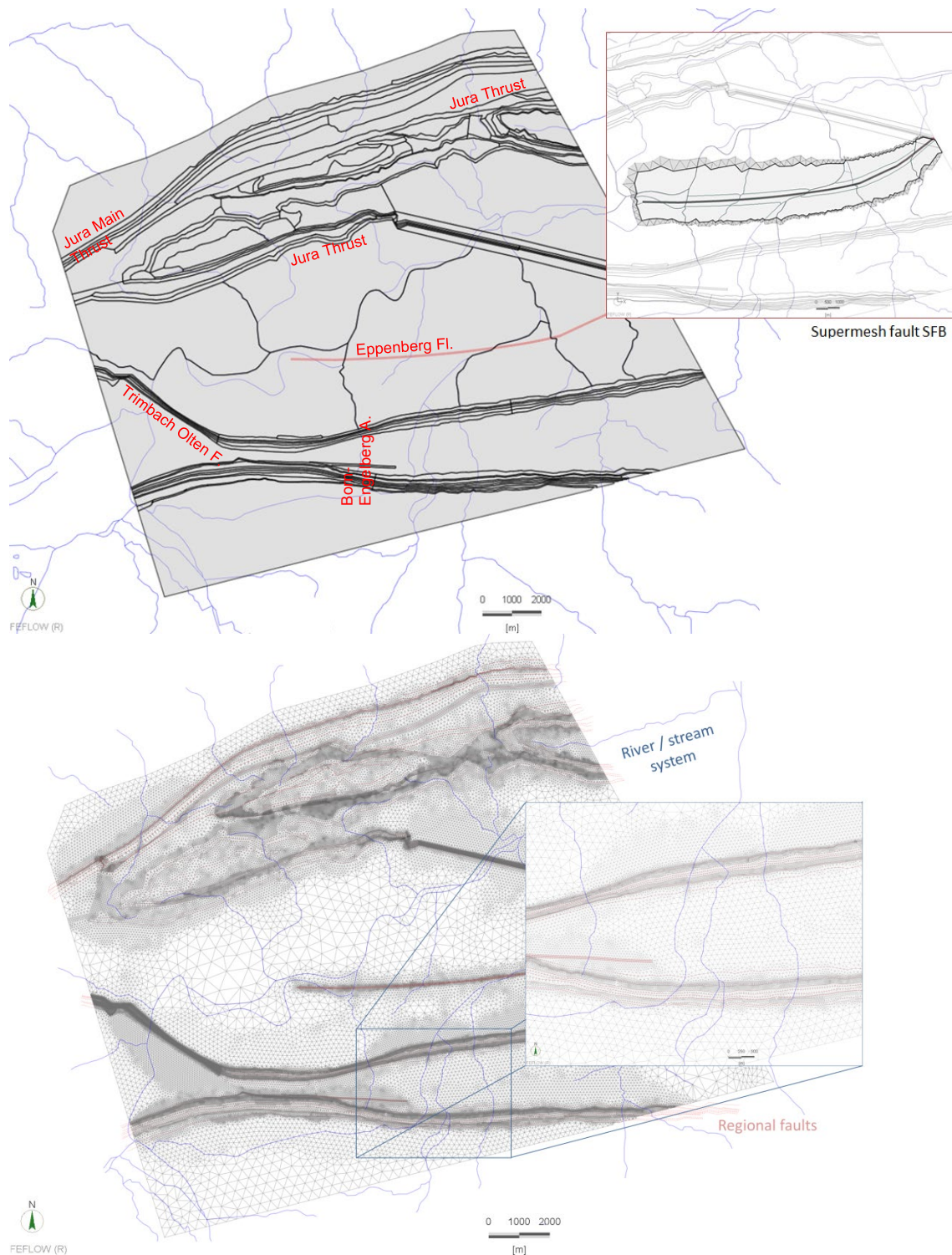


Fig. 3-4: Horizontal Discretisation. Top: Black lines represent borders of the super-polygons or trace lines where faults cut the respective regional faults. Bottom: Finite-Element mesh generated from meshing the super-polygons. The length of the triangles varies between 80 and 300 m in general and 8 and 15 m in zones of mesh refinement, e.g. near outcrops or along traces of faults (red lines indicate locations where the faults intersect the geological formations considered).

3.2.3 Vertical discretization

General aspects

3D-gridding follows a layered approach (i.e. in-depth repetition of the surface mesh) according to the horizon data as defined by the geologic regional model (see Chapter 3.1). The regional geological model contains the elevations (horizons) of 13 basic geological formations (from top to bottom: Quaternary, OSM, OMM, USM, Villigen Fm., Effingen Member, Oberer Dogger, Hauptrogenstein Fm., Passwang Fm., Opalinus Clay, Lias+Keuper, Oberer Muschelkalk, Anhydritgruppe). As argued above, additional subdivision of the Passwang Formation (2 layers), the Keuper-Lias unit (5 layers) and Effingen Member (3 layers) was introduced due to hydrogeological evidence (see also next chapter).

In addition, the model includes 4 regional faults, the Trimbach Olten Fault, the Born-Engelberg Anticline, the Eppenbergr Flexure and several Jura Thrusts, each represented by one or more fault planes (see Fig. 3-3). As each mesh layer has to be present in all the 5 blocks (see also Chapter 3.2.4) the resulting FEFLOW model consists of 92 model layers representing the 20 hydrogeological units (listed in Table 3-1) and the 4 regional faults.

In order to import the geological layer-based data from the geological model into the FEFLOW-model, the plug-in "GOCAD2Elevation" was used which automatically interpolates the elevation (and/or thickness) of FEFLOW nodes along corresponding horizons of the geological model.

Workflow

The general workflow of vertical discretization can be summarized as follows:

- Setup of a primary geometry of the 3D-model according to the layering of the geological model
- Definition of reference data "Geological Units" for the geol. formations and "Regional faults" for the regional faults considered
- Adaption or correction of model layers for smoother representation of the geological formations along the regional faults or outcrops, combined with necessary mesh refinements
- Vertical refinement of the regional geological formations Passwang and Lias+Keuper due to local hydrogeological evidence
- Adaption or correction of the divided layers for smoother representation of the geological formations along the regional faults or outcrops, combined with a second mesh refining

Tab. 3-1: Implemented layers of the 3D Model JS.

Geological Era	Model Layer (geol. units) of regional model	Hydrogeol. units considered in the hydrogeol. regional model	Model Layer (geol. units) of local model JS	Geological units considered in JS	Hydrogeol. Units in JS	Thicknesses of hydrogeol. units (at location of the borehole Schafisheim)
Quaternary	1	Quaternary	1	Quaternary	Quaternary	205 m
Tertiary (Molasse)	2	OSM	2	OSM	OSM	n/a
	3	OMM	3	OMM	OMM	n/a
	4	USM	4	USM	USM	372 m
Malm (Upper Jurassic)	5	Malm aquifer	5	Villigen Fm.	Malm aquifer	37 m
	6	Effingen Member	6	Upper Effingen Member	EFF 1	168 m
			7	Gerstenhübel-Schichten	EFF 2	30 m
			8	Lower Effingen Member	EFF 3	50 m
Dogger (Middle Jurassic)	7	Upper Dogger	9	Upper Dogger	RD1	5 m
	8	"Hauptrogenstein"	10	Klingnau Fm.	RD2	94 m
	9	"Passwang - Klingnau", not subdivided	11	Passwang Fm.	RD3	58 m
			12		RD4	8 m
	10	Opalinus Clay	13	Opalinus Clay	Opalinus Clay	81 m
Lias (Lower Jurassic)			14	Upper Lias	Clay-rich Lias	3 m
	Keuper (Triassic)	11	Lias + Keuper, not subdivided	15	Arietenkalk	Arietenkalk
16				Lias + Upper Mittelkeuper	Clay-rich Keuper (incl. lower Lias)	33 m
12		Keuper aquifer	17	Gansinger Dolomit / Schilfsandstein	Keuper aquifer	25 m
	13	Gipskeuper	18	Gipskeuper	Gipskeuper	75 m
Muschelkalk (Triassic)	14	Muschelkalk aquifer	19	Muschelkalk aquifer	Muschelkalk aquifer	60 m
	15	Anhydritgruppe	20	Anhydritgruppe	Anhydritgruppe	176 m

Additional hydrogeological classification

As argued in Chap. 3.1 and listed in Table 3-1, the complex units Lias and Keuper were divided, according to their average thickness indicated in brackets, into five sub layers, i.e. from top to bottom: "clay-rich Lias" (3 m), Arietenkalk (15 m), the "clay-rich Keuper incl. lower Lias", Keuper aquifer (25 m) and "Gipskeuper" (90 m).

The Passwang Formation was divided in a similar way into two sub layers, RD3 and RD4 (8 m), relating to the top elevation of the Opalinus Clay as reference.

Finally, the Effingen Member was divided into three sub layers, i.e. from top to bottom: EFF1 (upper part of the Effingen Member), EFF2 (30 m, Gerstenhübel Schichten) and EFF3 (50 m, lower Effingen Member), according to their average thickness related to the top elevation of the Upper Dogger as reference.

These thicknesses were chosen mainly based on evidence from the borehole Schafisheim.

3.2.4 Regional faults

In the geological dataset generated and provided by the SIMULTEC AG (see Gmünder et al. 2013a) for setting up the local models, regional faults are implemented as inclined faults. With respect to the local model JS, 4 regional faults, the Jura Thrusts (including the Jura Main Thrust), the Trimbach Olten Fault, the Eppenbergl Flexure and the Born-Engelberg Anticline were implemented as several inclined fault planes (Fig. 3-8). The handling of inclined faults in a FEFLOW model is illustrated by Fig. 3-5.

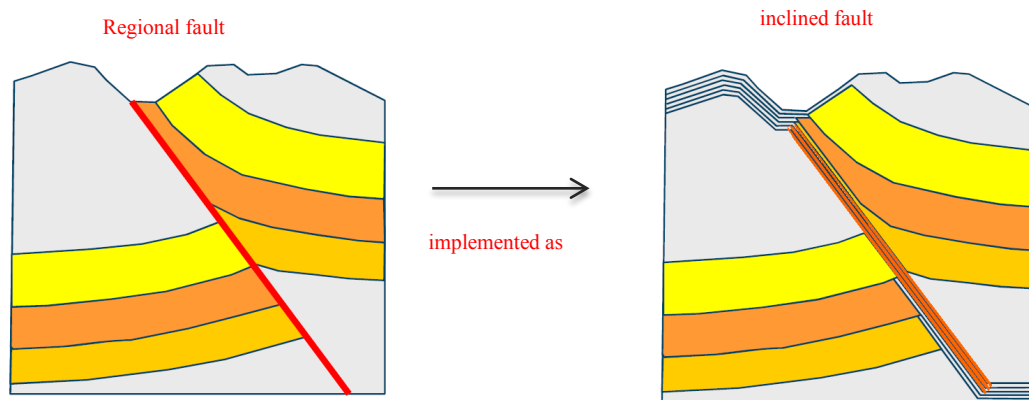


Fig. 3-5: Illustration of fault implementation in the local scale FEFLOW-Model.

In order to ensure a correct transition between the fault and the connected geological units, the corresponding intersection lines have to be present in the horizontal surface mesh (see Chapter 3.2.2). The situation is illustrated in Fig. 3-7 and Fig. 3-8. Fig. 3-6 shows parts of polygons of the horizontal super-mesh (black lines). The polygons represent intersection lines (projected onto the surface mesh) between a fault plane and the corresponding modelled geological horizons. The red line indicates an arbitrary reference line with numbered intersection points. These points refer to the numbered vertical (red) lines in Fig. 3-7 in order to illustrate where the geological horizons connect to the fault and how the layering is handled in this context.

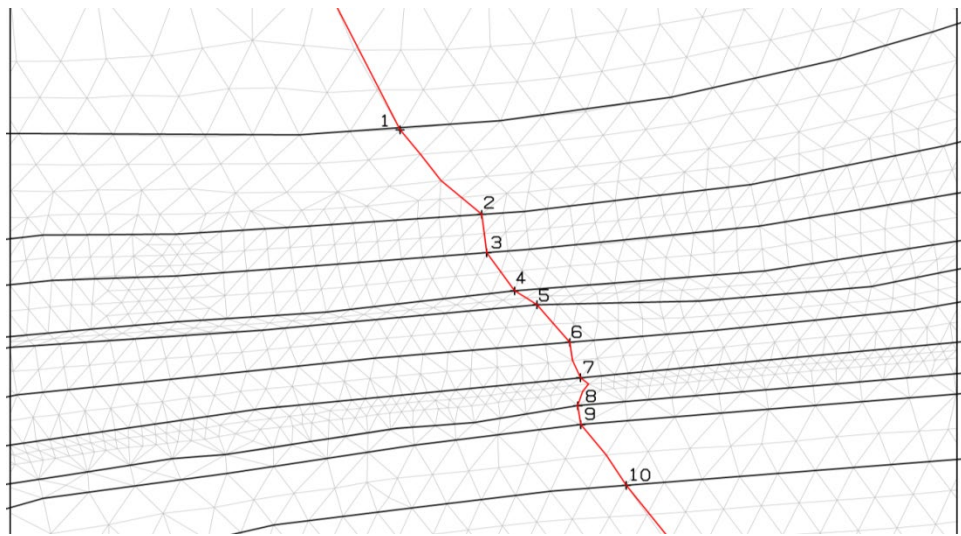


Fig. 3-6: Intersection between a fault trace and geological horizons (situation/surface mesh): Black lines indicate polygons of the super-mesh (i.e. surface projection of intersection lines), red indicates a reference line with numbered intersection points (to be compared with Fig. 3-7).

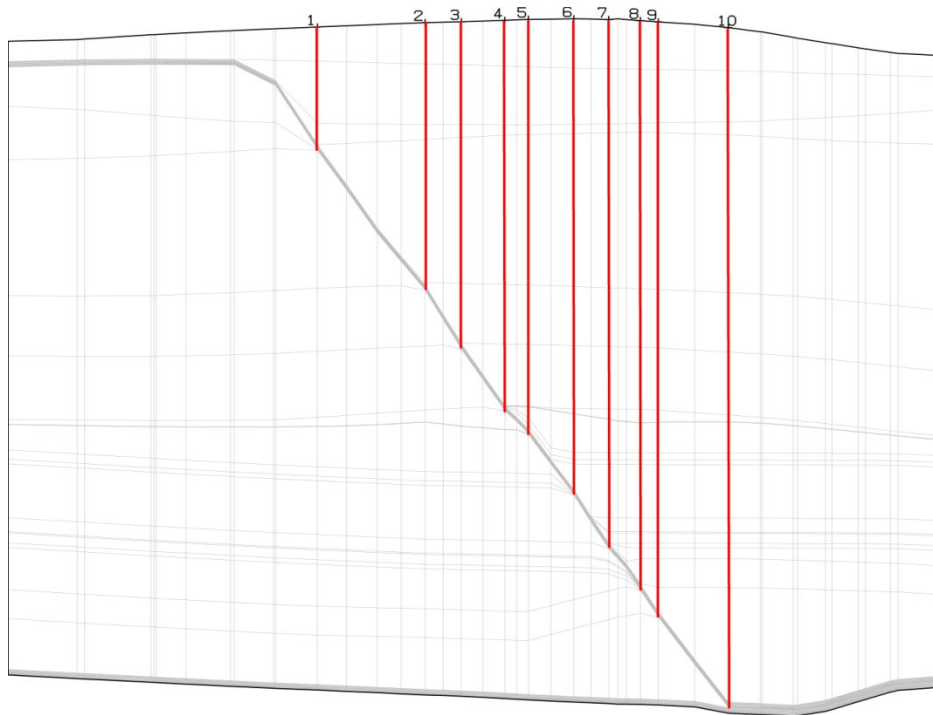


Fig. 3-7: Intersection between a fault and geological horizons (vertical section through reference line in Fig. 3-6).

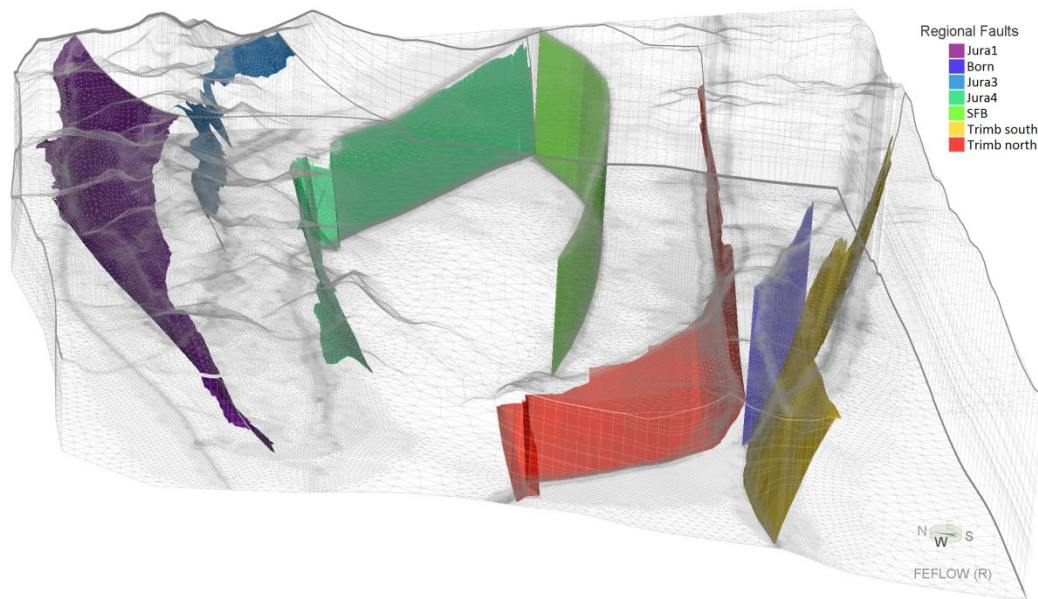


Fig. 3-8: 3D view from the west of the regional faults implemented as inclined and vertical faults. 2x vertical exaggeration.

In some rare cases, the connection between the fault plane and the connecting hydrogeological unit is not ideal. This is most obvious in the connection of the Malm aquifer along the elements connecting a Jura Thrust with the Eppenbergl Flexure (due to software reason, see Chapter 3.2.1) where hydraulic heads show a slight offset across these elements even though the fault plane has the same properties as the adjoining hydrogeological unit.

3.2.5 Composite mesh

In spite of all the numerical tools involved to discretize the complex 3D geometry, additional adaptations and corrections are necessary. In particular, the connections of geological layers along faults and outcrops need final (manual) interaction. The resulting 3D FEFLOW-model consists of 25,551,436 finite elements and 12,937,788 nodes in total. It contains 92 model layers (93 horizons), representing the 20 geological units listed in Table 3-1 and visualized in Fig. 3-9 to 3-11. As (partly) shown in Fig. 3-10 the elevation of the model domain varies from 400 to 900 masl on the top and between 200 and -1400 masl at the bottom.

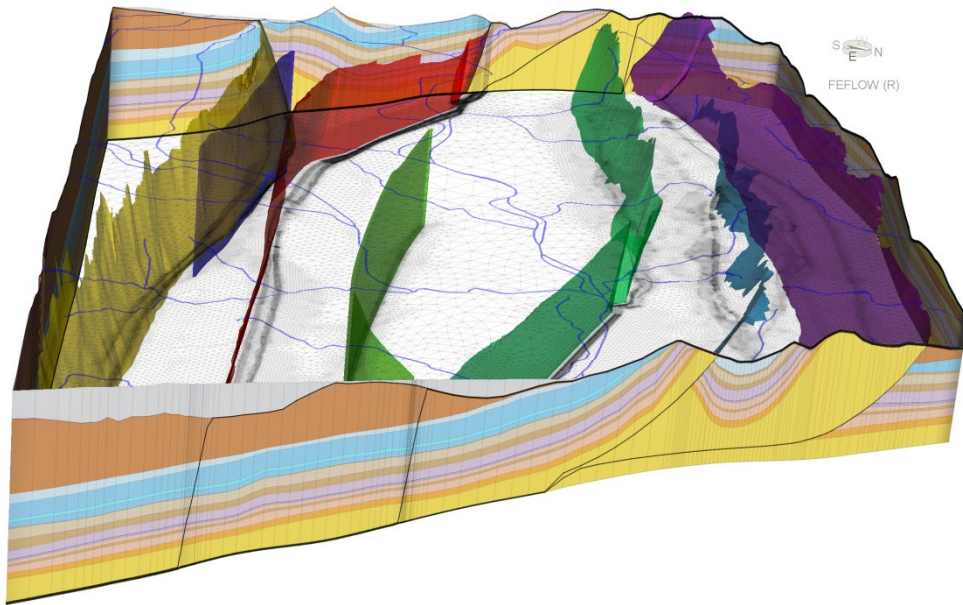


Fig. 3-9: 3D-View of the JS model from E. Lateral boundaries with geological layering, implemented faults and basic 2D-mesh along bottom of the domain. 2x vertical exaggeration.

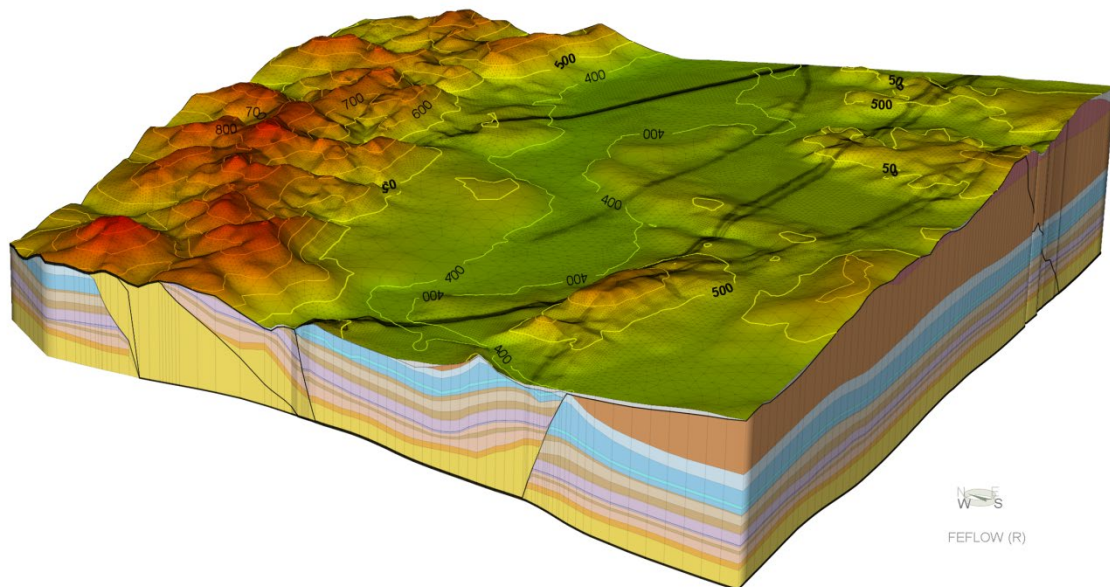


Fig. 3-10: 3D-View of the JS model. Lateral boundaries with geological layering, surface mesh with elevations. 2x vertical exaggeration.

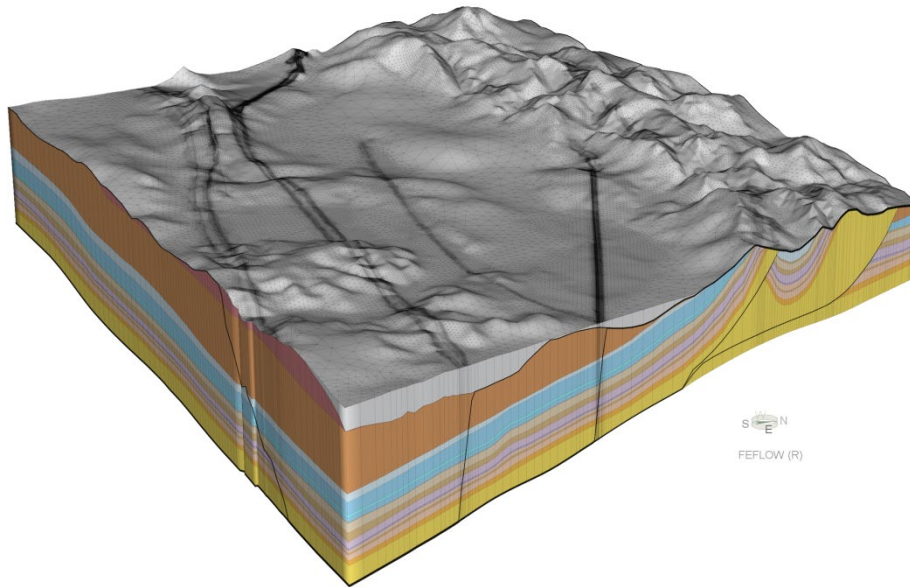


Fig. 3-11: 3D-View of the JS model from SE. Lateral boundaries with geological layering, surface mesh with fault traces. 2x vertical exaggeration.

3.3 Property assignment

3.3.1 General aspects

In rock aquifers the groundwater flow takes place in a complex system of pores, fissures, fractures, local and regional scaled fault structures. To model the flow in a scale required by the present project, the hydrogeological system has to be simplified. As described earlier the 4 relevant regional faults are considered as discrete model elements where different conductivity can be assigned in parallel and perpendicular direction. The flow properties of the smaller faults, fractures and fissures enter into a conductivity of a postulated homogeneous equivalent porous media. To consider the layered character of some geological units, they are supposed to have an anisotropic conductivity tensor with a higher conductivity parallel to bedding.

Like commonly applied in the finite element method, FEFLOW uses a cell-based definition of properties such as the hydraulic conductivity and K-values have to be assigned to each element of the 3D-mesh.

In order to accommodate the anisotropy of the hydraulic conductivity, FEFLOW-option "General Anisotropy with computed angles" is applied. This option makes use of the fact the principal axes of the 3D anisotropy tensor generally correlate with the geological layer structure and, provided that the 3D shape of the layers is known, the spatial rotation of the principal directions can be accomplished by computation. Provided (as assumed in the present case) the conductivity is orthotropic inasmuch the higher conductivity is parallel to the layering, and a lower conductivity is normal to the stratigraphy and the top and bottom faces of the elements fit the stratigraphic layering the transformation of the principal directions can be derived. Anisotropy is then computed on runtime based on the inclination/slope of the elements. To account for transversal conductivity of the faults, the latter have been represented by regular 3D-elements (see Chap. 3.2) and as such will be treated numerically as common elements with anisotropic features described above.

With respect to handling of layer conductivities in the vicinity of fault intersections similar issues arise as before during mesh construction. In this context, the hydraulic conductivities of discontinued layers have to be adapted (e.g. based on user-defined minimal thickness) and assigned to adjacent geological layers (which are therewith reused). In this way, a smooth transition of the conductivity along the faults can be obtained.

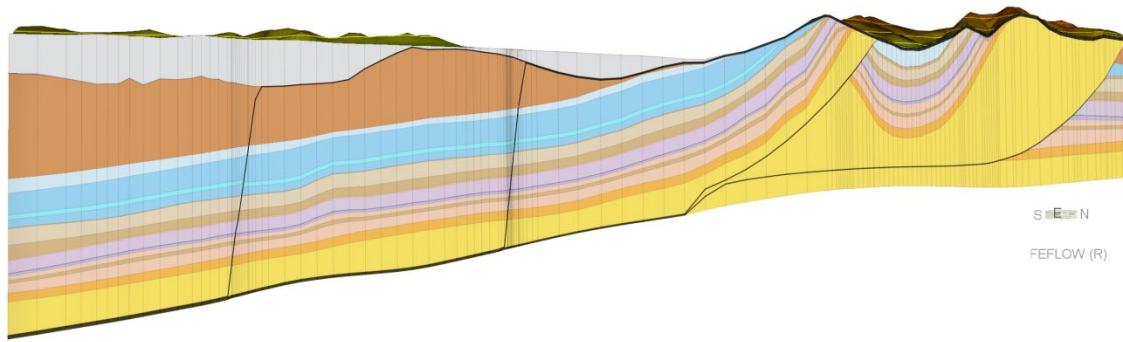


Fig. 3-12: Cross-section through the model domain indicating the layered stratigraphy of the model domain. Where the regular layering is "broken" at fault planes, discontinued layers are "reused" by assigning them to new hydrogeological units. 2x vertical exaggeration.

3.3.2 Hydraulic/Hydrogeological units

The model JS represents one link in the model chain from regional to local scale. Therefore, the regional hydrogeological model (Gmünder et al. 2013b) forms the basis of the conductivities to be assigned. In a first step, the geological units of the model JS obtain the values of the regional model as listed in Table 3-2 also taking into account regional heterogeneity (zonation) within those formations (see Gmünder et al. 2013b). In some units of the hydrogeological regional model, a spatially varying hydraulic conductivity has been assigned to account for different processes influencing the rock permeability (karstification, cementation, fracturing etc.). The assigned values and the arguments for these zonations are detailed in Gmünder et al. (2013b, Chapter 4.5). This spatial variability of the regional model has also been used for the respective units in the local scale model, namely for the Malm aquifer (Fig. 3-13a), the Hauptrogenstein aquifer (Fig. 3-13b) and the Muschelkalk (Fig. 3-13c) so that the local scale model is consistent with the regional model (see also Chapter 4.1.1) and boundary conditions necessary for the local scale model can easily be transferred from the regional model.

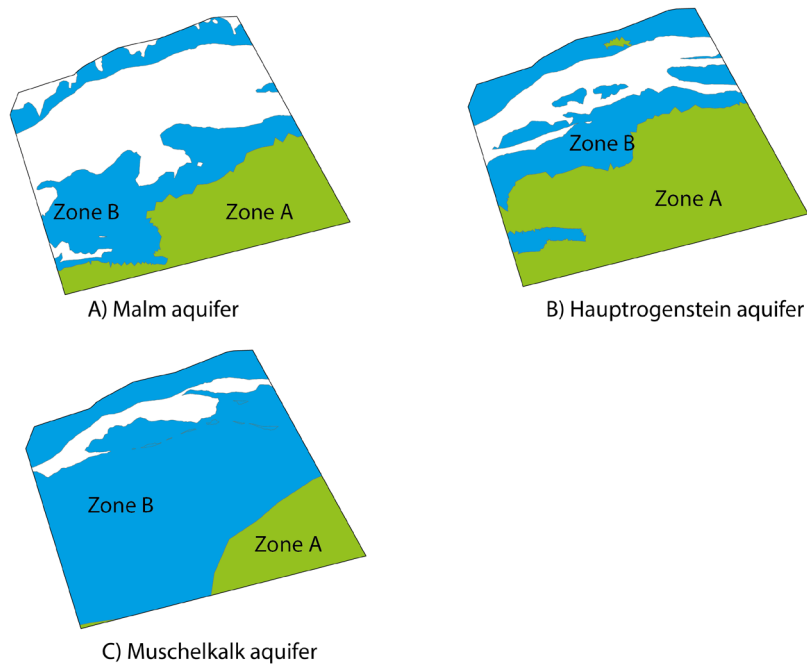


Fig. 3-13: Zones of Different Conductivities Implemented in the Local Model Jura-Südfuss (see Gmünder et al. (2013b) for a detailed discussion).

As described above (Chapter 2.1) additional, locally important hydrogeological units have been incorporated into the Passwang, Lias-Keuper and Effingen Member units of the model resulting in a higher vertical resolution. The hydraulic conductivity values assigned to these new layers were chosen based on hydrogeological considerations. The conductivities assigned to the regional model (Table 3-2) have been used to calculate correct conductivities for the newly created layers based on their (average) thicknesses (see Tab. 3-3). Therefore, the overall conductivity in the local model is consistent with the regional scale model.

Tab. 3-2: Hydraulic conductivities according the Regional Model (Gmünder et al 2013b). Note that in case of the Keuper aquifer, the whole local model is located in the same zone.

Layer	Description	Kh [m/s]	Kv [m/s]
1	Top Layer (Quaternary)	variable	variable
2	OSM	2.00E-8	2.00E-11
3	OMM	1.00E-6	1.00E-9
4	USM	Zonation	2.00E-11
5	Malm aquifer	Zonation	Zonation
6	Effingen Member	1.00E-11	1.00E-12
7	'Brown Dogger' / Rest-Dogger 1	1.00E-11	1.00E-12
8	Hauptrogenstein aquifer / Rest-Dogger 2	Zonation	Zonation
9	'Brown Dogger' / Rest-Dogger 3	1.00E-11	1.00E-12
10	Opalinus Clay	1.00E-13	2.00E-14
11	Lias	1.00E-13	2.00E-14
12	Keuper aquifer	Zonation	Zonation
13	Gypsum-Keuper	1.00E-14	1.00E-14
14	Muschelkalk aquifer	Zonation	Zonation
15	Anhydrit Group	1.00E-10	1.00E-10

Tab. 3-3: Hydraulic conductivities of the hydrogeologically refined formations Passwang, Keuper-Lias and Effingen Member.

Geological Unit of the Regional Model	Local Model Layer	Conductivity [m/s]	
		Horizontal K_h	Vertical K_v
Effingen Member	EFF1	$1 \cdot 10^{-11}$	$1 \cdot 10^{-12}$
	EFF2	$1 \cdot 10^{-11}$	$1 \cdot 10^{-12}$
	EFF3	$1 \cdot 10^{-11}$	$1 \cdot 10^{-12}$
'Brown Dogger' / Rest-Dogger 3	RD3	$8 \cdot 10^{-12}$	$1 \cdot 10^{-12}$
	RD4	$2 \cdot 10^{-11}$	$1 \cdot 10^{-12}$
Lias+Keuper	Clay-rich Lias	$1 \cdot 10^{-13}$	$1 \cdot 10^{-13}$
	Arietenkalk	$1 \cdot 10^{-12}$	$1 \cdot 10^{-12}$
	Clay-rich Keuper	$1 \cdot 10^{-12}$	$1 \cdot 10^{-12}$
	Keuper aquifer	$1 \cdot 10^{-9}$	$1 \cdot 10^{-9}$
	Gipskeuper	$1 \cdot 10^{-14}$	$1 \cdot 10^{-14}$

The resulting model layer structure with the considered hydrogeological units along representative cross sections (with 2x vertical exaggeration) is given in Fig. 3-14.

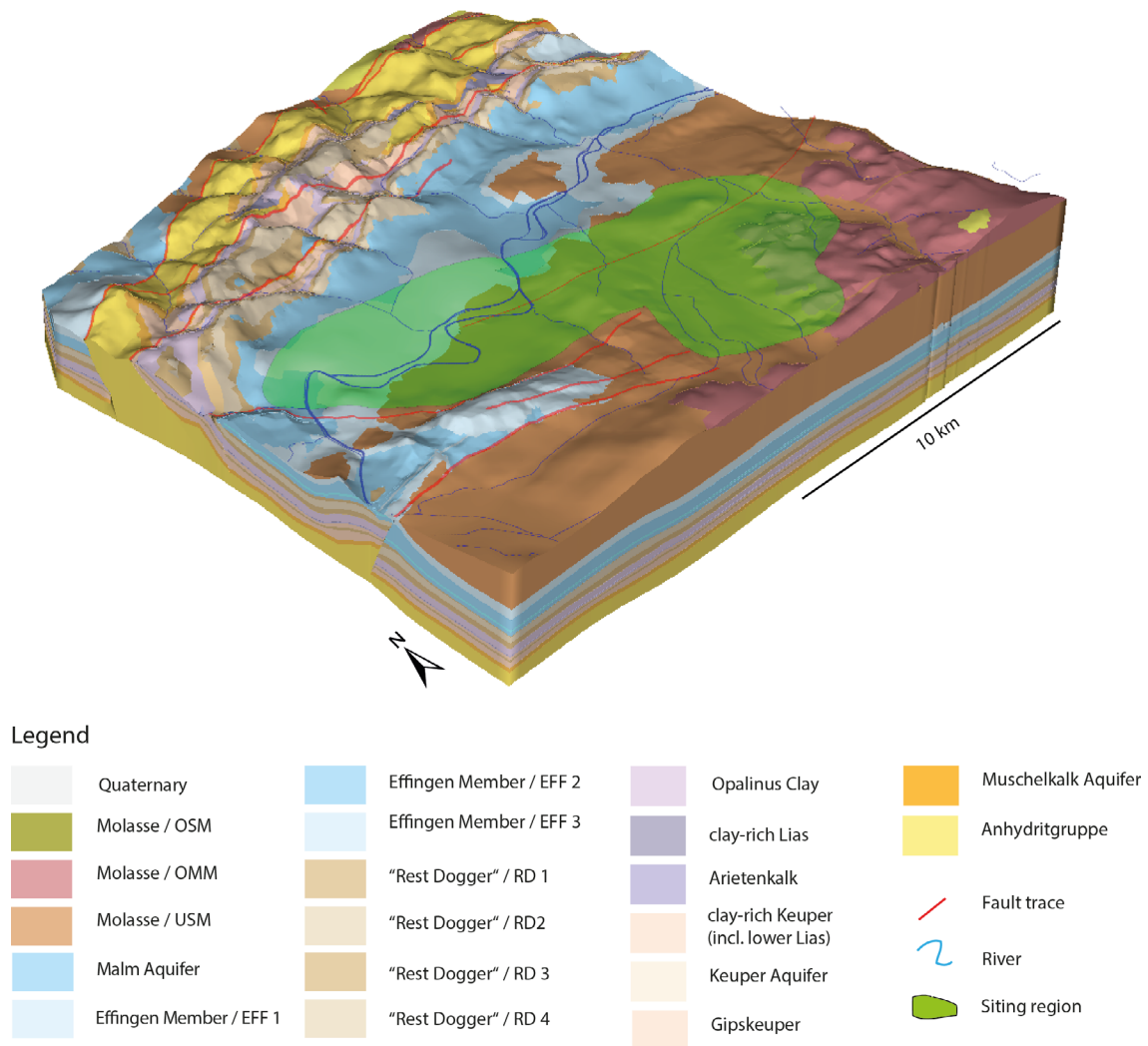


Fig. 3-14: 3D view of the implemented hydrogeological units without covering Quaternary. 2x vertical exaggeration.

3.3.3 Faults

As stated above faults are incorporated in the mesh using regular 3D-finite elements (in contrast to frequently used 2D-elements). Therefore, fault elements obtain (anisotropic) properties like other hydrogeological units. This method allows to easily accommodate the inherent uncertainty with respect to the fault behavior (connecting, sealing, etc.) so that different hypotheses can be investigated by assigning corresponding anisotropy tensors as explained in detail in Chap. 3.3.1. The hypothesis will be described below in Chap. 4ff.

3.4 Boundary conditions

Because the local model was cut-out of the regional model, the boundary conditions of the local model have to reflect the hydraulic conditions given by corresponding scenarios of the higher-scale model. These include Dirichlet boundaries, i.e. the so-called Fixed/Prescribed-Head Boundary Conditions (FH) along parts of the top and lateral aquifer boundaries as well as spatially distributed recharge (FQ) along the top boundary. The boundary conditions implemented along the 6 model boundaries are only shortly described below, detailed information, especially about the implemented surface boundary conditions, is given in Gmünder et al. (2013b).

3.4.1 Top/surface boundary

FH Boundary Conditions were implemented for the Quaternary-aquifer on the top of the model domain along and/or around the rivers or main streams according to Fig. 3-15.

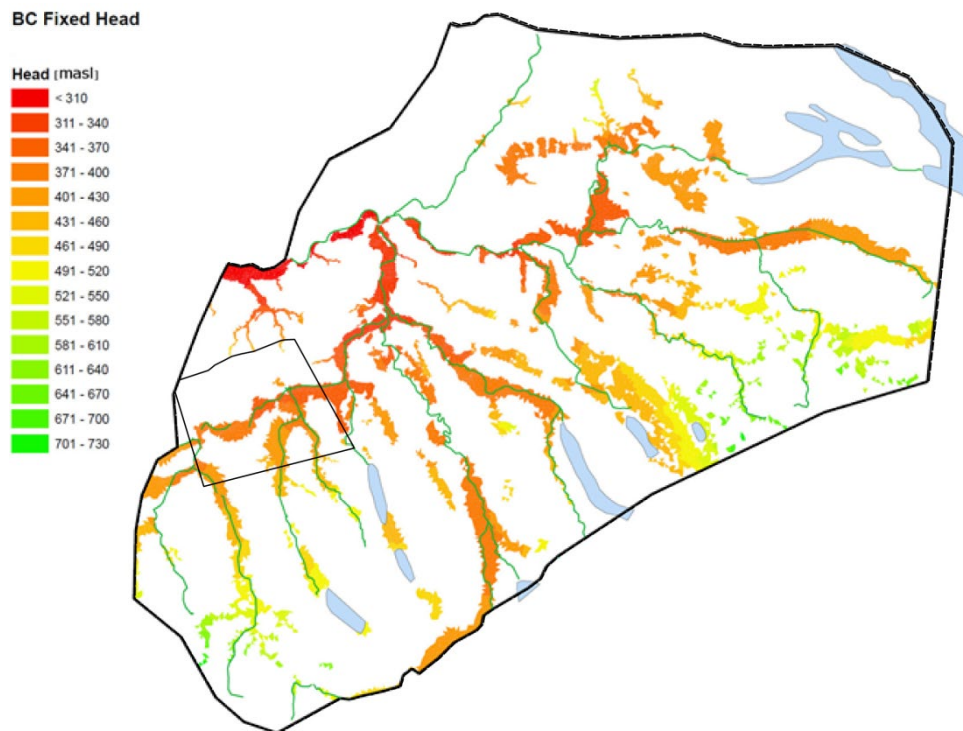


Fig. 3-15: Groundwater heads considered as fixed head boundary conditions at the top of the model domain in the Regional Model (Gmünder et al. 2013b).

Additionally, spatially distributed groundwater recharge is assumed along the top layer of the model. According to the regional model, a constant and homogeneous groundwater recharge rate of 139 mm/year or 85 mm/year has been chosen (see Fig. 3-16 and Fig. 3-17). This value was derived from the surface water flow corresponding to the 95th percentile of the annual flow of the main stream/river of the sub-basins (Q347, Sanford 2002).

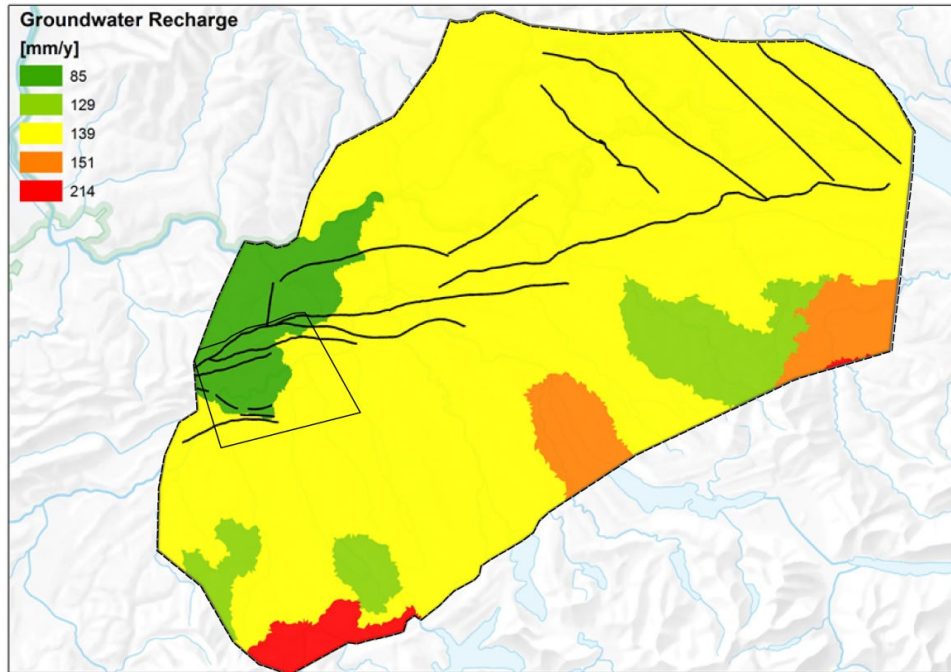


Fig. 3-16: Distribution of the groundwater recharge (precipitation) as considered in the regional model (Gmünder et al. 2013b).

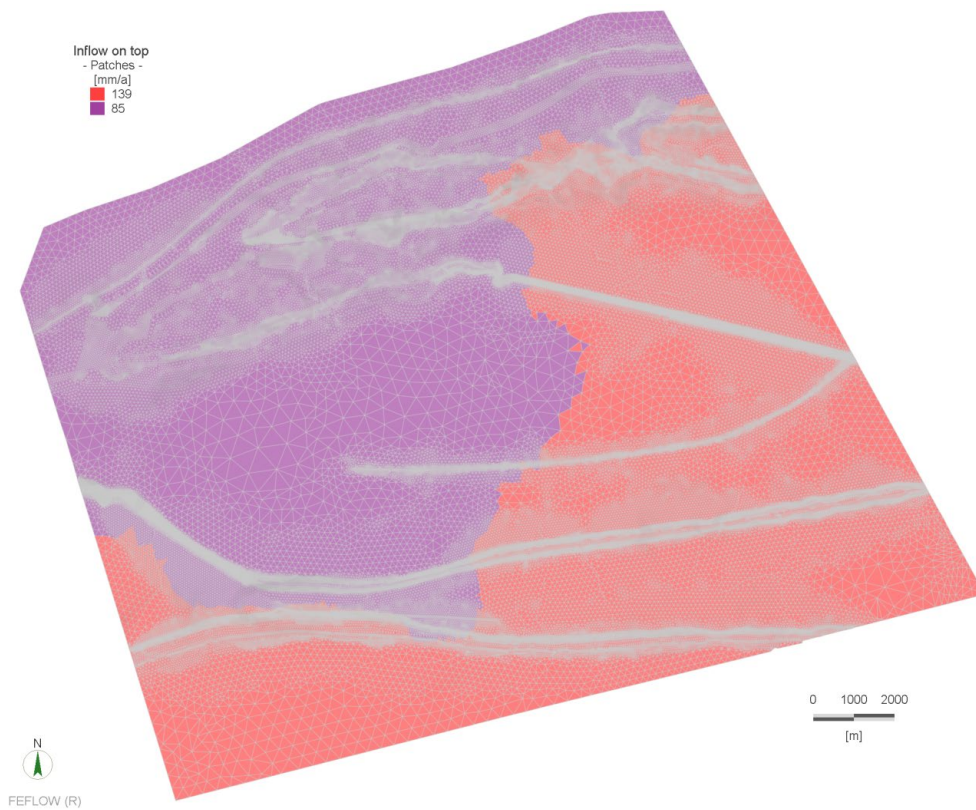


Fig. 3-17: Groundwater recharge as implemented in the model JS (compare with Fig. 3-16).

3.4.2 Lateral boundaries

According to their occurrences along the lateral borders, the Muschelkalk aquifer, Keuper aquifer, RD2 and Malm aquifer obtain FH conditions adopted from the regional model. For this purpose, the hydraulic heads of the considered boundary nodes represented by their 2D-coordinates were interpolated from results of the corresponding aquifer layer of the regional model. Boundary nodes along the additional, potentially transmissive units not present in the regional model and incorporated according Chap. 3.2, obtain the head values from the superior (joint) layer of the regional model. In order to properly map the head values along the faults at lateral boundaries, at first the corresponding node coordinates of the local model are projected onto the (vertical) fault of the regional model before head interpolation is accomplished.

3.4.3 Bottom

Crystalline basement rocks of relatively low conductivity are located below the bottom layer of the model so that the amount of water exchange with deeper formations can be neglected. Thus, no flow conditions have been implemented along the bottom boundary of the model.

4 Modelling results

4.1 Modelling strategy

A retraceable modelling strategy was adopted to ensure a balanced assessment of the key features and processes which govern groundwater flow conditions in the siting region Jura-Südfuss. The general workflow comprises the following elements (Figure 4-1):

- A consistent representation of groundwater flow conditions at all relevant scales was achieved by the nested modelling approach
- A set of complementary working hypotheses was specified, covering a wide spectrum of groundwater flow scenarios.
- The consistency of the (regional) simulations with the present day conditions was checked by comparison of the modelling results with the available field data. Sensitivity analyses were performed to investigate both conceptual uncertainties and parameter uncertainties.
- The simulation results were analysed and interpreted and the plausibility and consistency of the modelling results were evaluated by comparison with the regional scale simulations

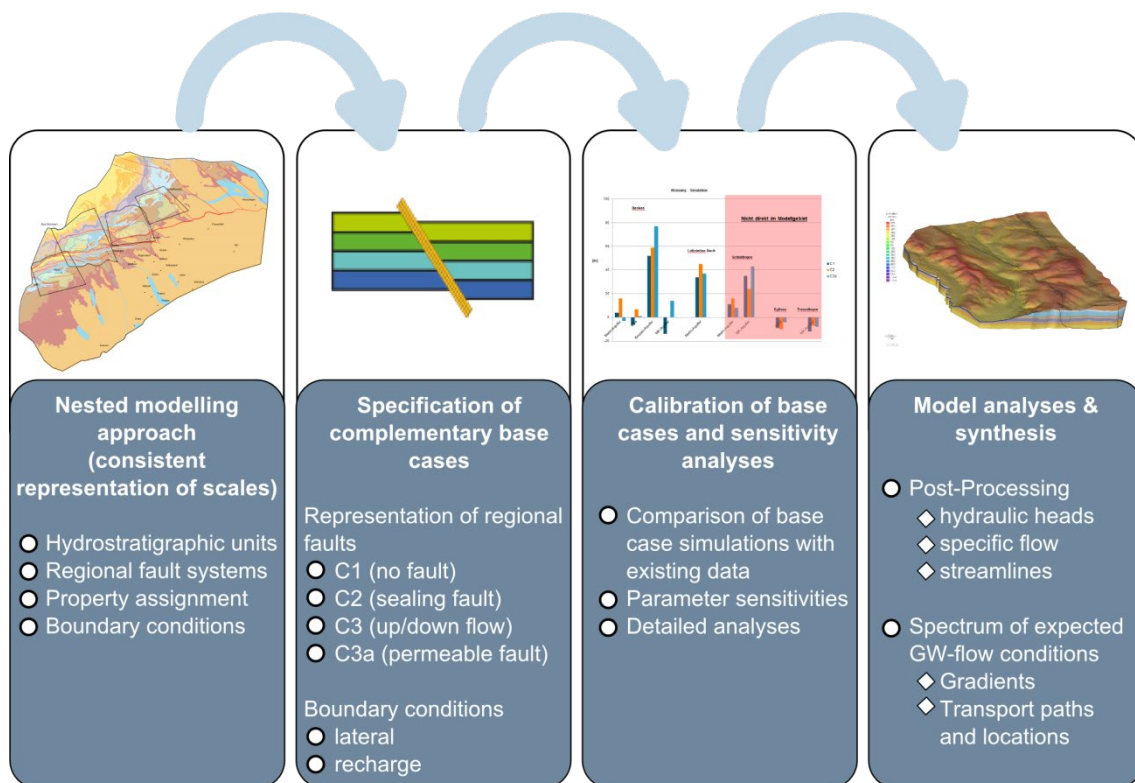


Fig. 4-1: Modelling strategy adopted for the hydrogeological simulations.

4.1.1 Nested modelling

As outlined in detail in Chapter 2 the siting region Jura-Südfuss is located in the (deformed) Tabular Jura and the Eastern Subjurassic Zone where local hydrogeological conditions are characterized by the following geological setting:

- The regional fault systems (Jura Thrusts, Born-Engelberg Anticline, Eppenbergr Flexure and Trimbach Olten Fault) occur within the model domain.
- Outcrops of all aquifers occur along topographic heights due to their large vertical (and horizontal) offset along some of the regional fault systems implying complicated groundwater circulation
- Clear evidence was found for regional scale variability of hydraulic conductivity in several hydrogeological units, such as the Malm aquifer, the Hauptrogenstein and the Muschelkalk aquifer

Understanding the impact of this geometrical and hydrogeological complexity on the local scale groundwater system requires detailed modelling by means of dense spatial discretisation. However, on the regional scale, minimum element size is restricted due to numerical execution time and memory constraints. In order to ensure a consistent description of groundwater flow on both, the regional and local scale, the solution is to use a nested modelling approach. The principle behind nested modelling is that, consistent with the large-scale groundwater circulation generated by the overall model, detailed local flow fields can be simulated using fine-scale sub-grids as long as lateral boundary conditions are suitably provided from higher scale results. In this context, the present model JS was implemented as local sub-grid of the large-scale regional model (Gmünder et al. 2013b) as described in more detail in Chapter 3.

4.1.2 Working hypotheses and base cases

The hydrogeological considerations together with its numerical implementation as described in Chap. 2 and Chap. 3, respectively, define reference conditions representing the currently most plausible model configurations with respect to geometry, parameters and boundary conditions. However, general uncertainties exist with respect to the impact of distinct components of the model (e.g. hydrogeological units, faults, etc.) on groundwater flow pattern. In particular, the potential role and significance of the hydraulic behaviour of the fault-zones is rather unknown. In this case, it is common practise to model the resultant effects based on different working hypotheses. Using the implementation of faults described in Chapter 3.3.3, it is possible to change their hydraulic behaviour by simply assigning corresponding conductivity parameters. In this context, 4 basic hypotheses have been defined (leading to 4 different base cases, see Fig. 4-2), each treating the role of the faults in a different manner:

- Hypothesis C1/Base case C1 ("throw only"): In this case, the faults are assumed non-existent. The controlling factor for flow along or across the (hypothetical) fault planes is the offset of the different hydrogeological units. If an aquifer is offset and abuts onto an aquitard, no flow is possible. In case of an aquifer being offset to abut onto another aquifer, these two aquifers are coupled and flow from one aquifer into the other is possible. The numerical model implements base case C1 by assigning the properties of the hydrogeological units to the adjacent elements of the faults.
- Hypothesis C2/Base case C2 ("sealing faults"): The faults are assumed to exhibit a very low hydraulic conductivity and therefore have a sealing effect. Because flow within the faults was limited to all directions even cross-flow between aquifers which abut through the offset would not be possible. This effectively divides the model domain into separate blocks. The

numerical model implements these conditions assigning a very low conductivity ($2e-14$ m/s) to the fault elements.

- Hypothesis 3/Base case 3 ("connecting faults"): In this case, flow along the fault planes (lateral and vertical) is possible while flow across the fault planes is prohibited (or at least only very limited flow is possible). This also divides the model domain into distinct blocks. However, flow along the fault from a deeper aquifer to a higher aquifer (or vice versa) is possible within each block. The numerical model implements base case C3 by assigning a relatively high conductivity ($1e-6$ m/s) to the outer elements of the faults while the central row of elements in the faults only have a very low conductivity ($2e-14$ m/s).
- Hypothesis 3a/Base case 3a ("fully connecting faults"): This case assumes the faults as fully active connections so that flow along the fault planes (lateral and vertical) as well as flow across the fault planes is possible. The numerical model implements base case C3a assigning a relatively high conductivity ($1e-6$ m/s) to all the elements of the faults (both outer and central row).

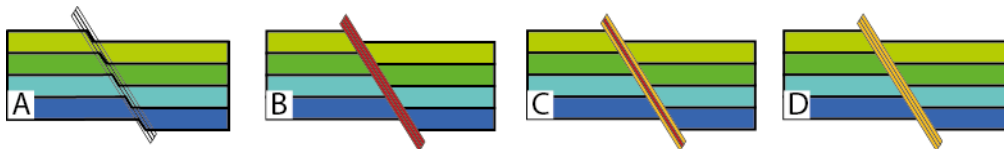


Fig. 4-2: Parameter assignment of the different elements of the faults for the different cases. Faults in the base cases are represented by 3 layers of elements. By assigning different hydraulic properties to the layers, the hydraulic behaviour of the fault can be changed. A) Base case C1: Fault elements are assigned with the same conductivities as the surrounding rocks. This effectively means that the fault does not exist and flow is governed by offset only. B) Base case C2: All fault elements are assigned very low conductivities. C) Base case C3: Fault elements on the outside are permeable, the central row of fault elements are assigned with very low conductivities. D) Base case C3a: All fault elements are assigned with high conductivities.

4.1.3 Sensitivity analyses

Uncertainties with respect to the role and significance of individual model components as well as the related parameter uncertainty necessitate the evaluation not only of the base cases behaviour but also of variations from the expected system behaviour. The systematic evaluation of this behaviour, including variations, has been performed by means of additional simulation runs as part of a sensitivity analysis (conceptual variations, parameter variations). For instance, the hydrogeological unit Arietenkalk has not been regarded as a locally important transmissive unit in the base cases defined above, but has been assigned higher conductivities in the sensitivity cases, effectively treating it as a transmissive while the remaining model was not changed. The unit RD4 (Sissach Member), a comparably thin unit just on top of the Opalinus Clay in the local scale model, has also been assigned with a higher conductivity in the sensitivity analyses as it may locally be a transmissive unit. A complete overview of parameters and boundary conditions used in the simulation runs (base and sensitivity cases) is given in Table 4-1.

Tab. 4-1: Overview on sensitivity cases performed with the local model JS.

Sensitivity Case	Base Case	Hydrogeol. unit	Conductivity Sensitivity case [m/s]	Conductivity Base Case [m/s]	Boundary conditions (from regional model)
C1-RD4	C1	RD4 (Sissach Member)	1×10^{-9}	1×10^{-12}	C1
C2-RD4	C2				C2
C3-RD4	C3				C3
C1-AKA	C1	Arietenkalk	1×10^{-8}	1×10^{-12}	C1
C2-AKA	C2				C2
C3-AKA	C3				C3

* AKA = Arietenkalk.

4.1.4 Modelling products and analysis

A thorough and comprehensive analysis of simulation runs involves numerous evaluation tasks yielding a manifold of output in terms of performance measures (i.e., hydraulic heads, groundwater fluxes, hydraulic gradients). In this context, each simulation run is discussed systematically based on a predefined set of so-called *modelling products* which have been organized as follows:

- Contour plots along selected surfaces (vertical/horizontal sections, geological boundaries, etc.)
- Profiles (tables and charts) along specified lines
- Maps of recharge/discharge areas
- 3D recharge/discharge paths (limitations of the method used to calculate the paths is detailed in Gmünder et al. (2013b))
- Vertical gradients through the host rock

The above mentioned products are presented in the following chapters. To avoid unnecessary repetition of results such as exact recharge or discharge locations etc., Chapter 4 is mostly descriptive while Chapter 5 summarizes and explains the results.

The position and orientation of the cross-sections shown in subsequent chapters and the appendices is given in Fig. 4-3 and is the same for all cross-sections in this report.

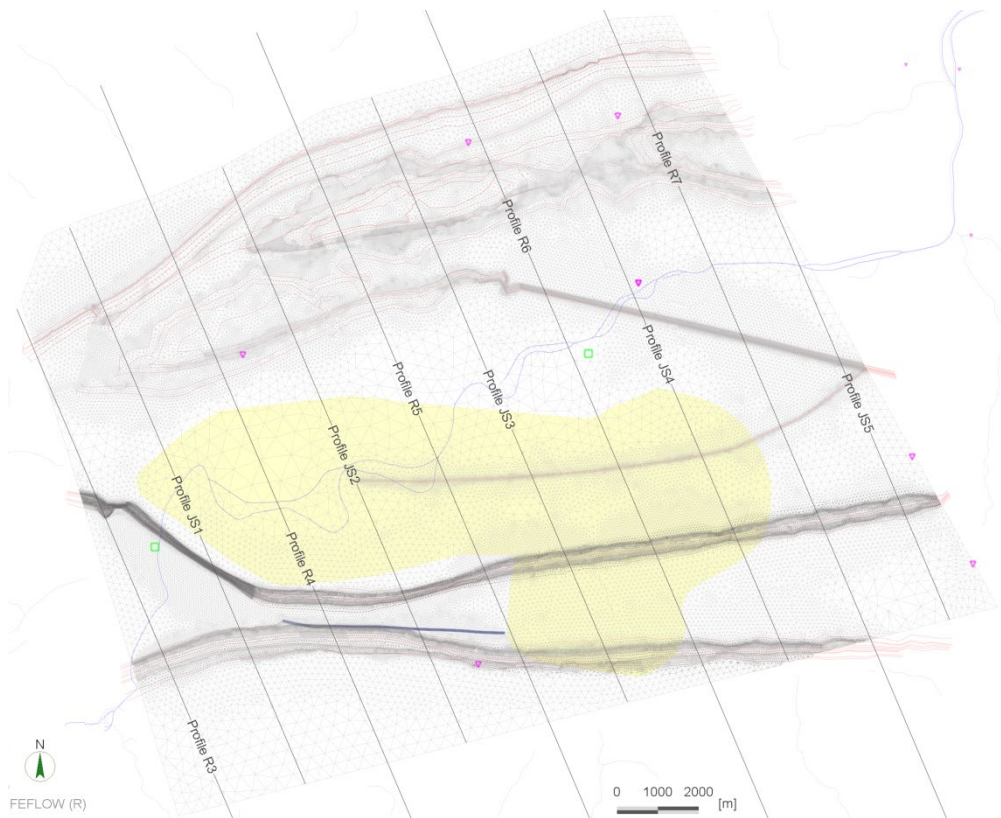


Fig. 4-3: Location of cross-sections in the model area.

4.1.5 Model calibration and consistency checks

In broad terms, model calibration refers to the process of gathering information about the model from measurements of what is being modelled. This includes the identification of model structure (e.g. the role of faults and aquifers) and the inherent heterogeneities defining hydraulic properties. For the model domain including the siting region Jura-Südfuss, a formal model calibration cannot be performed because not enough hydraulic observation data from boreholes is available. However, the larger scale regional hydrogeological model has been intensively checked against all available hydraulic measurements and provides a reliable picture of the regional flow pattern (Gmünder et al. 2013b). Thus, an acceptable agreement between the models at both scales will verify the local results to some extent.

Because a substantial model calibration cannot be carried out it is important to accomplish further checks in order to ensure plausibility and consistency of the modelling results. First, a comparison with results of the hydrogeological regional model is important to ensure the correct adoption of boundary conditions and hydrogeological parameters. This comparison is part of the modelling report for the hydrogeological regional model (Gmünder et al. 2013b).

4.2 Base case C1 ("throw only")

4.2.1 Hydraulic heads

As argued above Run C1 refers to a best guess parameter set and boundary conditions described in Chapter 3.3 and 3.4 assuming that the faults only affect the flow system according to the offset of the geological units (s. Chapter 4.1). Along the Jura Thrusts, a thick succession of the Anhydritgruppe crops out, effectively separating the model domain into a northern and southern part (with respect to the Jura Thrusts). In the following discussion (and subsequent chapters), the northern part is not analysed and discussed (the southern part contains the siting region). An overview of the model is given in Fig. 4-4.

Disregarding the Quaternary (surface) aquifer, the flow system is mainly represented by four aquifer layers (Malm aquifer, Hauptrogenstein aquifer, Keuper aquifer and Muschelkalk aquifer). Their flow fields, indicated by the distribution of hydraulic heads, are shown Fig. 4-5 and Fig. 4-6, vertical sections through the flow system are shown in Fig. 4-7.

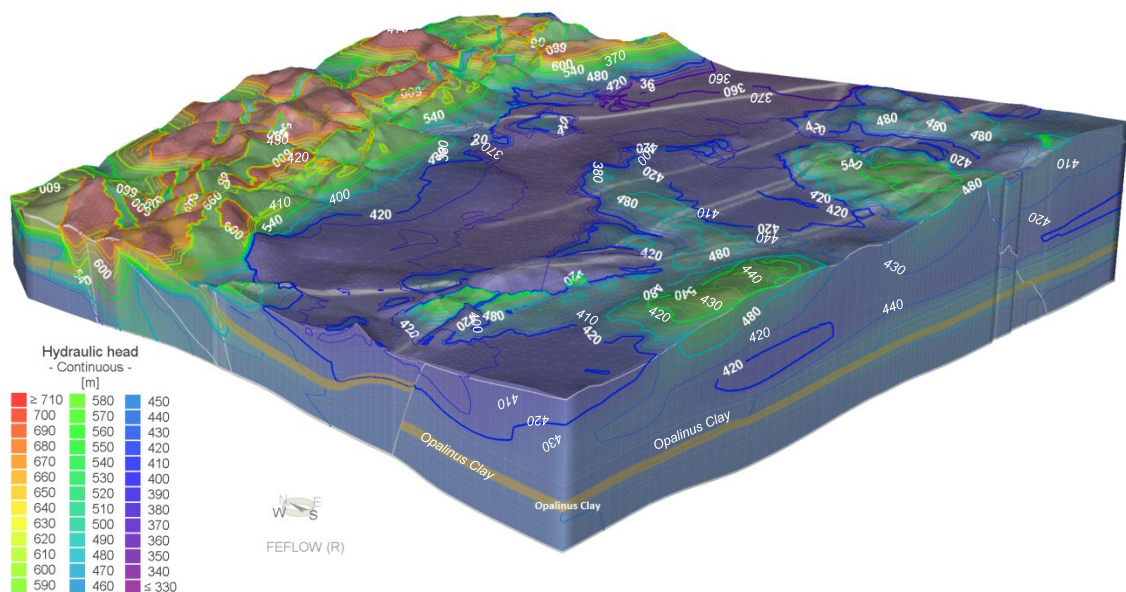


Fig. 4-4: Base case C1 - Overall 3D View of the simulated groundwater flow system. The Opalinus Clay is indicated by brown colors, 2x vertical exaggeration.

The *Malm aquifer* is a fractured or karst aquifer system. It mainly occurs south of the Jura Thrusts and has a number of outcrops in the Aare valley, notably below the Quaternary gravels in the Niederamt. Disregarding the small patches at the northern model boundary, simulated groundwater potential distributions of the Malm aquifer varies between 440 und 360 masl (Fig. 4-5a). Groundwater in the aquifer flows from the southern and northern areas towards the Aare valley. Due to the outcrop situation along the Jura Thrusts, the hydraulic head directly reflects the local topography where topographic high points also show the highest hydraulic heads while topographic low points (Aare valley) also have the lowest hydraulic heads.

The unit RD2 (*Hauptrogenstein*) also occurs as a fractured or karst aquifer system with an average thickness of ~100 m in the model domain. The simulated groundwater head close to the Jura Thrusts ranges between 670 to 420 masl. Groundwater in the aquifer generally flows from the north-west towards the south. Because of the vertical offset along the western part of the

Trimbach Olten Fault, the flow pattern looks discontinuous. The northern part of the aquifer (at the northern model boundary) is hydraulically decoupled from the southern part due the thick Anhydritgruppe cropping out along the Jura Thrusts (Fig. 4-5b). As in the Malm aquifer, the hydraulic heads are controlled by the local topography.

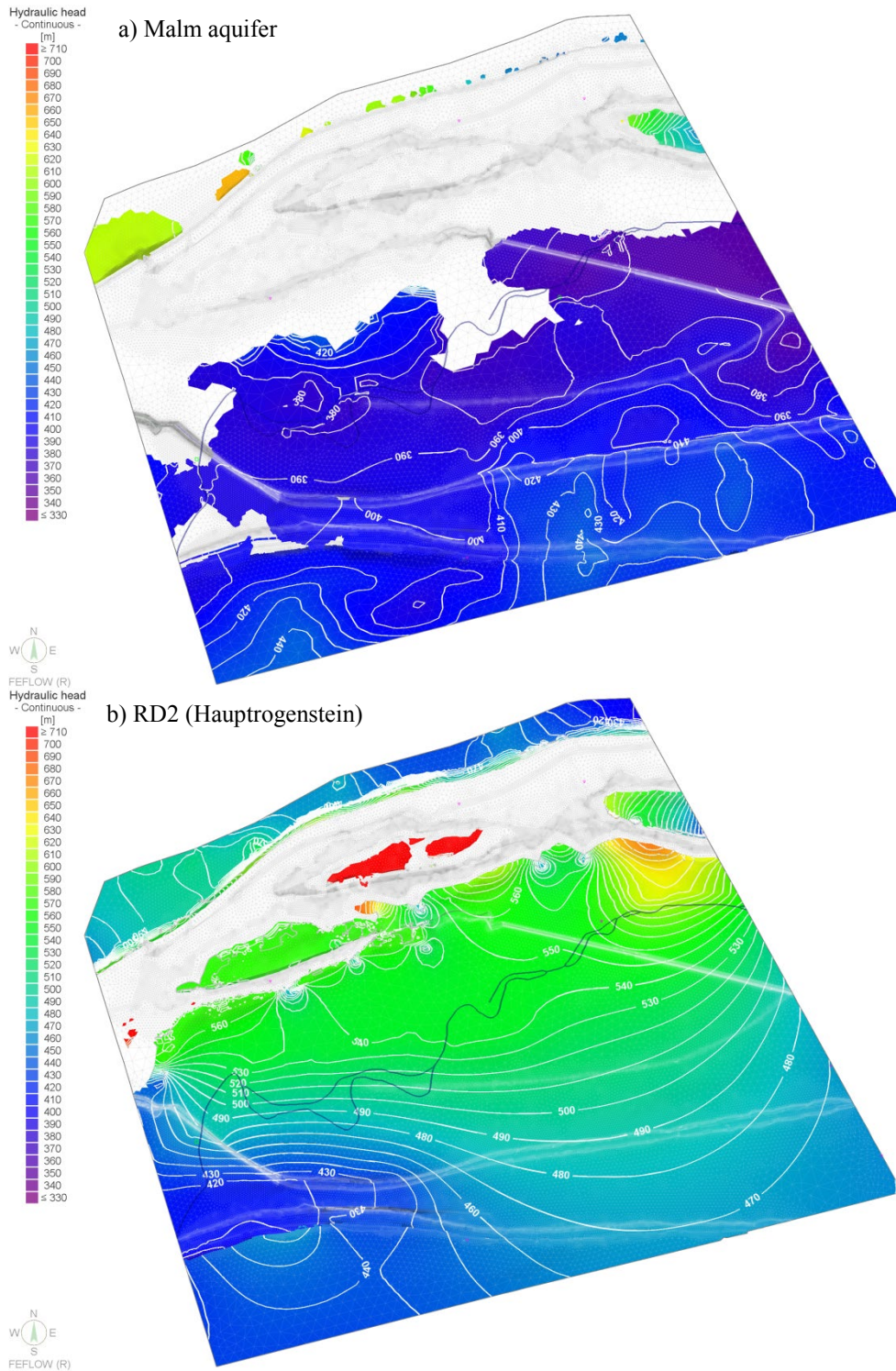


Fig. 4-5: Base case C1 – Simulated head fields along aquifers above the Opalinus Clay.

The ***Keuper aquifer*** is modelled as an aquifer system of 25 m thickness occurring below the Opalinus Clay (Fig. 4-6a). Simulated hydraulic heads of the Keuper aquifer vary between > 700 and 440 masl. Groundwater (in the southern block) in the aquifer generally flows from the north-west (along the Jura Thrusts) towards the south. Maximum hydraulic heads were again simulated according to the topographic high points along the Jura Thrusts (with the highest heads located along the Salhöhe in the centre of the Jura Thrusts).

The ***Muschelkalk aquifer*** is a significant regional fractured or karst aquifer located below the Keuper aquifer (Fig. 4-6b). Between the two aquifers, the lower conductive Gipskeuper acts as an aquitard. The simulated distribution of hydraulic heads in the Muschelkalk aquifer vary between 560 und 410 masl and groundwater generally flows from the western parts of the Jura Thrusts towards the lateral borders of the model exhibiting only a slightly different flow pattern as the Keuper aquifer.

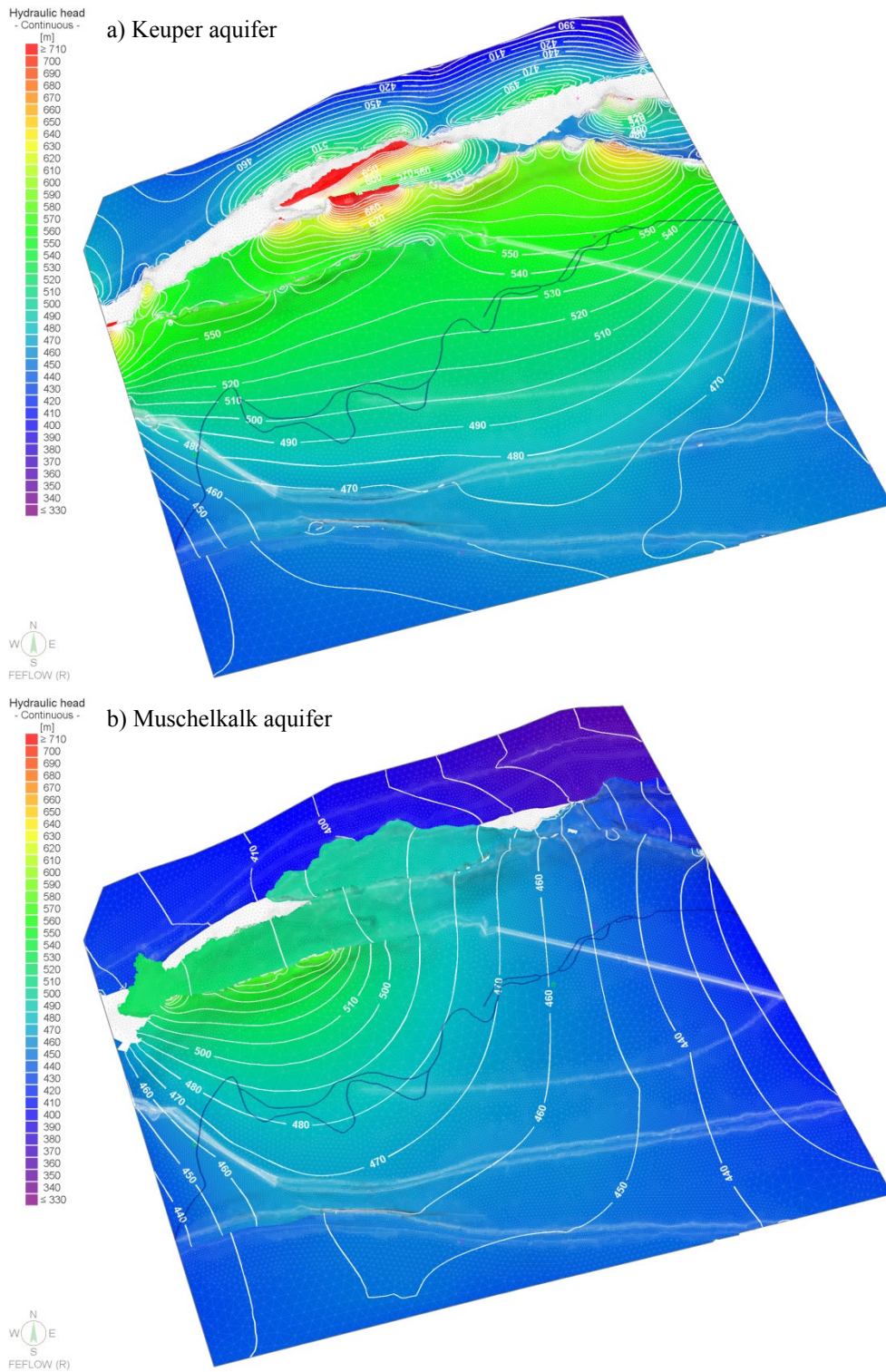


Fig. 4-6: Base case C1 – Simulated head field along aquifers below the Opalinus Clay.

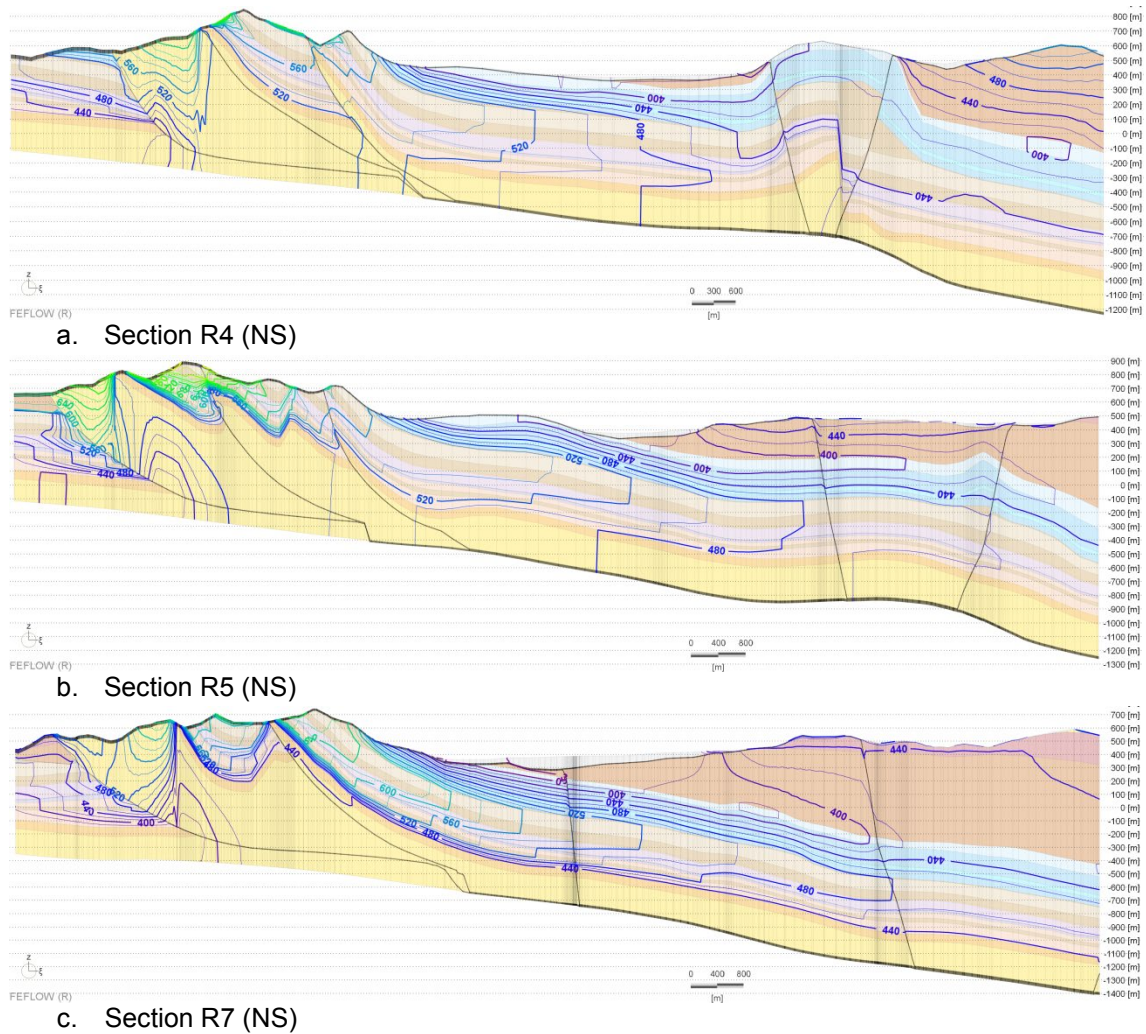


Fig. 4-7: Base case C1 – Simulated head field along vertical sections (location see. Fig. 4-3). 2x vertical exaggeration.

To assess vertical flow through the Opalinus Clay, head differences across the Opalinus Clay were evaluated as shown in Fig. 4-8 (gradients for all simulations are also given in appendix A). Regions with positive gradients indicate that hydraulic heads in the aquifer above the Opalinus Clay are higher than those in the aquifer below the Opalinus Clay, implying downward directed groundwater flow, regions with negative gradients represent upward directed groundwater flow. The complex pattern of fault planes and the vertical offsets along these planes also causes a complicated distribution of gradients within the model domain. Flow direction within the siting region is mainly directed downwards while at the western boundary (of the siting region), flow is directed upwards.

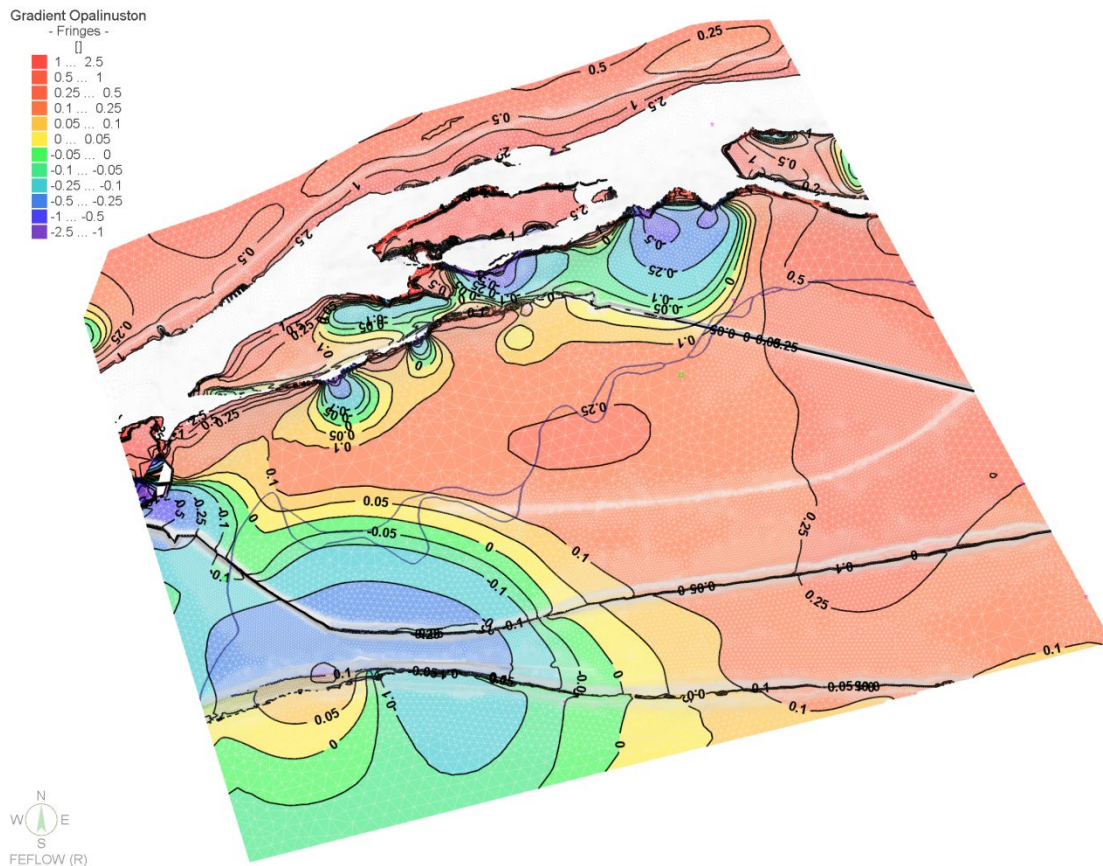


Fig. 4-8: Base case C1 – Vertical gradients in the Opalinus Clay.

4.2.2 Recharge and discharge paths

In order to assess discharge paths of groundwater from the Malm aquifer and Muschelkalk aquifer particle tracking has been carried out. The particles were started from given points in the aquifers considered. While tracking along the direction of flow (i.e. forward tracking) the paths run to discharge points when reaching a model boundary. Tracking in the opposite direction (i.e. backward tracking) the particles follow the recharge paths until a model boundary is reached indicating where groundwater originates from. Fig. 4-9 and Fig. 4-10 show the used starting points in the area of the model domain Jura-Südfuss. The starting points are always located at the shown xy-position, their vertical position is adjusted so that the points lie in the center of the aquifer. Starting points for the Hauptrogenstein aquifer have been distributed accordingly (but are not explicitly shown in Fig. 4-9 or 4-10).

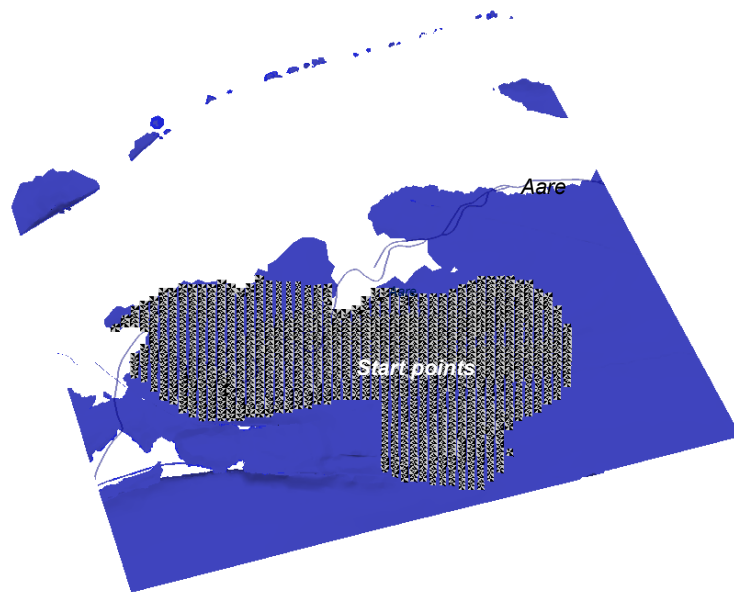


Fig. 4-9: Location of starting points for the path line computations in the Malm aquifer.

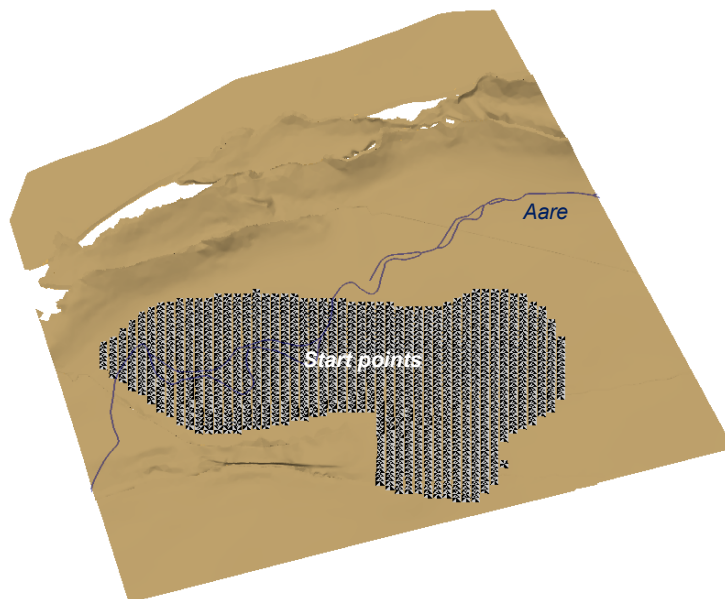


Fig. 4-10: Location of starting points for the path line computations in the Muschelkalk aquifer.

Fig. 4-11 shows calculated discharge paths (forward tracking) starting in the Malm aquifer as well as recharge paths obtained by backward tracking. The resulting path lines show that discharge areas of the Malm aquifer are mainly located in the Aare valley, mainly in the area of Niederamt and Wildegg. Some minor discharge areas are also located in the Suhre valley while other discharge path lines leave the model domain to the east. Several recharge areas can be identified within the model domain. Some recharge occurs close to the Jura Thrusts in the area of Lostorf (along the Dottenberg and Gugen) where path lines indicate recharge into the Quaternary flowing into the Malm aquifer. Additional recharge is indicated in the area around

the Engelberg (southeast of Olten) and at the Gönert (south of Aarau). The latter is caused by path lines crossing the overlying Molasse sediments.

Fig. 4-12 show calculated recharge and discharge areas for the Hauptrogenstein aquifer. Recharge areas are located in outcrops along the Jura Thrusts while discharge mainly occurs outside of the model domain. Most path lines leave the model towards the south and west. Only one notable (but small) discharge area is located within the model domain located just north of Lostorf.

The forward path lines starting in the Muschelkalk aquifer (Fig. 4-13) show that recharge occurs at the outcrops of the Muschelkalk aquifer in the northern model area just north of the Dottenberg and Gugen (north of Lostorf) while discharge occurs outside of the model domain towards the east, west and south. The regional model simulated the main discharge in the area of Birmenstorf in the Reuss valley and in the area of Aarburg just outside of the model domain in the west.

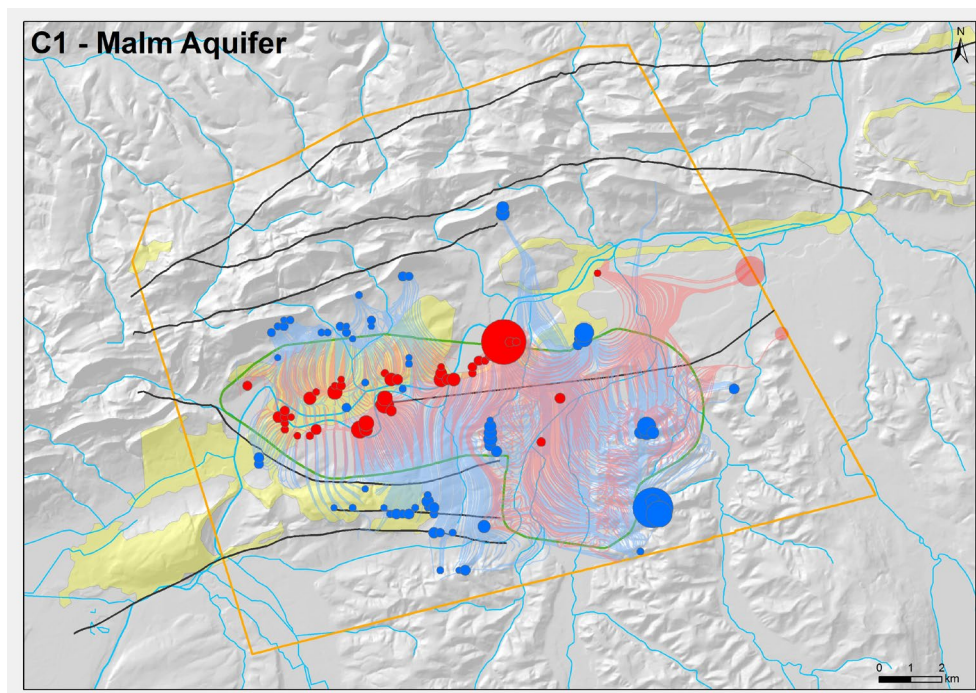


Fig. 4-11: Base case C1 – Calculated path lines starting in the Malm aquifer. (Blue: recharge path; red: discharge paths, green polygon depicts the siting region, strong colors indicate pathlines reaching the top of the model, pale colors indicate pathlines leaving the model along the lateral boundaries).

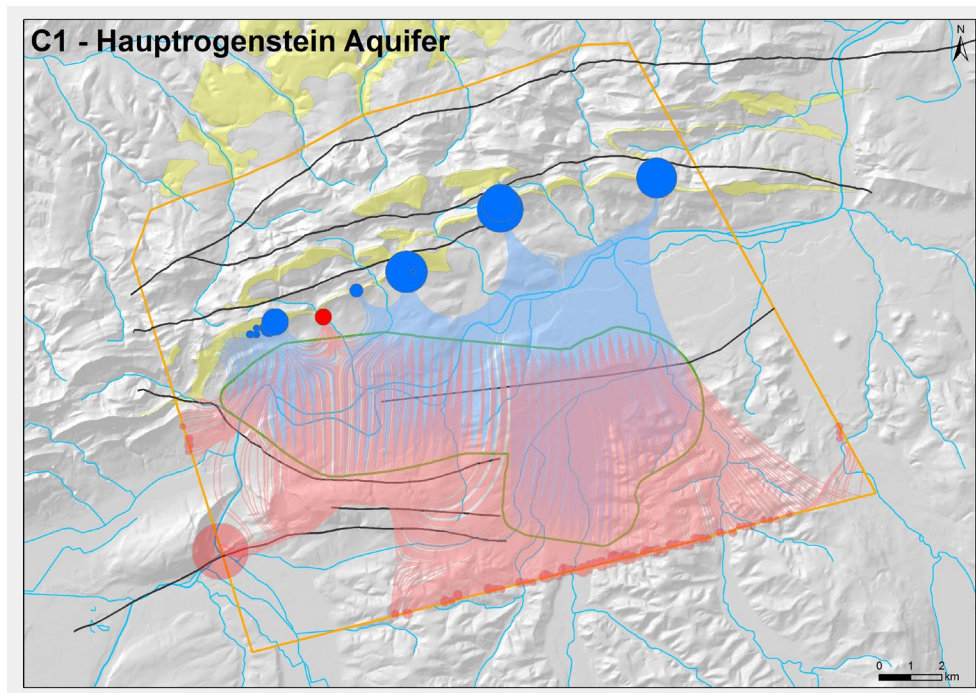


Fig. 4-12: Base case C1 – Calculated path lines starting from the Hauptrogenstein aquifer. (Blue: recharge path; red: discharge paths, green polygon depicts the siting region, strong colors indicate pathlines reaching the top of the model, pale colors indicate pathlines leaving the model along the lateral boundaries).

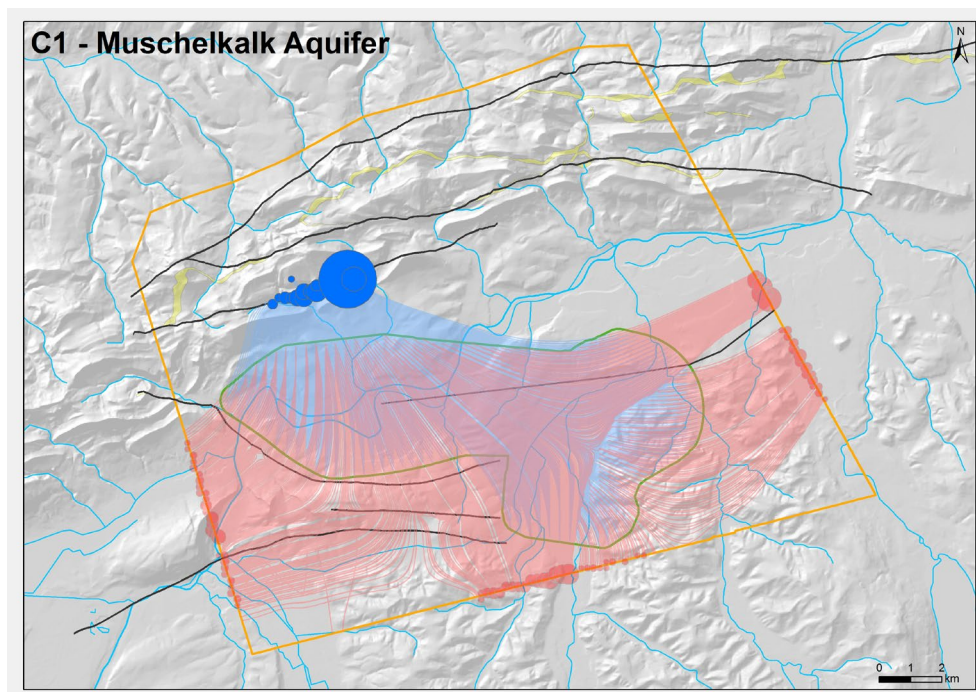


Fig. 4-13: Base case C1 – Calculated path lines starting from the Muschelkalk aquifer. (Blue: recharge path; red: discharge paths, green polygon depicts the siting region, strong colors indicate pathlines reaching the top of the model, pale colors indicate pathlines leaving the model along the lateral boundaries).

4.2.3 Sensitivity Runs

The sensitivity runs performed based on base case C1 refer to the hypotheses that the two layers RD4 (Sissach Member) and Arietenkalk (see Chapter 3.3) located above and below the Opalinus Clay are considered to be more conductive (i.e. water conducting layers).

C1-RD4

In case **C1-RD4**, the conductivity of unit RD4 (Sissach Member) was increased by 3 orders of magnitude (Table 4-1). At recharge areas in outcrops of the Sissach Member, an increase of hydraulic heads has been simulated but these increased hydraulic heads do not propagate far into the model domain. The rest of the model domain only shows small changes of hydraulic heads (see Fig. 4-14 and 4-15), the overall flow field is not significantly changed.

C1-AKA

In case **C1-AKA**, the conductivity of the Arietenkalk was increased by 4 orders of magnitude, i.e. from 1×10^{-12} m/s to 1×10^{-8} m/s (Table 4-1). The increased conductivity leads to higher hydraulic heads along outcrops close to the Jura Thrusts (mainly in the area north of the Dottenberg) where calculated heads are up to 200m higher than in the base case (where the Arietenkalk is treated as an aquitard) (Fig. 4-16 and Fig. 4-17). These increased hydraulic heads also lead to a change of the vertical hydraulic gradients with the flow direction being reversed in the western part of the siting region (see appendix A).

Both sensitivity cases show that an increased drainage locally increases the simulated hydraulic heads but do not show a significant influence on the flow field of the other aquifers in the model. The increased hydraulic heads do not propagate far into the model domain but diminish quickly and hence only cause locally increased heads (usually in the recharge areas). In discharge areas, the enhanced drainage due to the higher conductivity leads to a decrease of hydraulic heads.

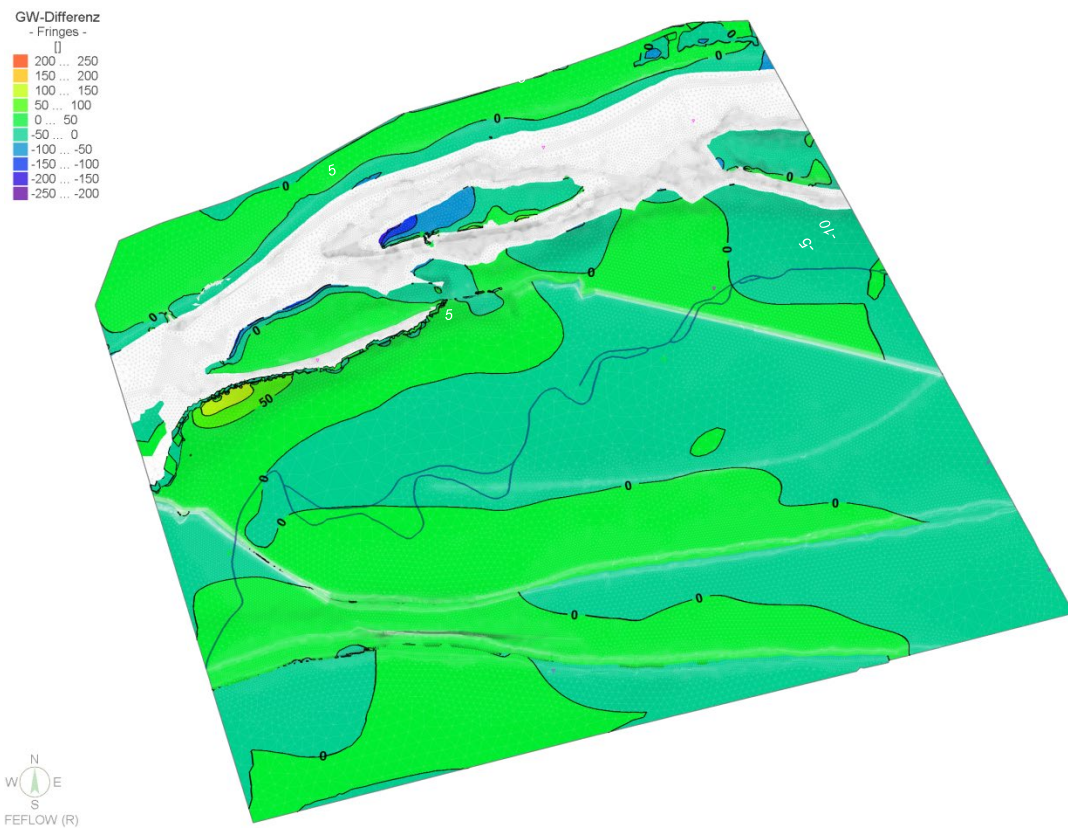


Fig. 4-14: Sensitivity case C1-RD4 – Simulated head differences in RD4 (Sissach Member) compared to base case C1.

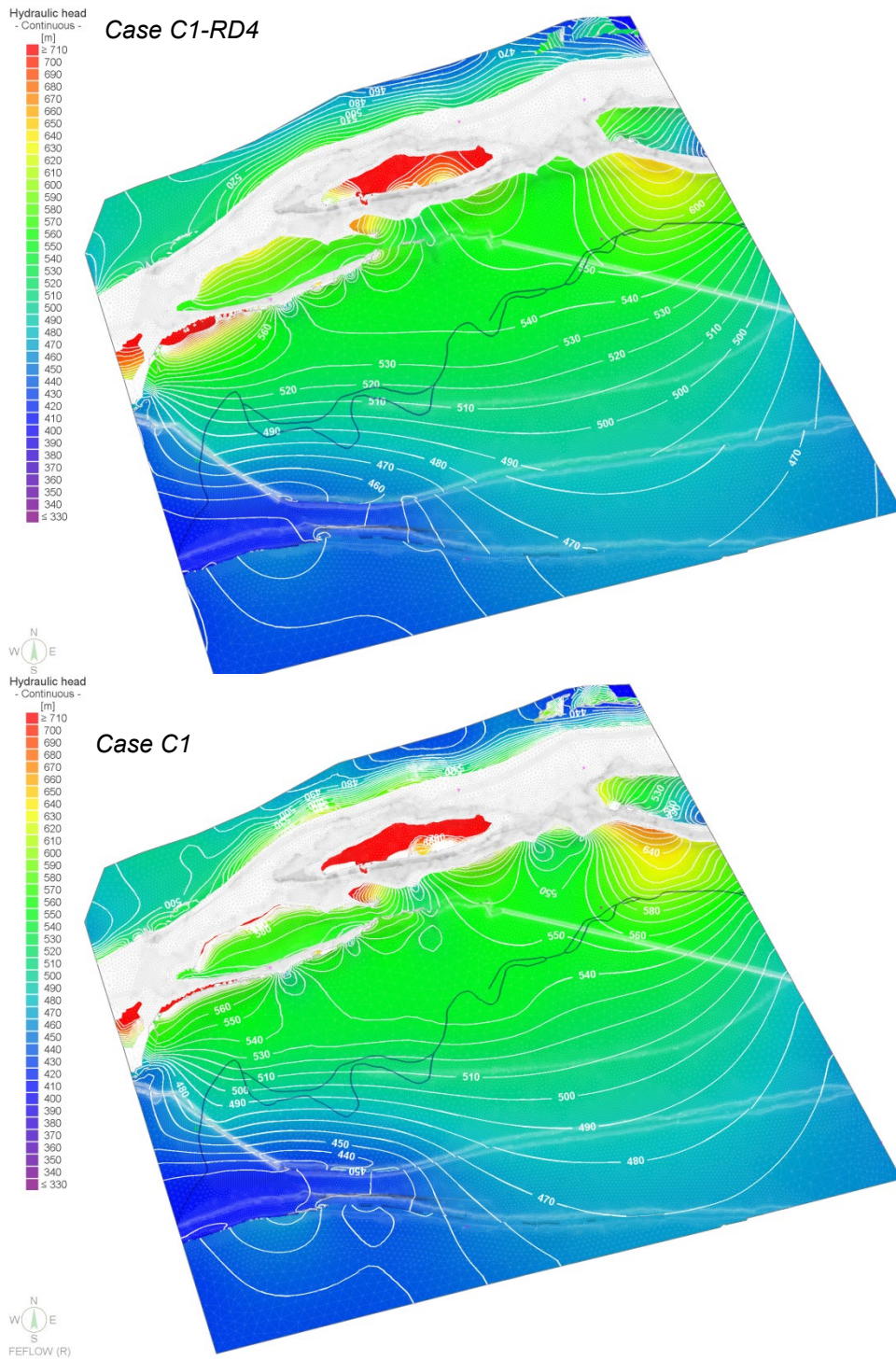


Fig. 4-15: Sensitivity case C1-RD4– Simulated head field in RD4 (Sissach Member) compared to base case C1.

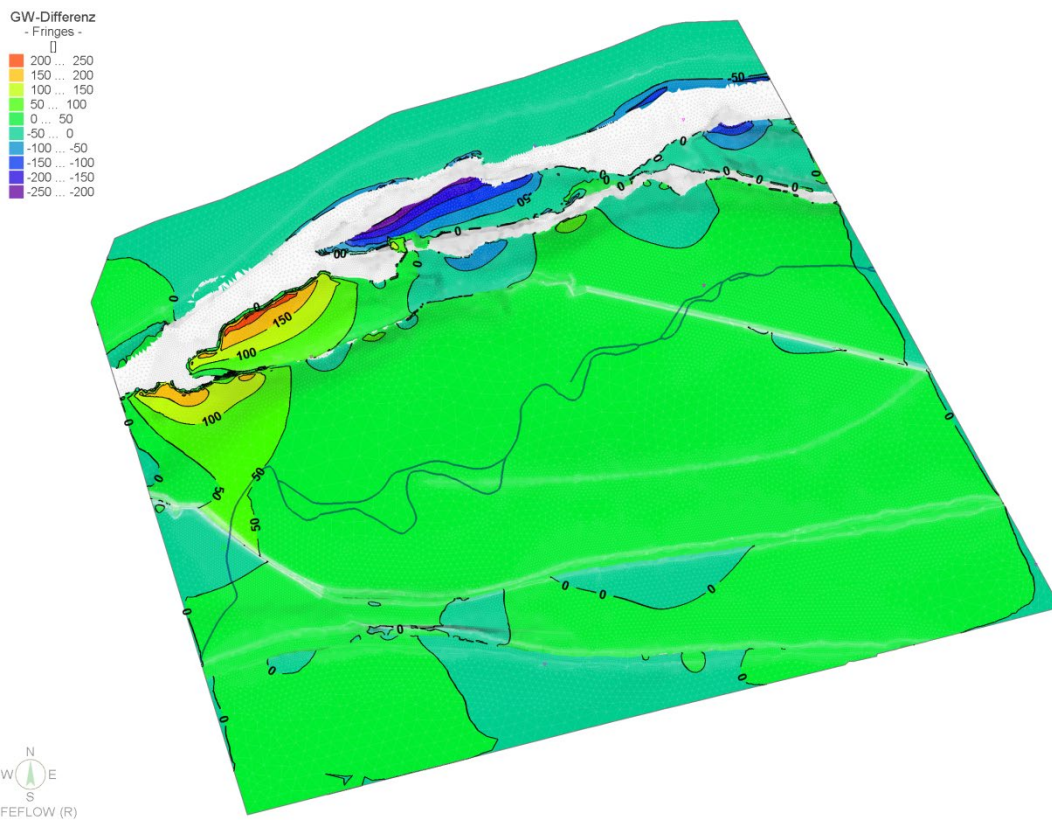


Fig. 4-16: Sensitivity case C1-AKA – Simulated head differences in the Arietenkalk compared to the base case C1.

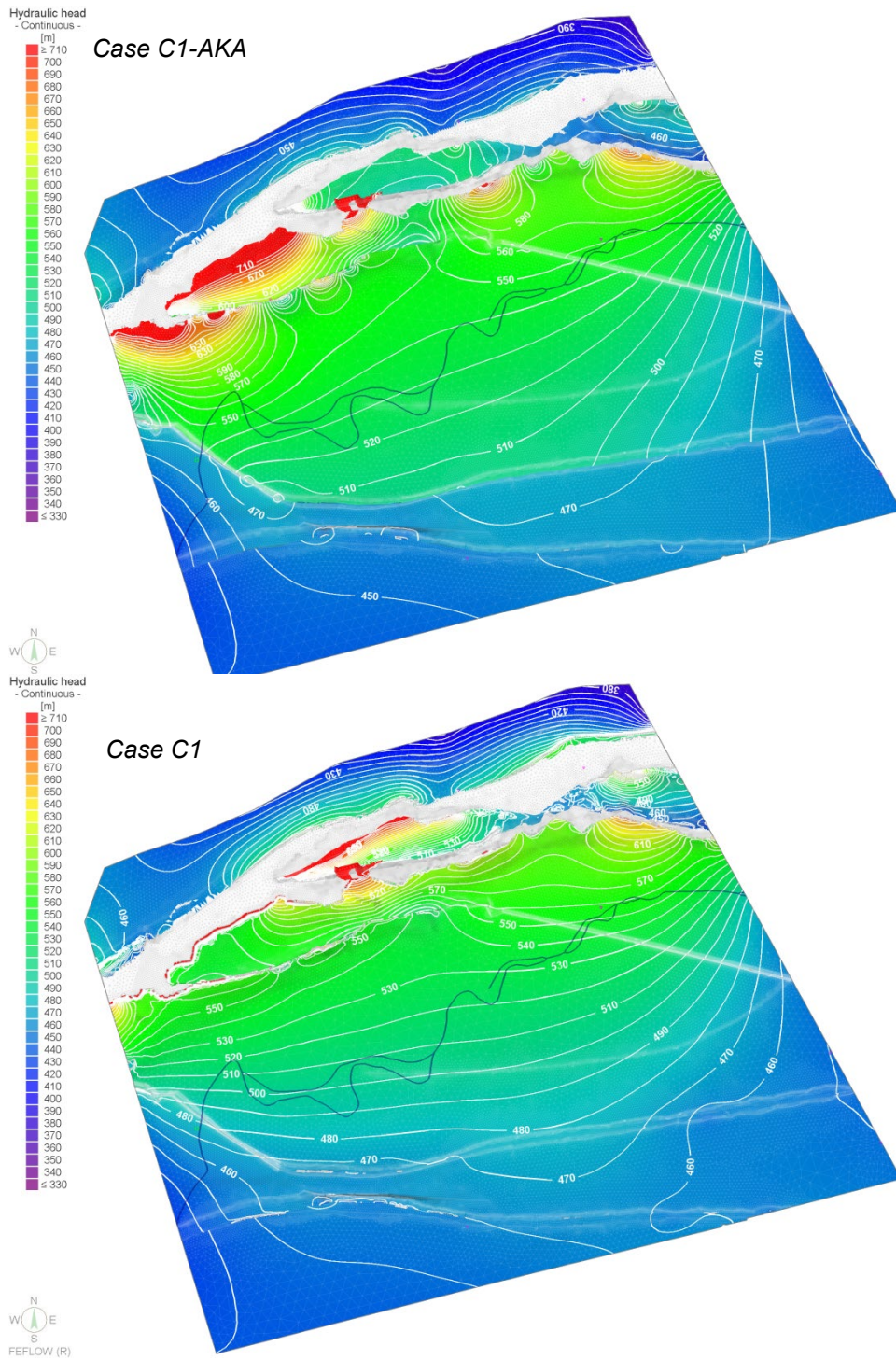


Fig. 4-17: Sensitivity case C1-AKA – Simulated head field in the Arietenkalk compared to the base case C1.

4.3 Base case C2 ("sealing faults")

4.3.1 Hydraulic heads

Run C2 refers to a best guess parameter set and the boundary conditions described in Chapter 3.3 and 3.4, assuming that the faults are of very low conductivity (hypothesis "sealing fault", s. Chapter 4.1). The computed flow fields are shown in Fig. 4-18 and Fig. 4-19. Vertical sections through the flow system are shown in Fig. 4-20.

It can generally be observed that simulated head distributions in the aquifers are discontinuous across the regional faults because of their prescribed hydraulic barrier effect.

Simulated hydraulic heads in the *Malm aquifer* vary between 370 and 440 masl (Fig. 4-18a). Again disregarding the patches along the northern model boundary, groundwater in the Malm aquifer flows from the northern parts towards the Aare valley indicating large discontinuities along the impermeable fault planes. The Eppenberg Flexure and the Born-Engelberg Anticline in the centre and south of the model domain effectively channel the flow towards the east. The Eppenberg Flexure shields the potential discharge areas north of it from the areas south of it so that in the area of Schafisheim, a hydraulic depression develops (though this might also be caused by the boundary conditions taken from the regional model).

The simulated head distribution in RD2 (*Hauptrogenstein*) shows a large discontinuity along the Eppenberg Flexure. The barrier effect of the fault results in head offsets of up to 70 meters along the fault. Groundwater at the northern side of the Eppenberg Flexure first roughly flows from east to west, following hydraulic head changes from 670 to 530 masl, and then to the east and north-east on the southern side of the impermeable Eppenberg Flexure (Fig. 4-18b). Close to the Jura Thrusts, local potential discharge areas occur in topographically low areas.

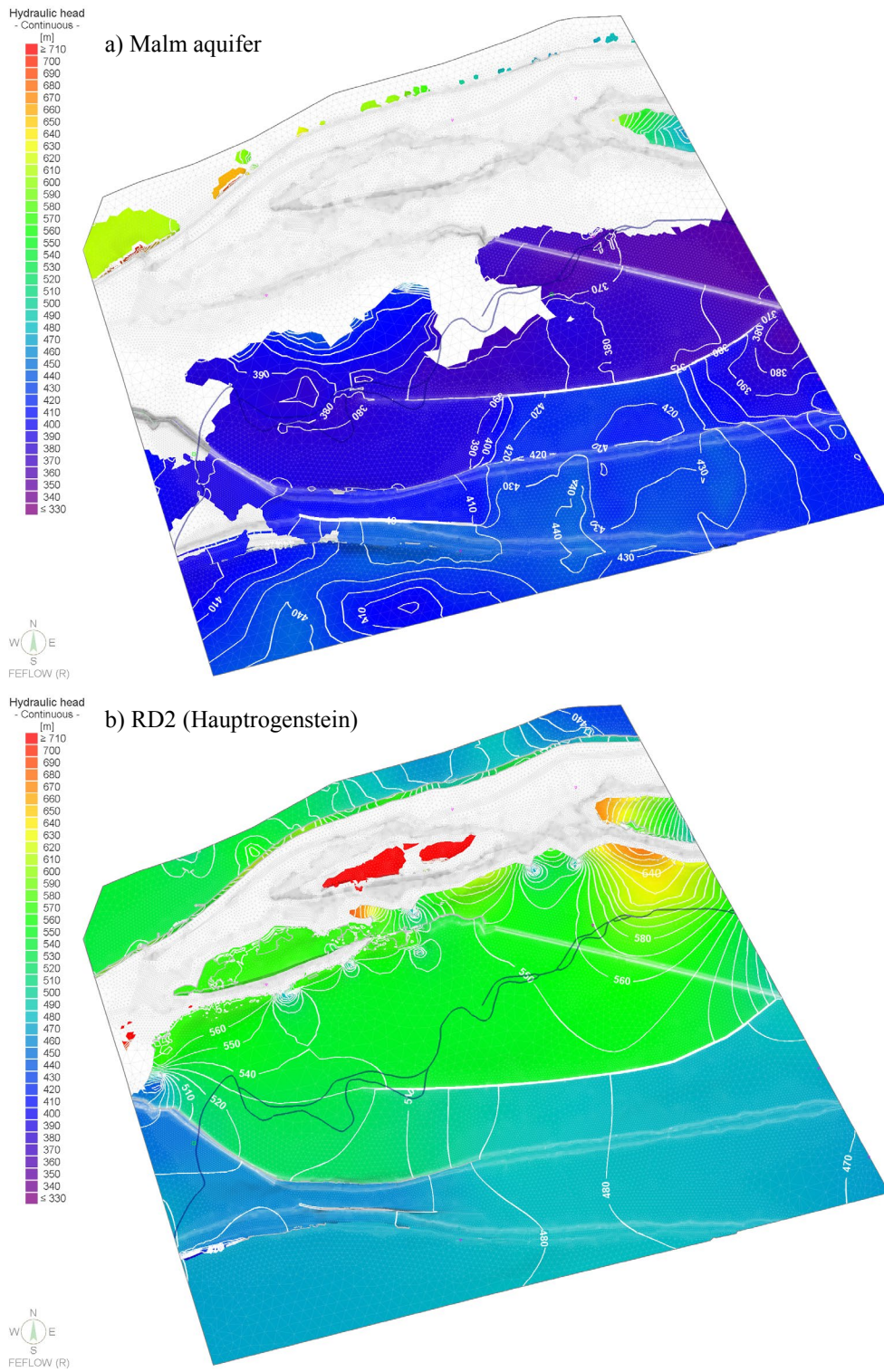


Fig. 4-18: Base case C2 – Simulated head field along aquifers above the Opalinus Clay.

The simulated head distribution in the *Keuper aquifer* of base case C2 shows that groundwater flows from topographically high areas close the Jura Thrusts towards the south and east, around the Eppenberg Flexure and then towards the east. The developing flow pattern is comparable to the flow pattern in the Hauptrogenstein aquifer though recharge areas are located more in the central part of the Jura Thrusts and, since they are topographically higher, the absolute values of the simulated hydraulic heads are also higher ($> 710\text{masl}$, see Fig. 4-19a). Again local minima of hydraulic heads occur at topographically low points close to the Jura Thrusts. At the western border in the area of Hauenstein, the high hydraulic heads are, at least in part, caused by the boundary conditions taken from the regional model.

In scenario C2, the simulated heads in the *Muschelkalk aquifer* vary between 570 and 510 masl. Groundwater flows from north-west mainly to the south-east indicating discharge areas outside of the model domain (Fig. 4-19b). Again, the Eppenberg Flexure channels the flow towards the eastern model boundary though offsets along the fault plane are small because the main recharge areas are located along the western part of the Jura Thrusts.

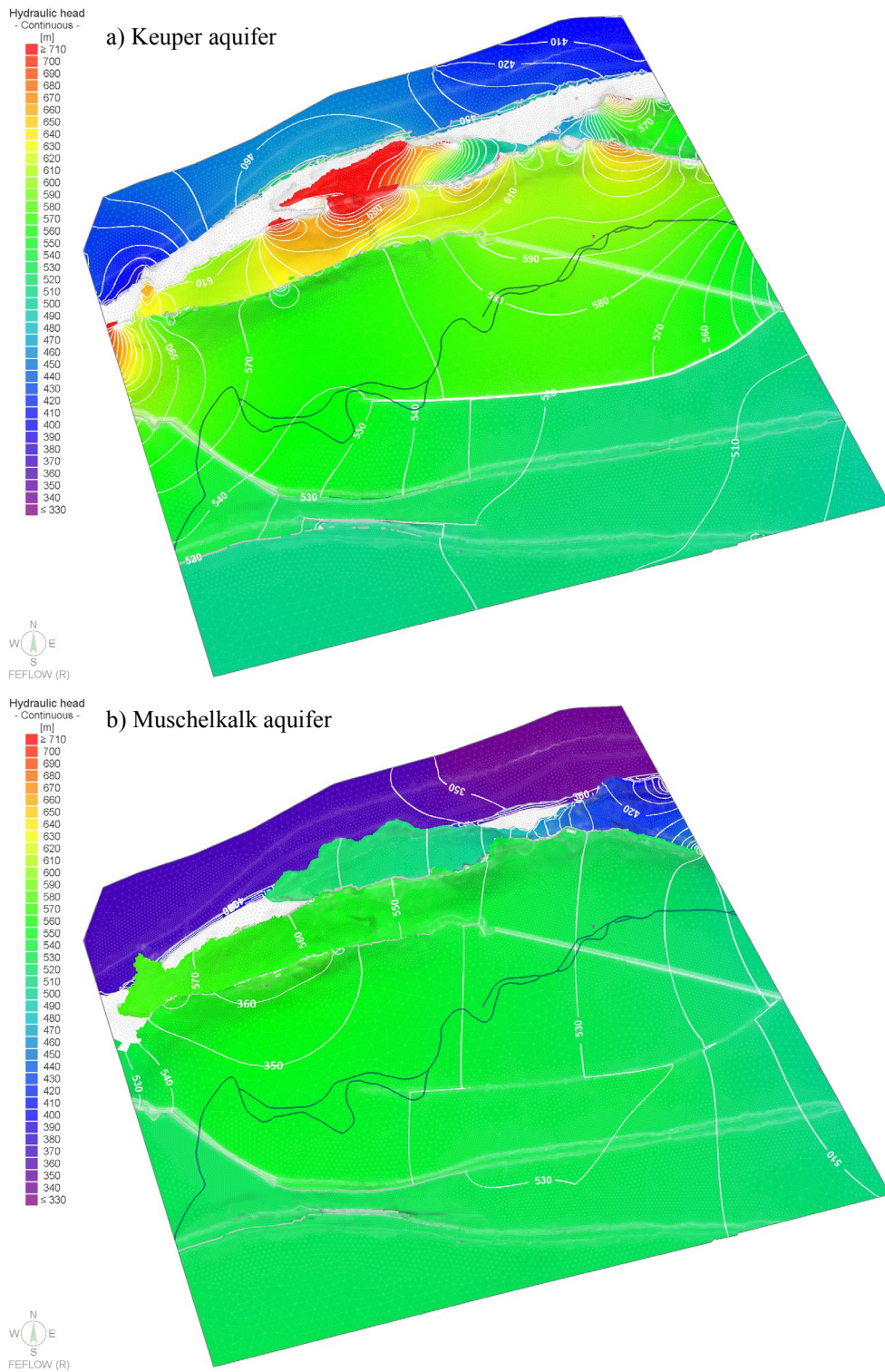


Fig. 4-19: Base case C2 – Simulated head field in aquifers below the Opalinus Clay.

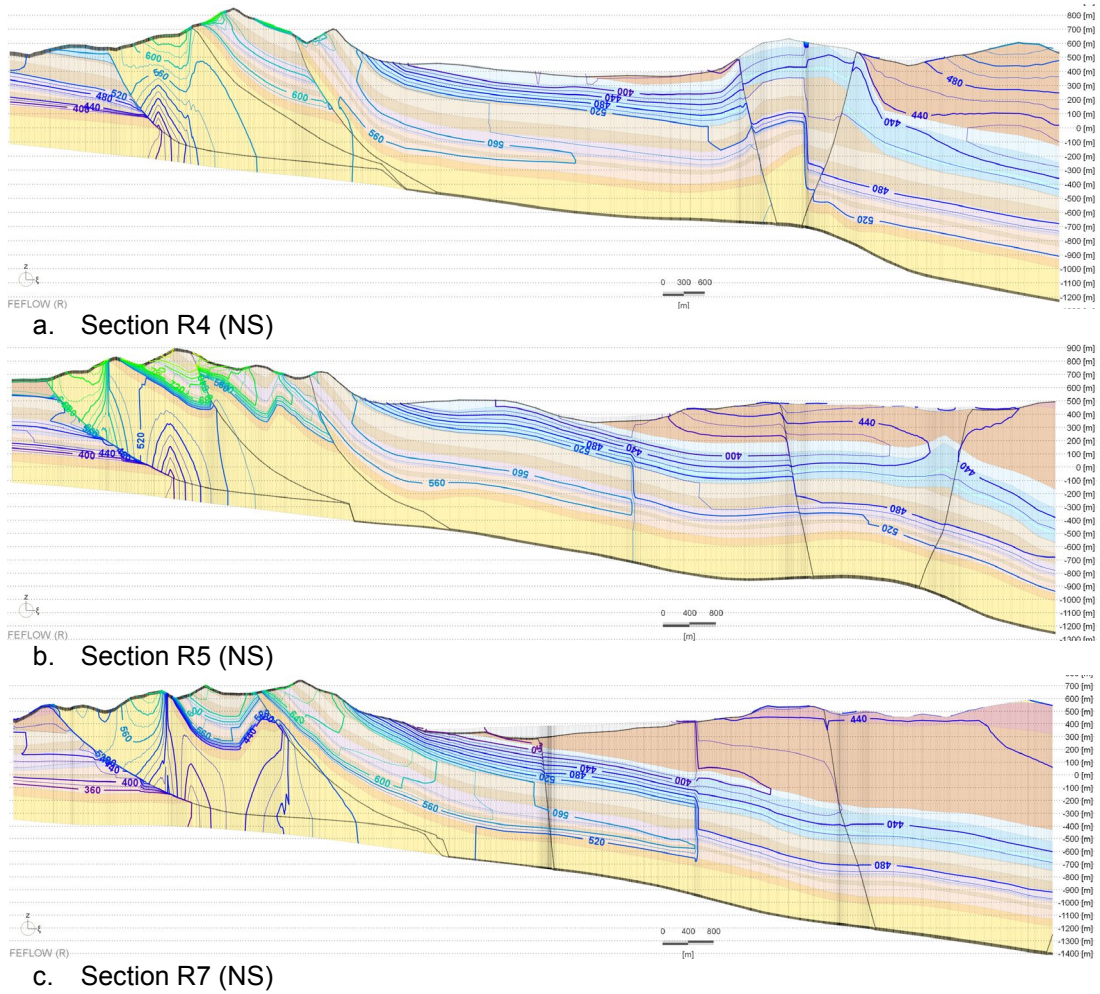


Fig. 4-20: Base case C2 – Simulated head field along vertical sections (location see Fig. 4-3). 2x vertical exaggeration.

Fig. 4-21 shows the vertical gradients within the siting region through the Opalinus Clay. Negative head differences throughout the siting region indicate mainly upward directed flow. Only at the outcrops close to the Jura Thrusts, large downward directed gradients (2.5) have been calculated (in areas of recharge).

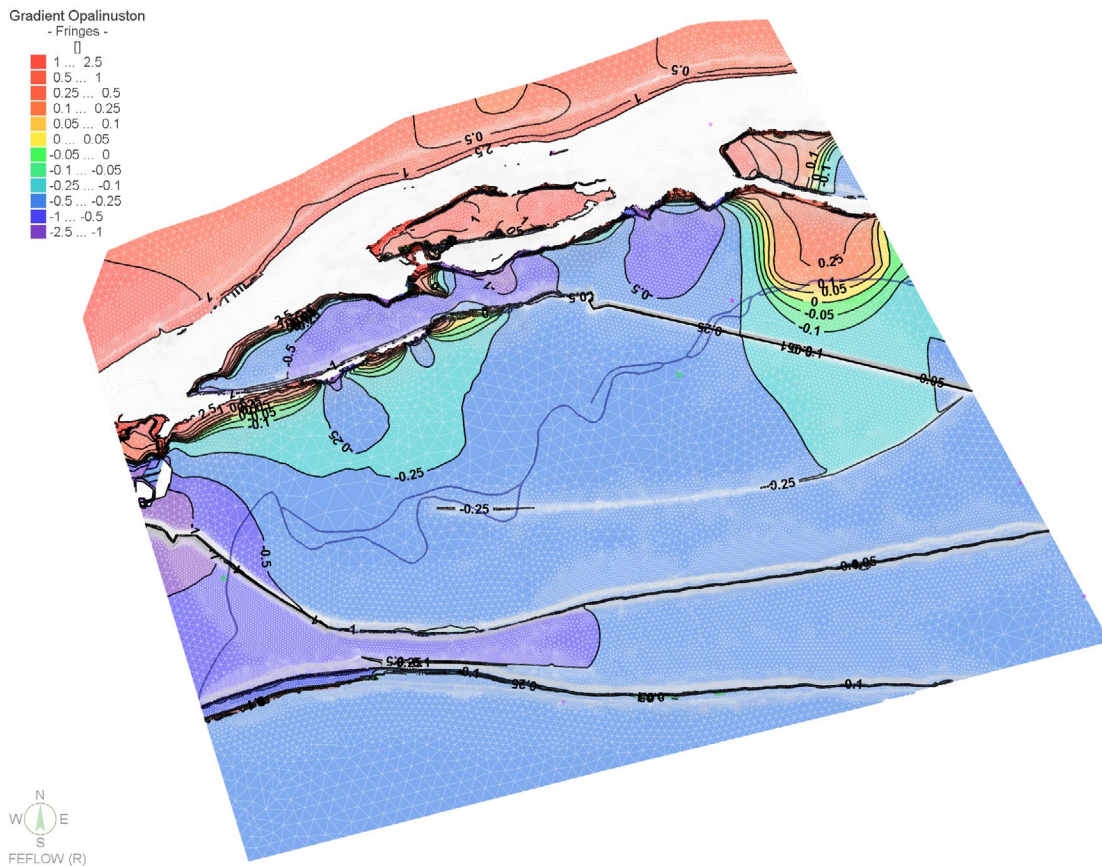


Fig. 4-21: Base case C2 – Vertical gradients in the Opalinus Clay.

4.3.2 Recharge and discharge paths

In order to assess discharge paths of groundwater from the Malm aquifer, Hauptrogenstein aquifer and Muschelkalk aquifer, particle tracking has been carried out. The particles were started from given points in the aquifers considered. While tracking along the direction of flow (i.e. forward tracking) the paths run to discharge points when reaching a model boundary. Tracking in the opposite direction (i.e. backward tracking) the particles follow the recharge paths until a model boundary is reached, indicating where groundwater originates from. Fig. 4-8 and Fig. 4-9 show the used starting points in the area of the siting region Jura-Südfuss.

Fig. 4-22 shows calculated discharge paths (forward tracking) starting from the Malm aquifer as well as recharge paths obtained by backward tracking. The resulting path lines show discharge areas of the Malm aquifer located in the Aare valley (Niederamt) and in the Suhre valley while some path lines leave the model domain at the eastern model boundary. Recharge paths mainly run from the northern hills (close to the Jura Thrusts, through the Quaternary) and the southern model area (in the vicinity of the Born-Engelberg Anticline, partly through the Molasse) towards the Aare valley. Another recharge area is located just south of Aarau.

Fig. 4-23 shows calculated discharge and recharge areas of the Hauptrogenstein aquifer. Recharge areas are mostly located close to the Jura Thrusts though some recharge is also indicated from outside of the model domain (south). Discharge areas within the siting region occur in the Aare valley, south of Lostorf and south of Aarau. Some discharge paths also leave the mode domain towards the east, west and south. Discharge within the siting region must occur through the overlying hydrogeological units (Malm aquifer and/or Molasse) as there are no outcrops of the Hauptrogenstein aquifer in this area. The main discharge areas (according to

the number of path lines reaching a model boundary) are again in the area of Niederamt, in the area just north of Lostorf and in the area of Trimbach (the latter being just outside of the model domain).

The path lines starting in the Muschelkalk aquifer (Fig. 4-24) show that groundwater in the aquifer flows from the north to the southern, western and eastern model boundaries, no discharge paths arrive at the model surface. The main discharge area of the Muschelkalk aquifer in the regional model has been calculated in the area of Laufenburg with path lines flowing around the Lägern in the east, flowing back north of the Lägern (through the siting region Jura Ost) towards the Rhine valley.

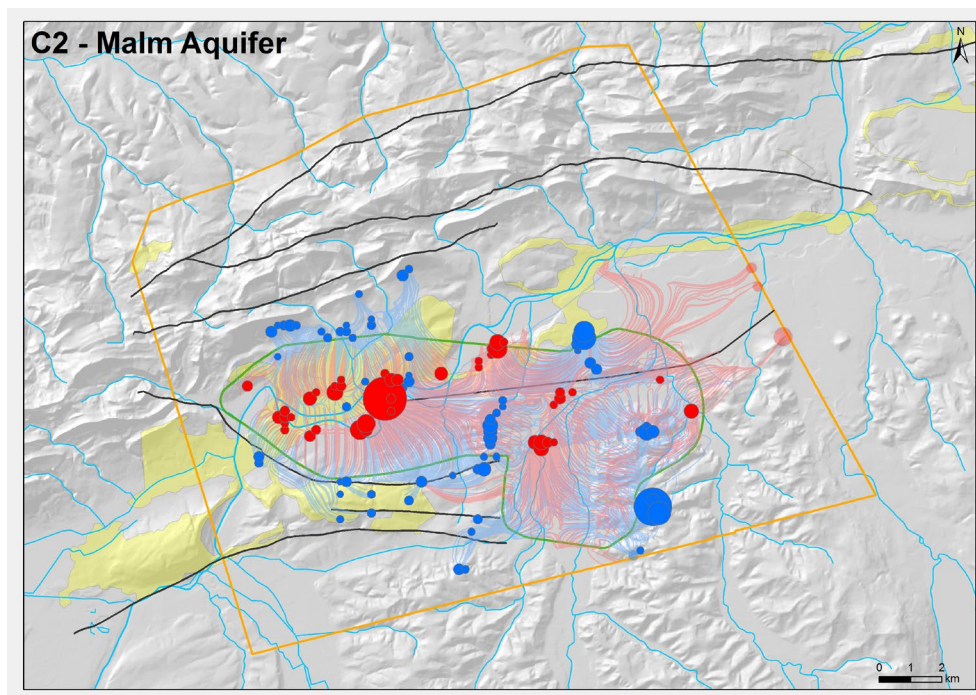


Fig. 4-22: Base case C2 – Calculated path lines starting in the Malm aquifer. (Blue: recharge path; red: discharge paths, green polygon depicts the siting region, strong colors indicate pathlines reaching the top of the model, pale colors indicate pathlines leaving the model along the lateral boundaries)

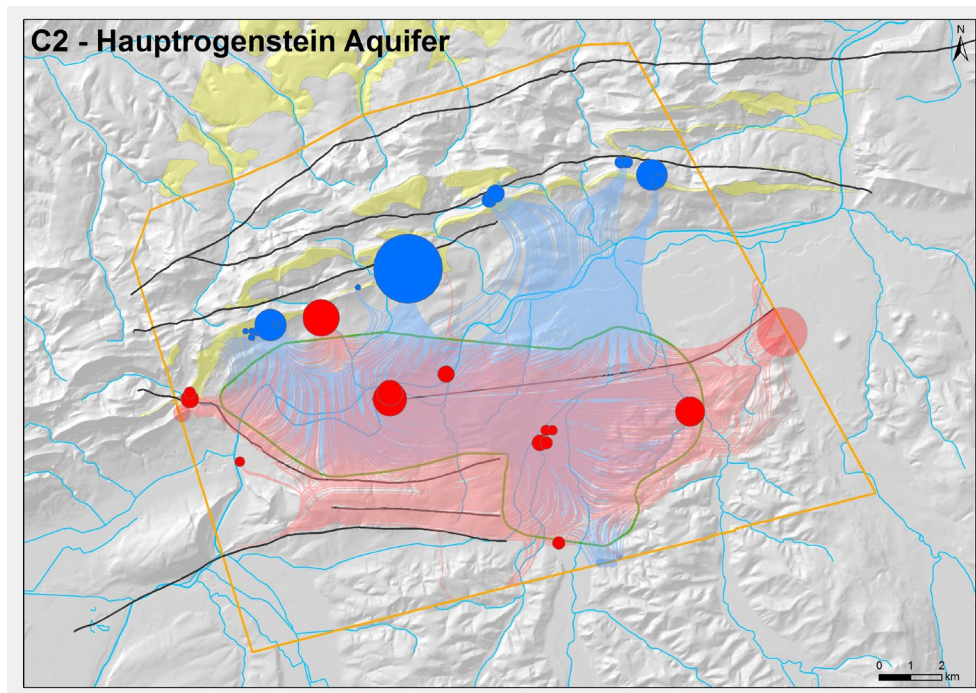


Fig. 4-23: Base case C2 – Calculated path lines starting from the Hauptrogenstein aquifer. (Blue: recharge path; red: discharge paths, green polygon depicts the siting region, strong colors indicate pathlines reaching the top of the model, pale colors indicate pathlines leaving the model along the lateral boundaries).

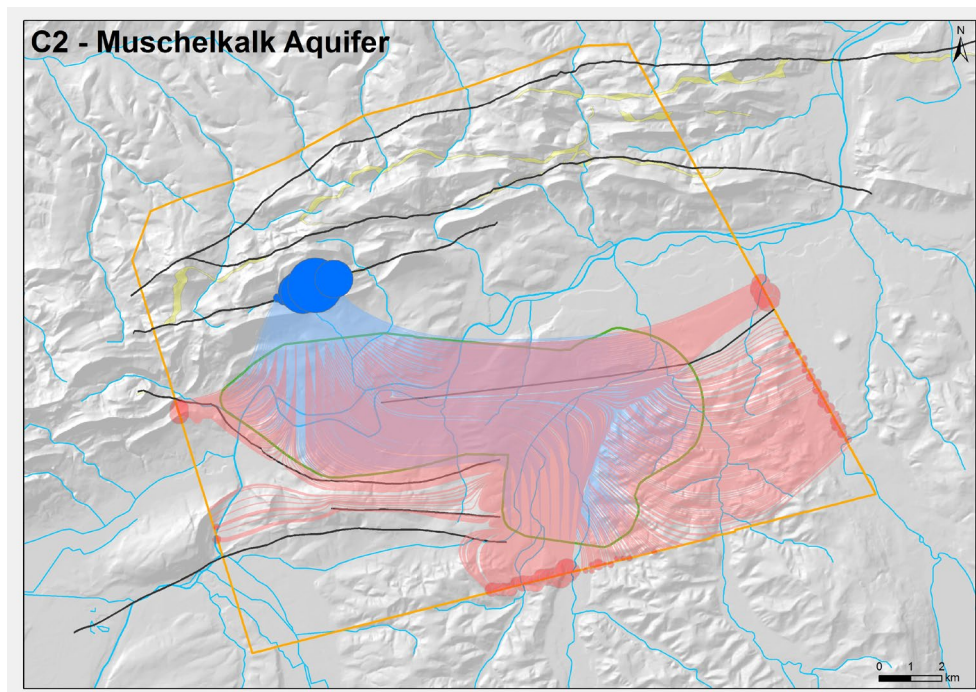


Fig. 4-24: Base case C2 – Calculated path lines starting from the Muschelkalk aquifer. (Blue: recharge path; red: discharge paths, green polygon depicts the siting region, strong colors indicate pathlines reaching the top of the model, pale colors indicate pathlines leaving the model along the lateral boundaries).

4.3.3 Sensitivity Runs

The sensitivity runs performed based on base case C2 refer to the hypotheses by which the two hydrogeological units RD4 (Sissach Member) and Arietenkalk (see Chapter 3.3) located below the Opalinus Clay are considered to be more conductive (i.e. water conducting layers).

C2-RD4

Comparable to case C1-RD4, increasing the conductivity of RD4 results in slightly higher hydraulic heads compared to the base case in areas of potential recharge (mainly close to the Jura Thrusts). The general flow direction still is comparable to the base case (though there the Sissach Member is treated as an aquitard). In potential discharge areas, the simulated hydraulic heads decrease due to the enhanced drainage (Fig. 4-25 and 4-26).

C2-AKA

In case **C2-AKA**, the conductivity of the Arietenkalk was increased by 4 orders of magnitude, i.e. from 1×10^{-12} m/s to 1×10^{-8} m/s (Table 4-1). The main recharge areas are located along topographically high areas towards the west of the Jura Thrusts while flow is mainly directed towards the east (Fig. 4-27 and Fig. 4-28). The increased heads however do not propagate far into the model domain. Where local discharge is possible, the higher heads are immediately relieved and hydraulic heads are lower than in the base case. The increased heads do modify the absolute values of the vertical gradient through the Opalinus Clay but do not generally change flow direction (which is still upwards) within the siting region.

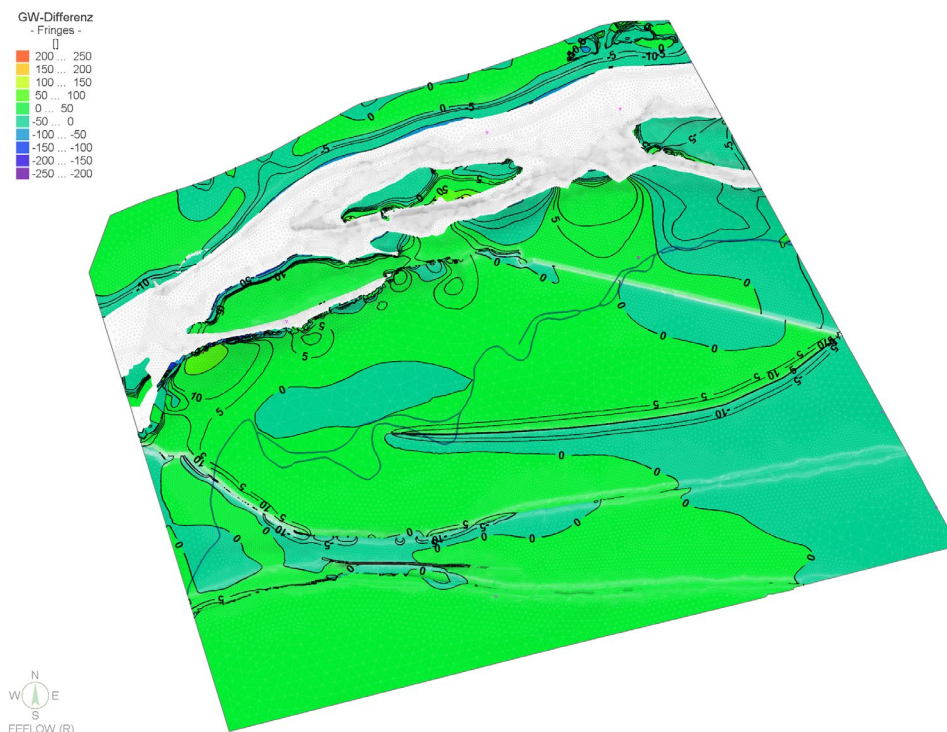


Fig. 4-25: Sensitivity case C2-RD4 – Simulated head field differences in RD4 (Sissach Member) compared to the base case C2.

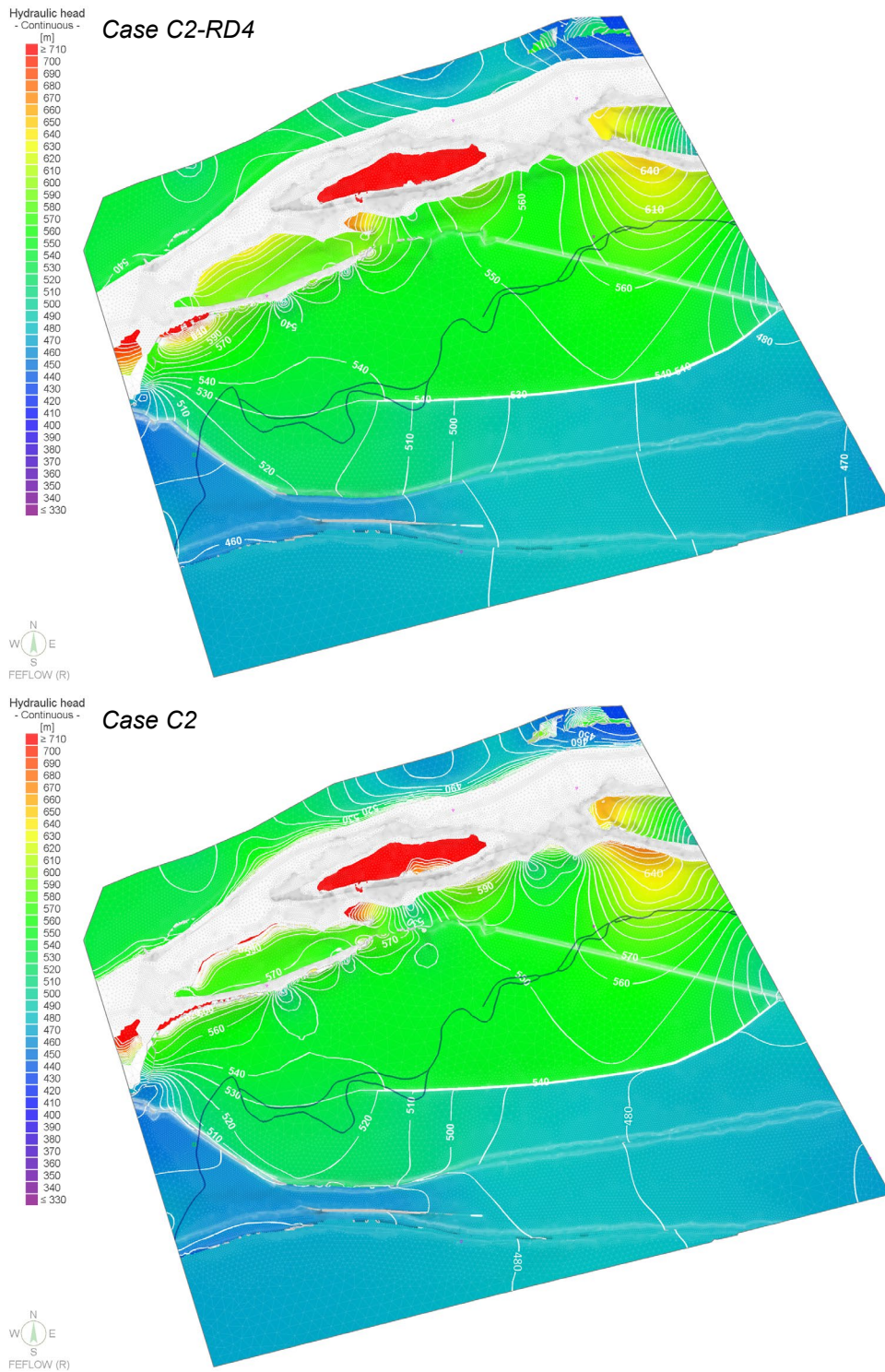


Fig. 4-26: Sensitivity case C2-RD4 – Simulated head field in RD4 (Sissach Member) compared to the base case C2.

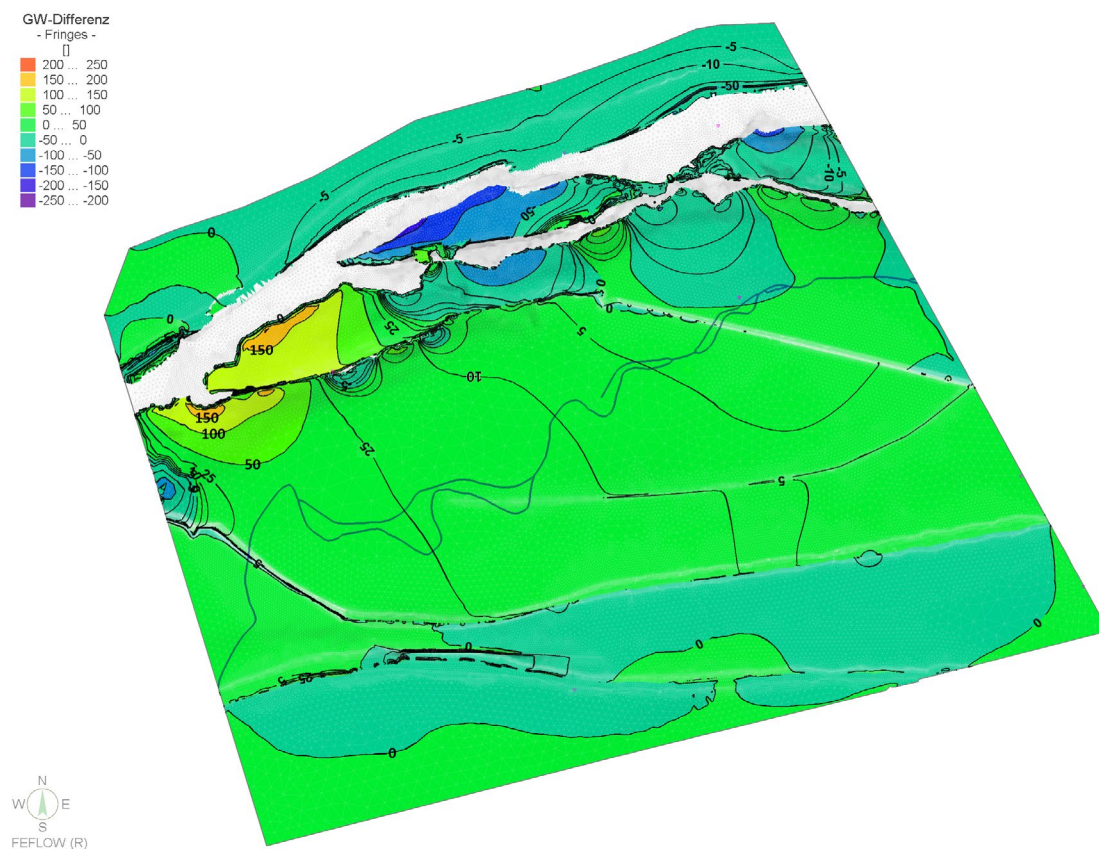


Fig. 4-27: Sensitivity case C2-AKA – Simulated head differences in the Arietenkalk compared to the base case C2.

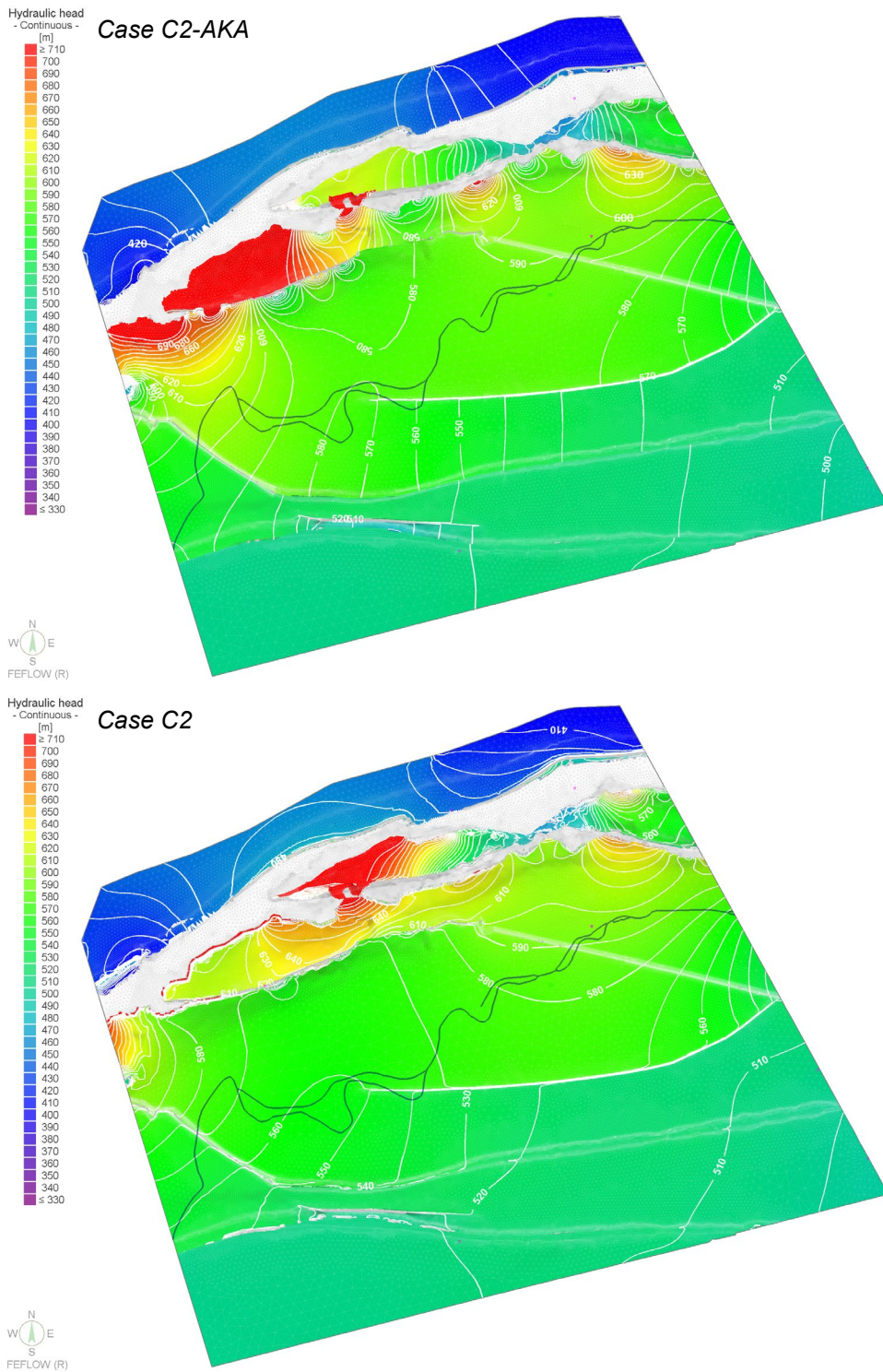


Fig. 4-28: Sensitivity case C2-ACA – Simulated head field in the Arietenkalk compared to the base case C2.

4.4 Base case C3 ("connecting faults")

4.4.1 Hydraulic heads

Run C3 refers to a best guess parameter set and the boundary conditions described in Chapter 3.3 and 3.4 under the hypothesis "connecting faults", meaning that groundwater flow across the faults is disabled. However, because flow along the faults is possible, water exchange between the layers of the multi-aquifer system can evolve. The computed flow fields are shown in Fig. 4-29 and Fig. 4-30. Vertical sections through flow system are shown in Fig. 4-31.

Simulated hydraulic heads in base case C3 in the *Malm aquifer* vary between 460 and 360 masl, indicating groundwater discharge into the Aare valley (Fig. 4-29a). Because vertical water exchange along the fault planes is allowed, a significant impact from the faults is observed, especially in the surroundings of the Eppenbergl Flexure. Since groundwater is able to flow along the fault plane, hydraulic pressure can be relieved resulting in slightly lower hydraulic heads than were simulated for the previous base cases.

The simulated head distribution in RD2 (*Hauptrogenstein*) ranges from 390 to above 700 masl (Fig. 4-29b). The hydraulic connections along the fault planes allow exchange and interaction between the different aquifers and generally lead to low hydraulic heads along the Eppenbergl Flexure. As a consequence, flow is generally directed towards the Eppenbergl Flexure.

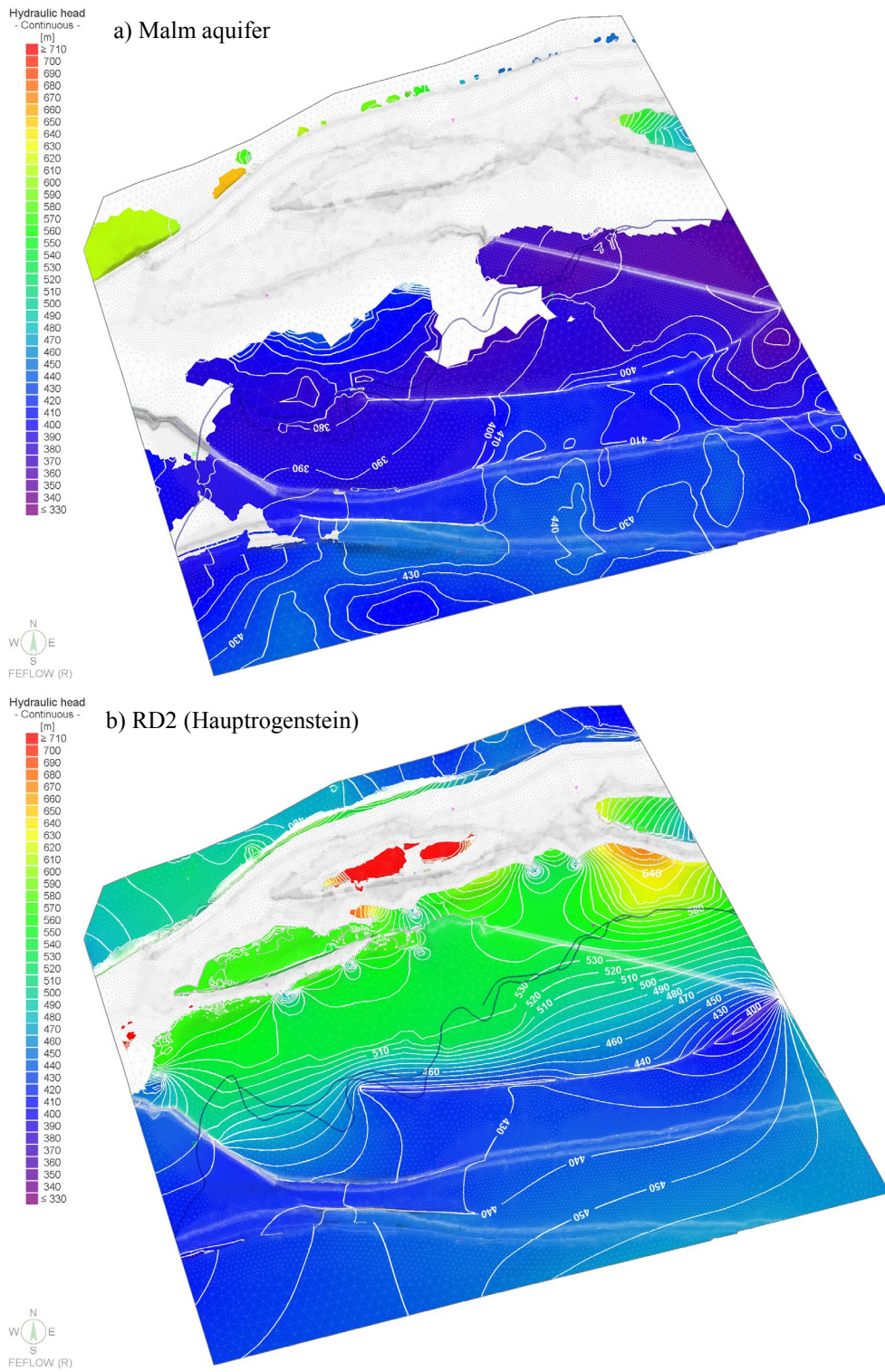


Fig. 4-29: Base case C3 – Simulated head field along aquifers above the Opalinus Clay.

The simulated flow pattern in the **Keuper aquifer** with heads ranging between >710 to 460 masl (Fig. 4-30a) looks similar to that of base case C2 (comp. Fig. 4-19a). Main differences occur in the surroundings of the faults. Due to the vertical flow along the fault planes, the simulated heads are lower than in base case C2. Comparable to flow directions in the Hauptrogenstein, flow is also directed towards the Eppenberg Flexure. Since the Eppenberg Flexure and the Born-Engelberg Anticline largely shield the southern part of the model domain from the simulated recharge areas close to the Jura Thrusts and upward directed flow along the fault planes is possible, simulated hydraulic heads on the southern side of the flexure are lower than on the northern side. Also, at the western model boundary, a hydraulic depression develops.

The simulated hydraulic heads in the **Muschelkalk aquifer** (Fig. 4-30b) vary between 570 and 390 masl. Its flow pattern is comparable to that of base case C2 although the simulated heads, due to the vertical flow along the fault planes, are lower. Again, the Eppenberg Flexure and the Born-Engelberg Anticline shield areas in the south from the recharge areas in the north. In addition, pressure can be relieved through the outer, permeable parts of the fault plane. This leads to a groundwater depression along the Eppenberg Flexure at the eastern model boundary. Low hydraulic heads also occur along the western and eastern model boundary close the Jura Thrusts which are caused by the boundary conditions taken from the regional model.

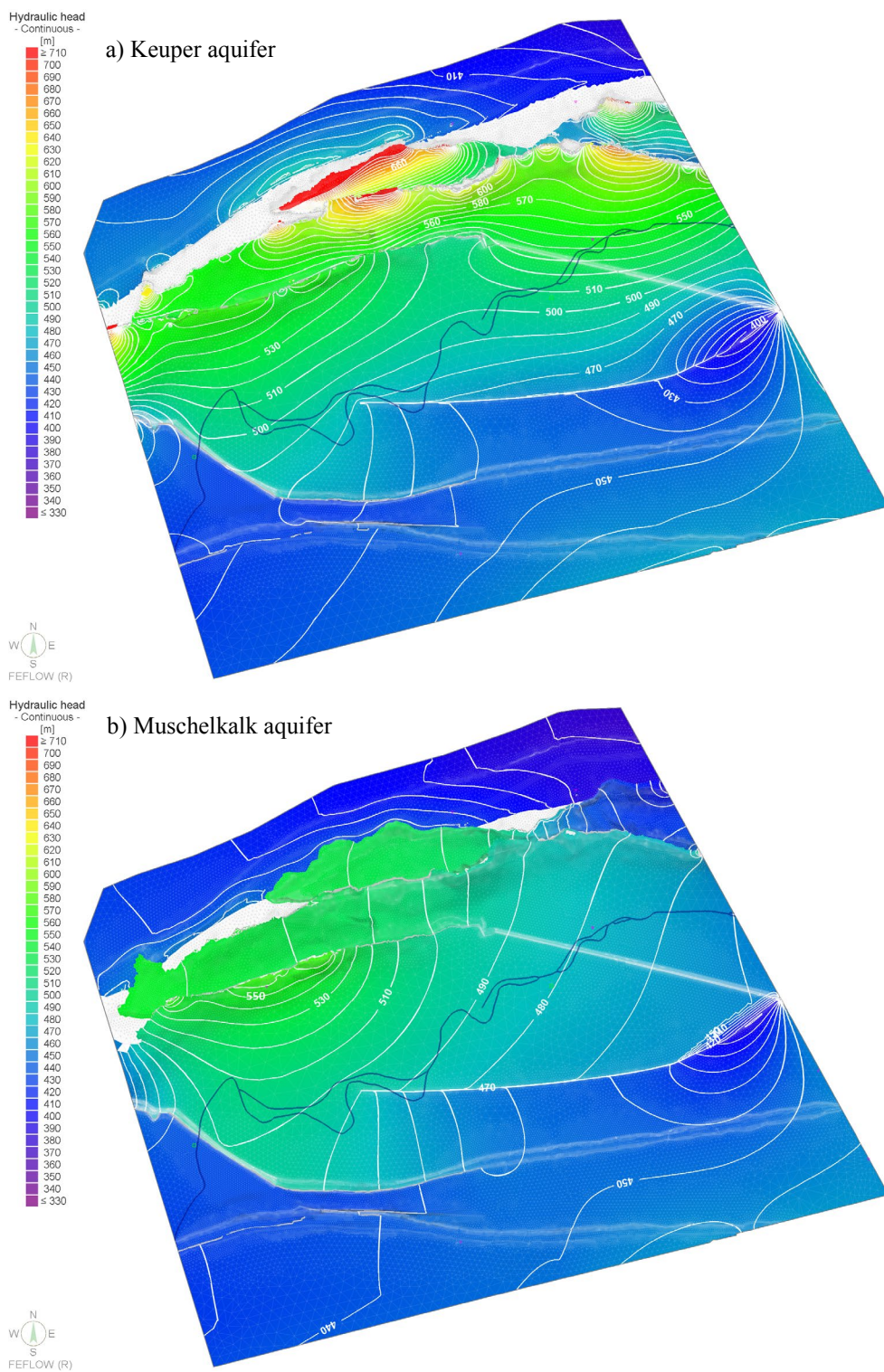


Fig. 4-30: Base case C3 – Simulated head field along aquifers below the Opalinus Clay.

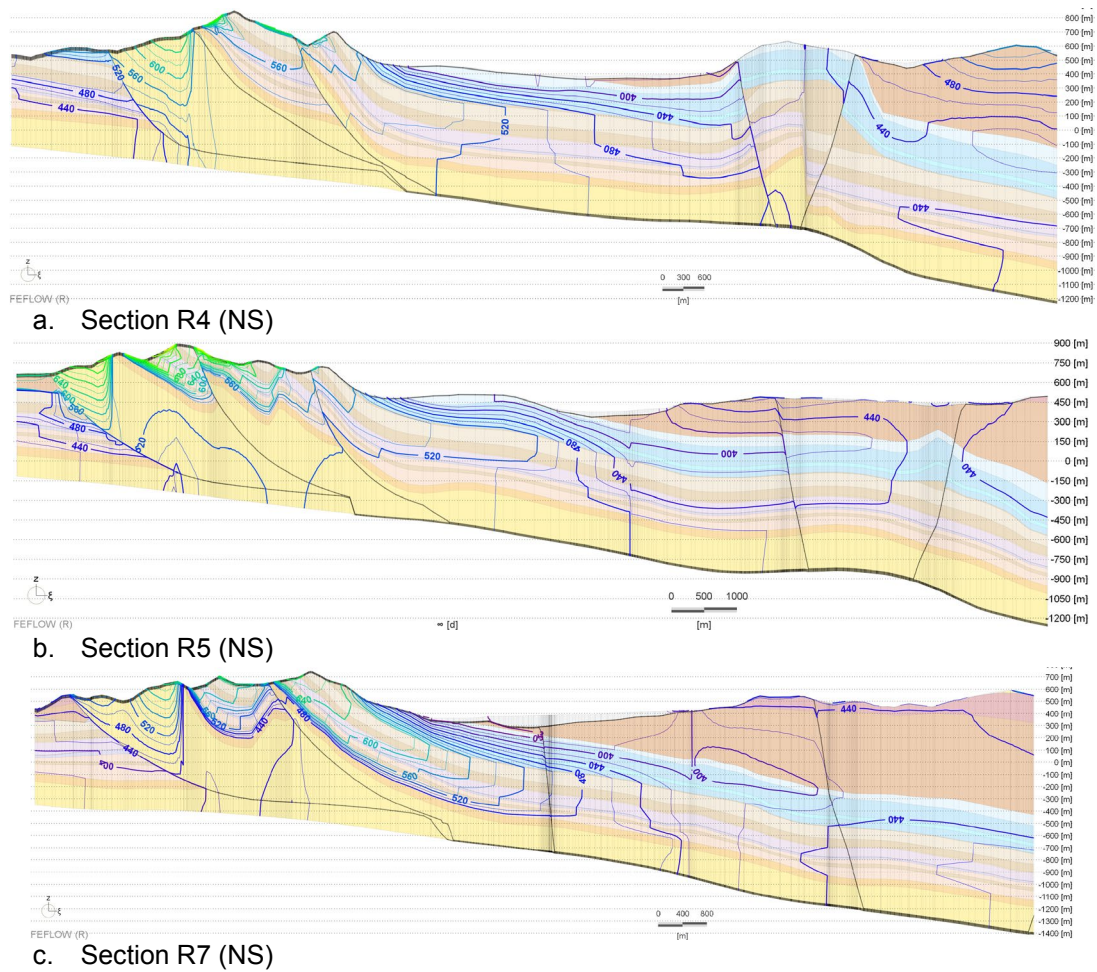


Fig. 4-31: Base case C3 – Simulated head field along vertical sections (location see Fig. 4-3). 2x vertical exaggeration.

Vertical gradients through the Opalinus Clay are shown in Fig. 4-32. Along topographically high points (recharge areas), vertical gradients are naturally directed downwards. This downward directed gradient changes towards upward directed gradients away from the recharge area with the highest (upward directed) vertical gradients close to the Eppenbergl Flexure.

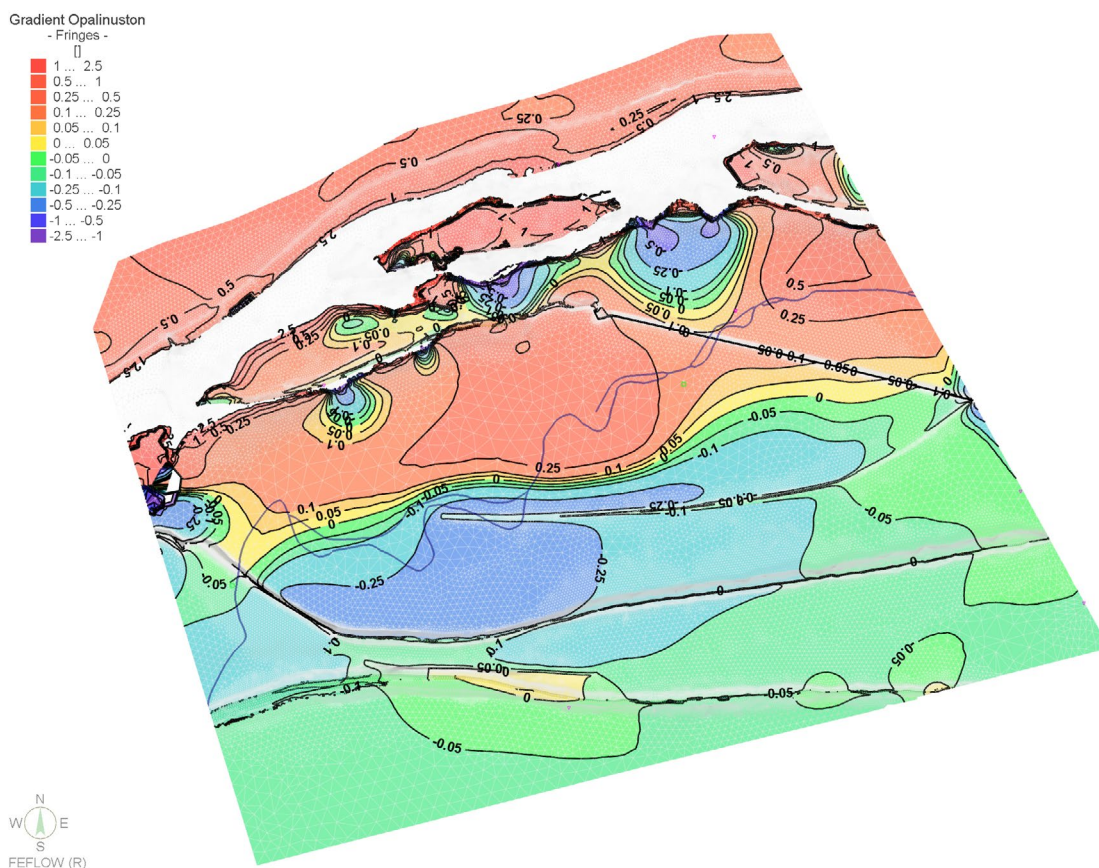


Fig. 4-32: Base case C3 – Evaluation of head differences in the Opalinus Clay.

4.4.2 Recharge and discharge paths

In order to assess discharge paths of groundwater from the Malm aquifer and Muschelkalk aquifer, particle tracking has been carried out. The particles were started from given points in the aquifers considered. While tracking along the direction of flow (i.e. forward tracking) the paths run to discharge points when reaching a model boundary. Tracking in the opposite direction (i.e. backward tracking) the particles follow the recharge paths until a model boundary is reached, indicating where groundwater originates. Fig. 4-8 and Fig. 4-9 show the used starting points in the area of the siting region Jura-Südfuss.

Fig. 4-33 shows calculated discharge paths (forward tracking) starting in the Malm aquifer as well as recharge paths obtained by backward tracking. The resulting path lines show that a large part of discharge traces of the Malm aquifer are located in, or close to, the Aare valley (Niederamt). Other discharge areas occur along the Eppenbergl Flexure (southern side, lower Suhretal) caused by the vertical flow along the fault plane. Only a few path lines leave the model domain at the eastern model boundary. Recharge paths mainly run from the outcrops close to the Jura Thrusts (between the Dottenberg and the Gugen, north of Lostorf, through the Quaternary), outcrops (or the Molasse) in the south along the Born-Engelberg Anticline and the southern model boundary towards the siting region.

Fig. 4-34 shows the simulated recharge and discharge paths in the Hauptrogenstein aquifer. While recharge areas are concentrated along topographically high points close to the Jura Thrusts, discharge areas are primarily located in the area of Niederamt and along the Eppenbergl Flexure. Minor discharge areas also occur just north of Lostorf and at the western and eastern model boundary.

The forward path lines starting in the Muschelkalk aquifer (Fig. 4-35) show that recharge areas are still located close to the Jura Thrusts while discharge within the model domain occurs along the Eppenbergr Flexure and in the Aare valley (Niederamt). Other discharge paths leave the model domain towards the west, south and east. The regional model here indicated discharge in the area of Aarburg (just outside the model domain) and in the area of Baden in the Limmat valley.

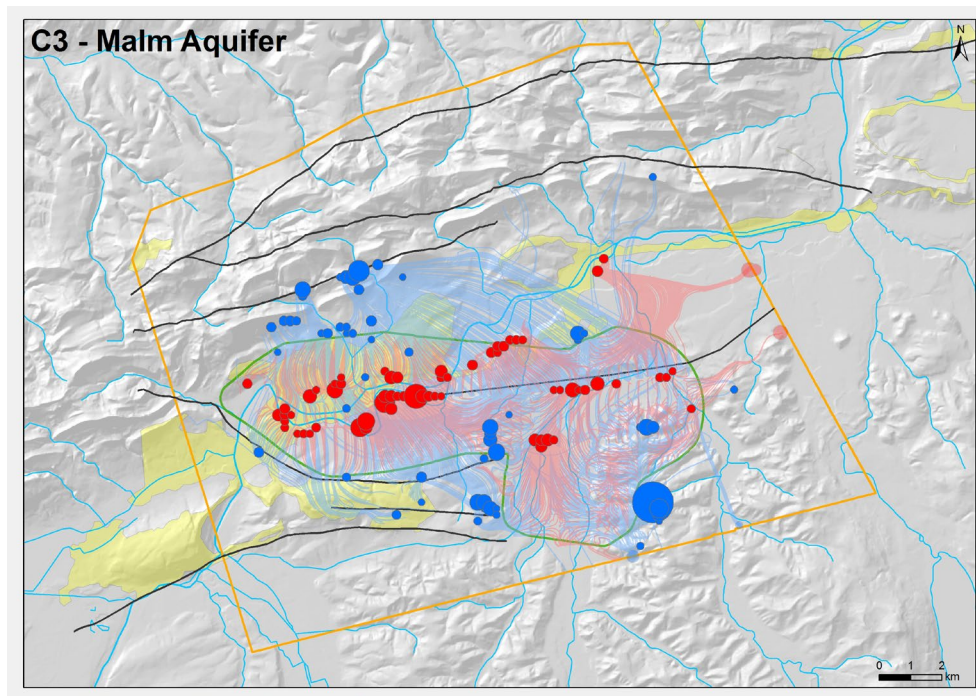


Fig. 4-33: Base case C3 – Calculated path lines starting from the Malm aquifer. (Blue: recharge path; red: discharge paths, green polygon depicts the siting region, strong colors indicate pathlines reaching the top of the model, pale colors indicate pathlines leaving the model along the lateral boundaries).

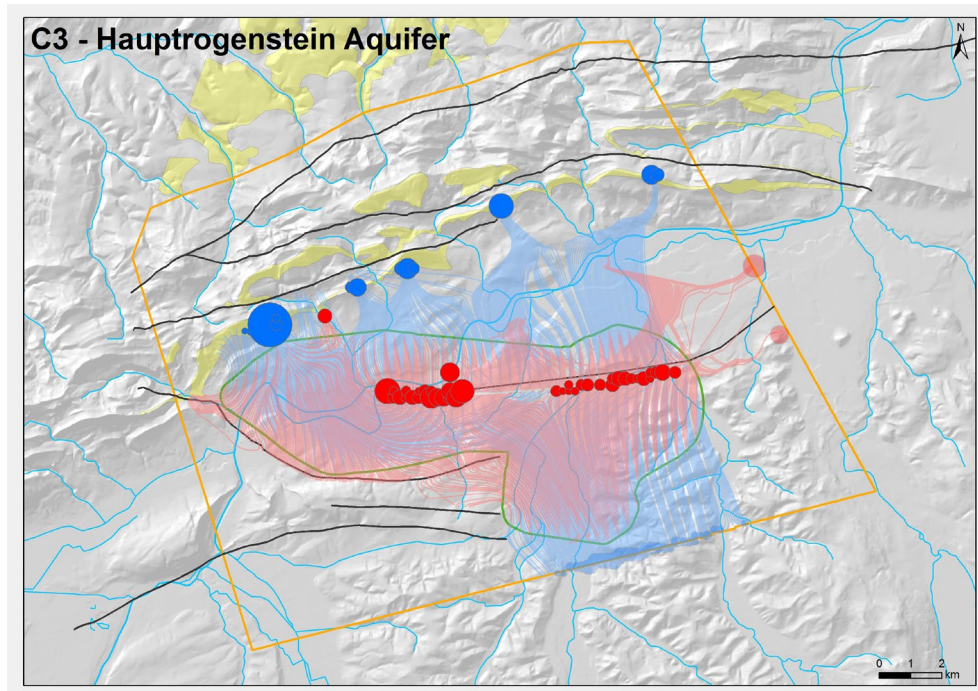


Fig. 4-34: Base case C3 – Calculated path lines starting in the Hauptrogenstein aquifer. (Blue: recharge path; red: discharge paths, green polygon depicts the siting region, strong colors indicate pathlines reaching the top of the model, pale colors indicate pathlines leaving the model along the lateral boundaries).

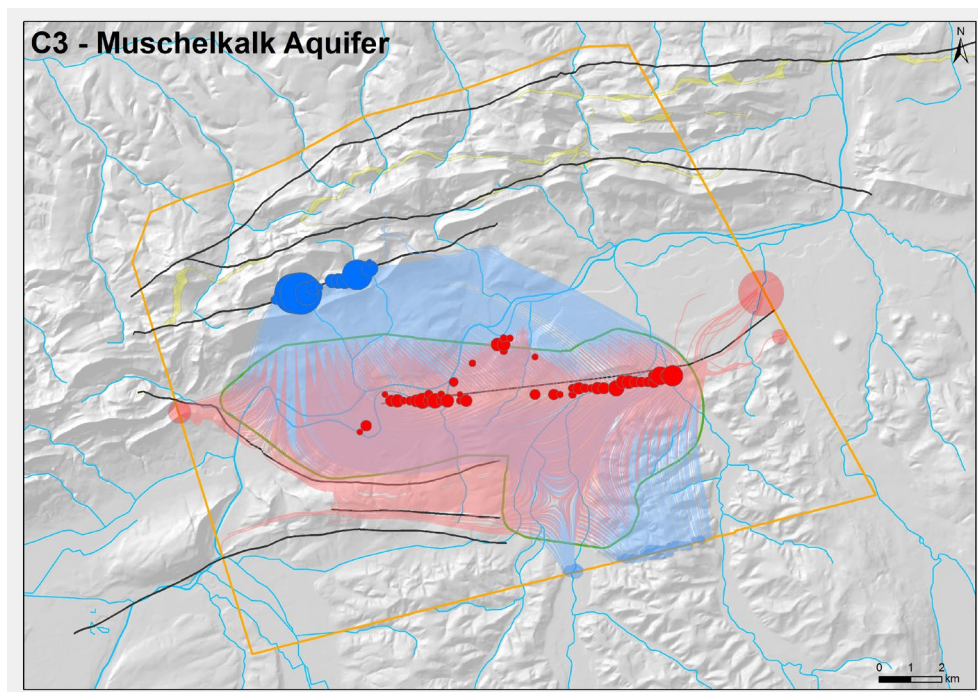


Fig. 4-35: Base case C3 – Calculated path lines starting in the Muschelkalk aquifer. (Blue: recharge path; red: discharge paths, green polygon depicts the siting region, strong colors indicate pathlines reaching the top of the model, pale colors indicate pathlines leaving the model along the lateral boundaries).

4.4.3 Sensitivity Runs

The sensitivity runs performed based on base case C3 refer to the hypotheses by which the two hydrogeological units RD4 (Sissach Member) and Arietenkalk (see Chapter 3.3) located above and below the Opalinus Clay are considered to be more conductive (i.e. water conducting layers).

C3-RD4

Fig. 4-36 and Fig. 4-37 show the simulated head distribution of sensitivity case **C3-RD4** where the conductivity of the Sissach Member (RD4) was increased by 3 orders of magnitude compared to the base case. As in sensitivity case C2-RD4, the more effective drainage increases the hydraulic heads in the areas of recharge (close to the Jura Thrusts) while heads are decreased in areas of discharge (e.g. the permeable fault planes).

C3-AKA

In case **C3-AKA**, the conductivity of the Arietenkalk was increased by four orders of magnitude, i.e. from 1×10^{-12} m/s to 1×10^{-8} m/s (Table 4-1). The increased conductivity again increases the hydraulic heads within the Arietenkalk in areas of local recharge (Fig. 4-38 and Fig. 4-39). Again, where local discharge is possible, the increased drainage causes lower hydraulic heads than in the base case.

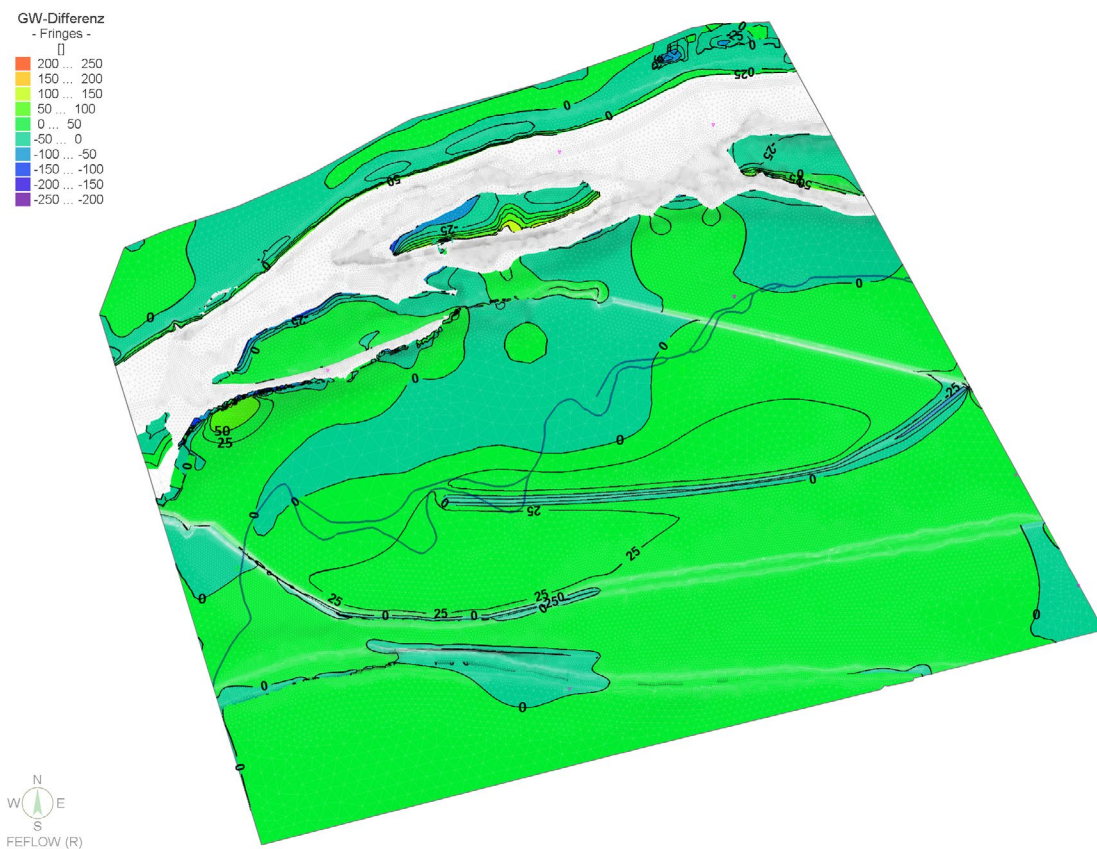


Fig. 4-36: Sensitivity case C3-RD4 – Simulated head field differences in RD4 (Sissach Member) compared to base case C3.

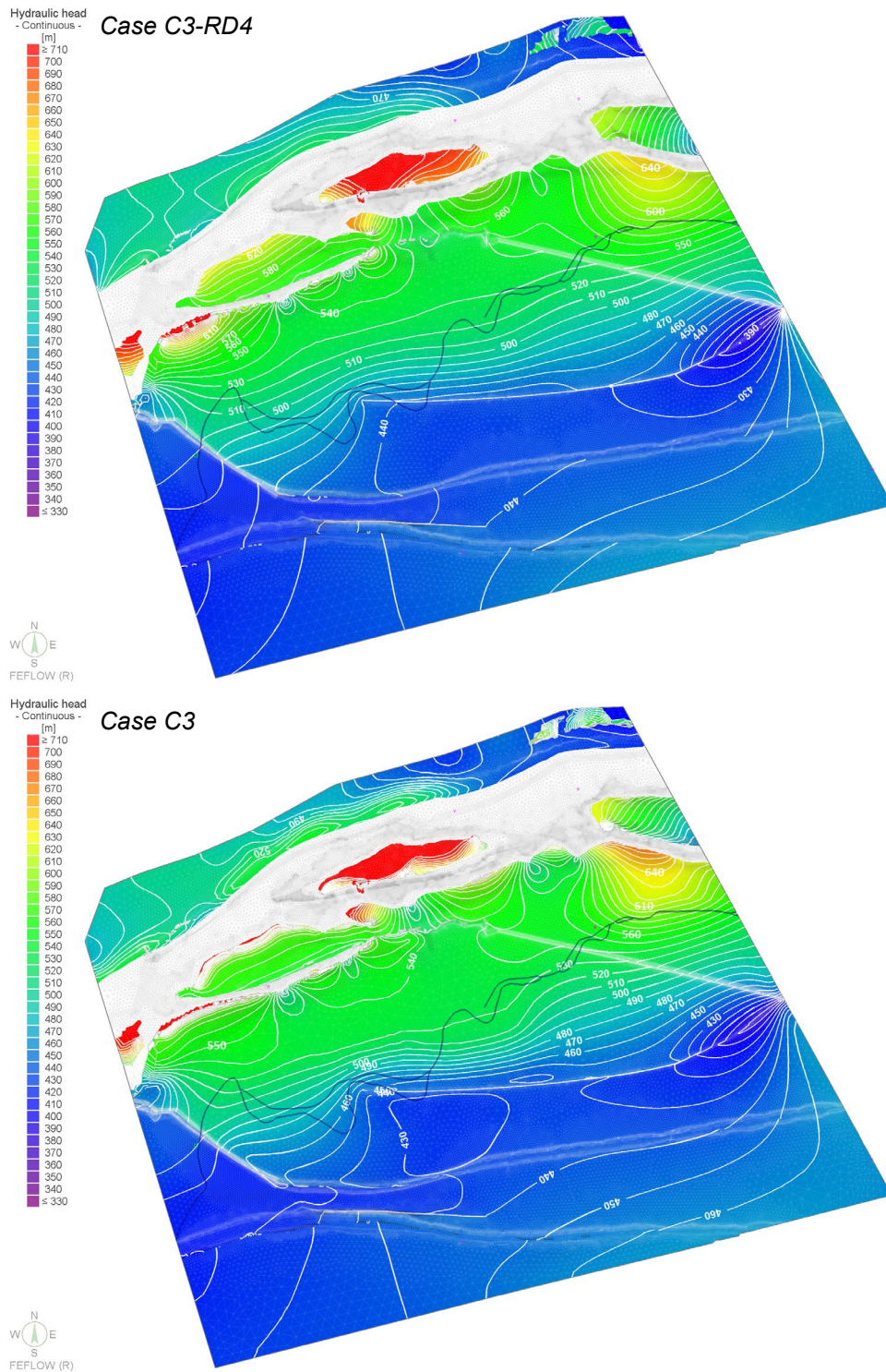


Fig. 4-37: Sensitivity case C3-RD4 – Simulated head field in RD4 (Sissach Member) compared to base case C3.

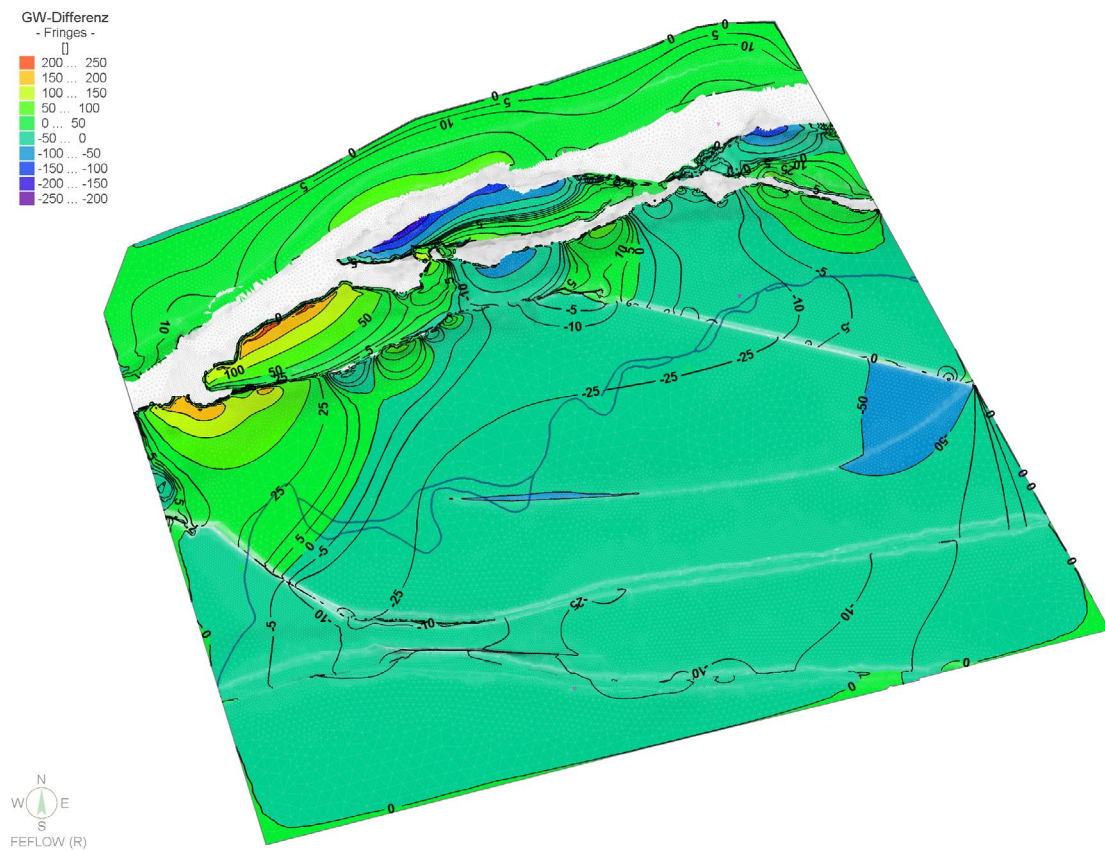


Fig. 4-38: Sensitivity case C3-AKA – Simulated head field differences in the Arietenkalk compared to base case C3.

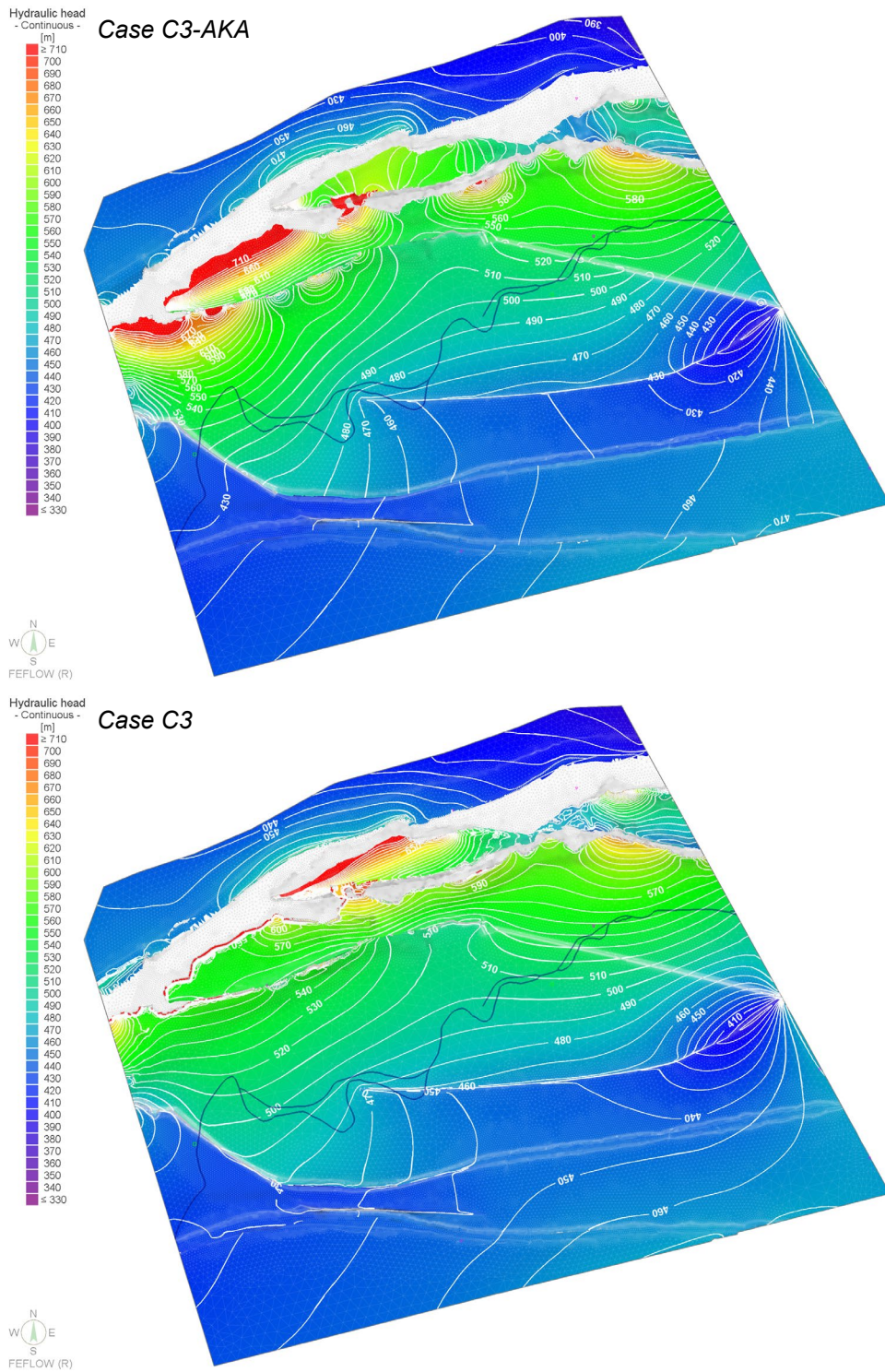


Fig. 4-39: Sensitivity case C3-ACA – Simulated head field in the Arietenkalk compared to base case C3.

4.5 Base case C3a ("fully connecting faults")

4.5.1 Hydraulic heads

Run C3a refers to a best guess parameter set and the boundary conditions described in Chapter 3.3 and 3.4, representing the hypothesis "fully connecting faults", meaning that groundwater flow across and along the faults is possible. Consequently, water exchange across the faults as well as between the layers of the multi-aquifer system can evolve. The computed flow fields are shown in Fig. 4-40 and Fig. 4-41. Vertical sections through flow system are shown in Fig. 4-42.

Base case C3a differs from C3 by also allowing flow across the fault planes. The flow fields of C3a are more or less comparable to those of C3 though the shielding and channelling effect of the impermeable faults in base case C3 is not visible anymore. Groundwater contours of all the aquifers become continuous and smooth along the faults because of their assigned hydraulic properties (permeable).

Simulated hydraulic heads in the *Malm aquifer* vary between 430 and 360 masl, indicating groundwater recharge areas mainly in the northern hills and groundwater discharge into, and along, the Aare valley and in the area of Schafisheim where a groundwater depression close to the Eppenberg Flexure develops (Fig. 4-40a).

The hydraulic head in RD2 (*Hauptrogenstein*) ranges from 670 to 380 masl (Fig. 4-40b). Similar to base case C3, a local groundwater depression with low hydraulic heads (380 masl) occurs along the Eppenberg Flexure. A maximum hydraulic head of 670 masl is calculated in outcrops close to the Jura Thrusts (in the northern block). Groundwater flow is directed towards the Eppenberg Flexure where the high hydraulic heads can relieve through the permeable fault.

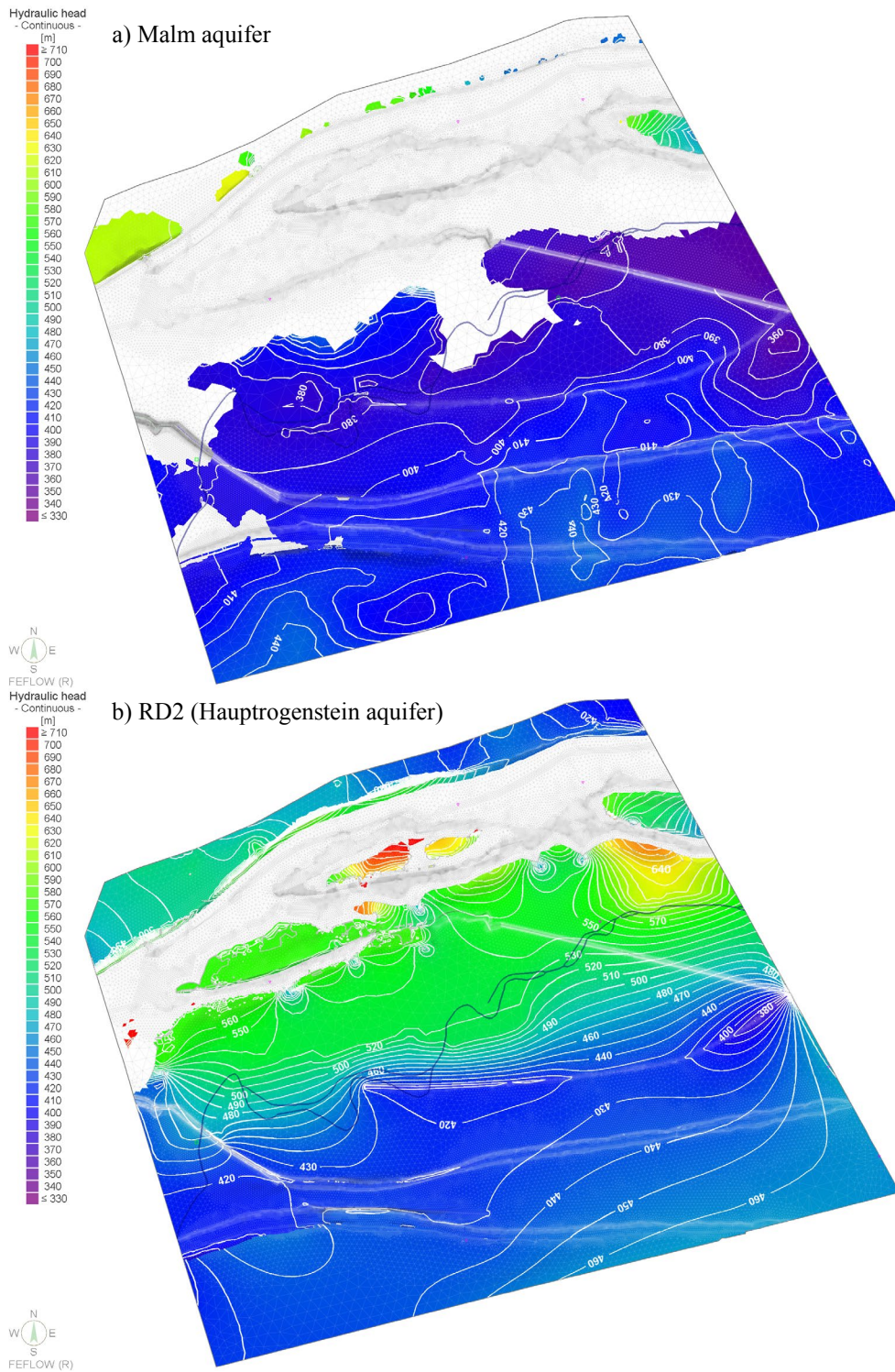


Fig. 4-40: Base case C3a – Simulated head field along aquifers above the Opalinus Clay.

The simulated head distribution in the *Keuper aquifer* shows a very similar pattern to that of base case C3. Local minima of hydraulic heads develop close to the Jura Thrusts, depending on the topography. Flow in general is directed from the topographic high points close to the Jura Thrusts towards these local minima or towards the Eppenberg Flexure (Fig. 4-41a).

The simulated heads in the *Muschelkalk aquifer* also show the highest hydraulic heads (up to 570 masl) close to the Jura Thrusts (north of Lostorf). Flow is primarily directed towards the Eppenberg Flexure (Fig. 4-41b). As in the Keuper aquifer, the groundwater depression at the eastern model boundary along the Eppenberg Flexure marks a local discharge area.

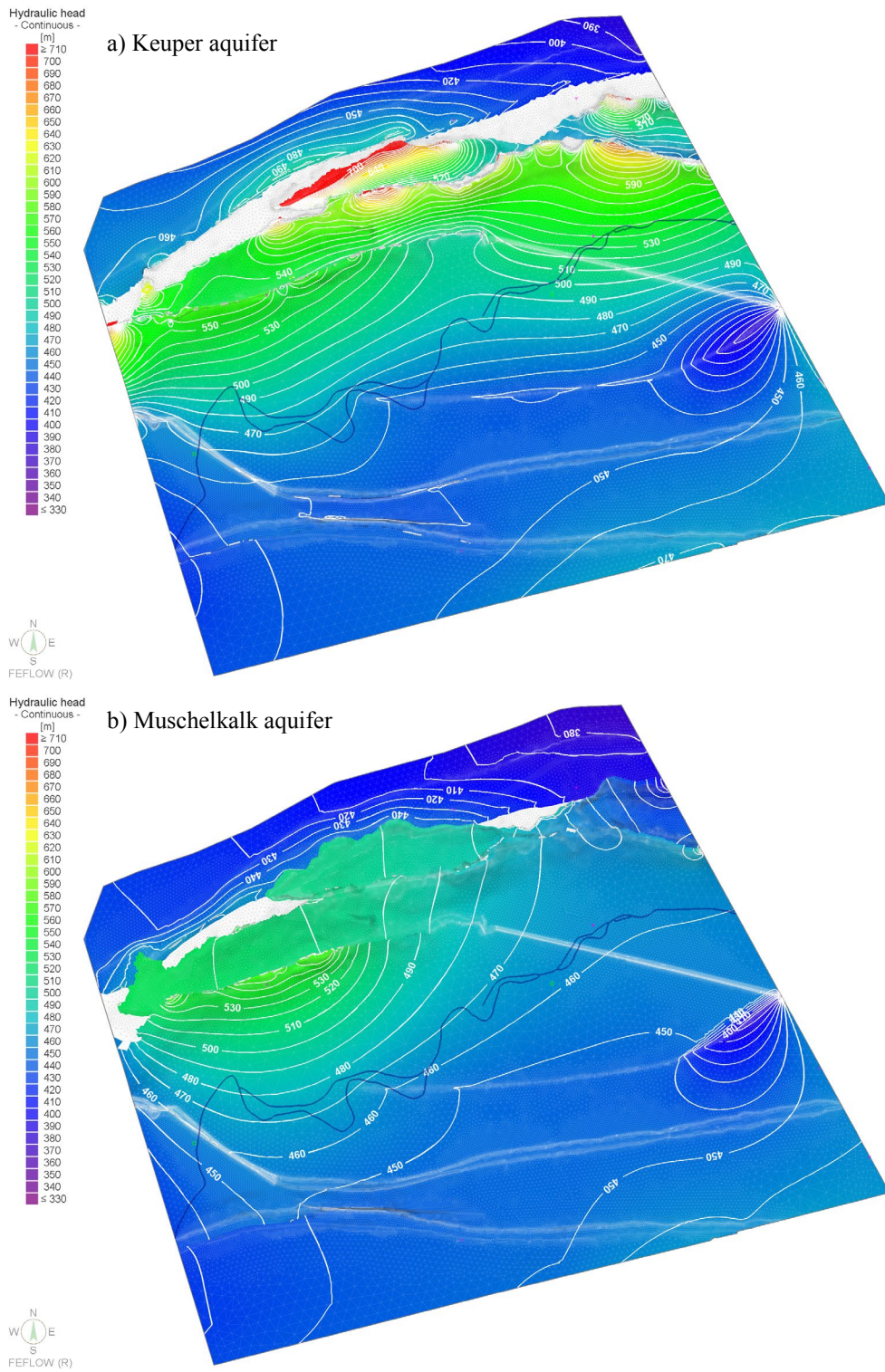


Fig. 4-41: Base case C3a – Simulated head field along aquifers below the Opalinus Clay.

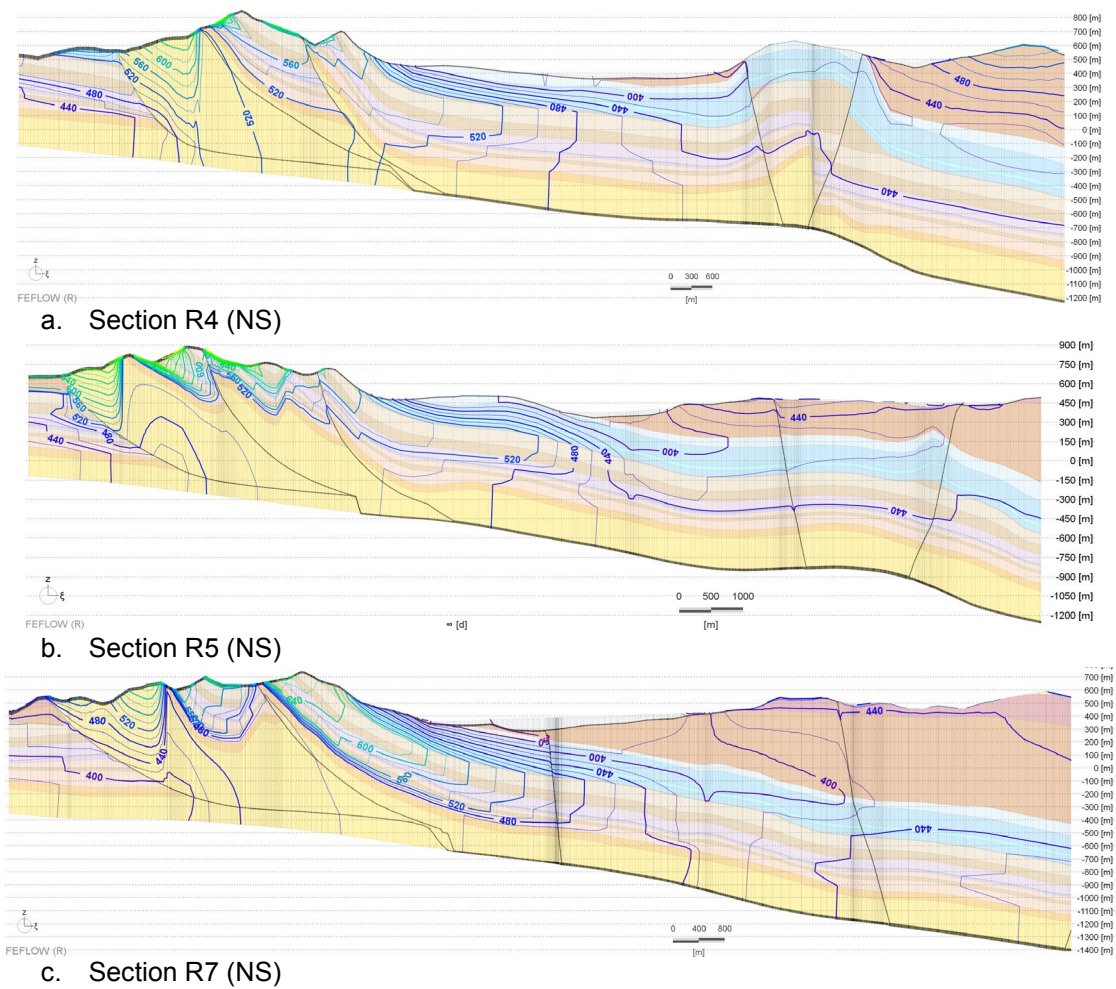


Fig. 4-42: Base case C3a – Simulated head field along vertical sections (Location see Fig. 4-1). 2x vertical exaggeration.

Vertical gradients through the Opalinus Clay are shown in Fig. 4-43. The head differences in the siting region show a very similar distribution pattern to that of base case C3. Mainly close to the Jura Thrusts, positive values indicate downward directed gradients (in recharge areas). Close to the Eppenbergr Flexure (mainly between the Eppenbergr Flexure and the Born-Engelberg Anticline), upward directed gradients develop. The change from upward to downward directed gradients is subparallel to the Aare valley and Eppenbergr Flexure, hence within the siting region, a change from upward to downward directed flow is indicated.

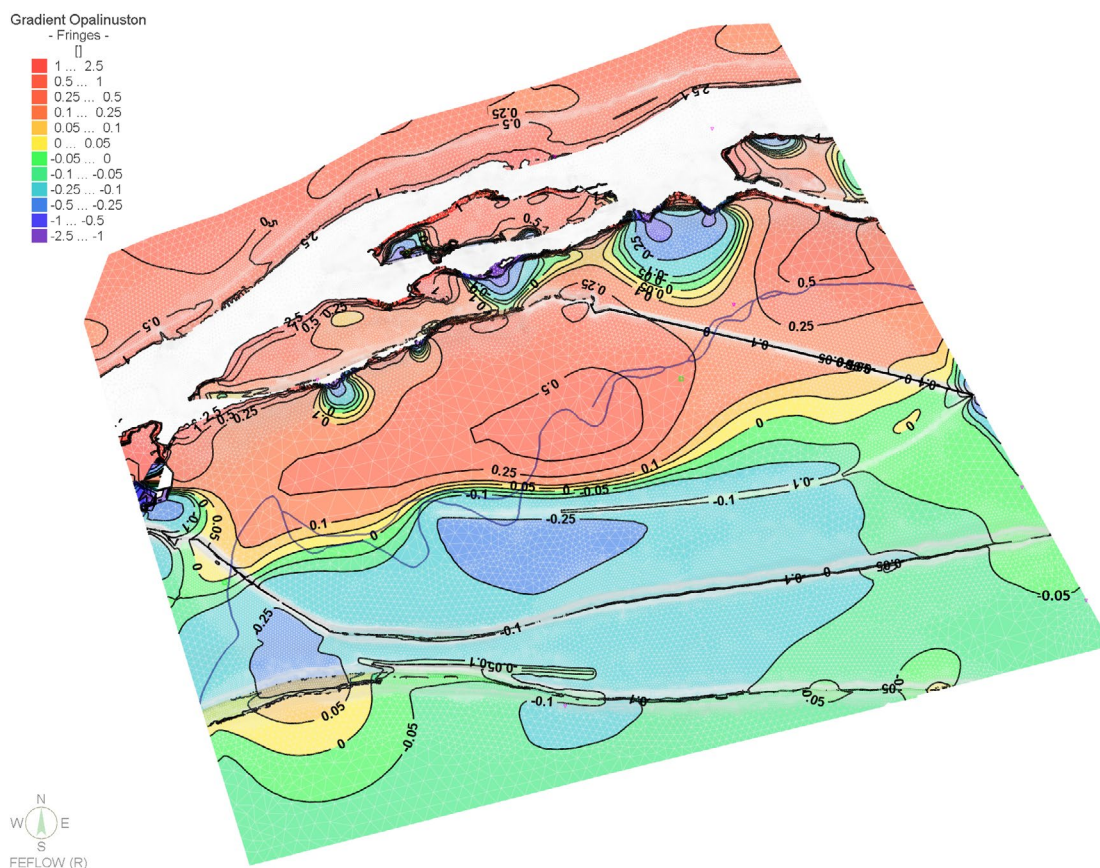


Fig. 4-43: Base case C3a – Vertical gradients in the Opalinus Clay.

4.5.2 Recharge and discharge paths

In order to assess discharge paths of groundwater from the Malm aquifer and Muschelkalk aquifer particle tracking has been carried out. The particles were started from given points in the aquifers considered. While tracking along the direction of flow (i.e. forward tracking) the paths run to discharge points when reaching a model boundary. Tracking in the opposite direction (i.e. backward tracking) the particles follow the recharge paths until a model boundary is reached, indicating where groundwater originates. Fig. 4-8 and Fig. 4-9 show the starting points in the area of the siting region Jura-Südfuss.

Fig. 4-44 shows calculated discharge paths (forward tracking) starting from the Malm aquifer as well as recharge paths obtained by backward tracking. The results are similar to those of base case C3. The discharge locations of the Malm aquifer are situated in the Aare valley (Niederamt) as well as along the Eppenbergr Flexure, south of Aarau and the Suhre valley. Some of the path lines also leave the model domain to the east. Recharge paths trace back to the south (the Jura Thrusts, between the Dottenberg and the Gugen, indicating recharge into Quaternary), to the area south of Suhr (where recharge occurs through the Molasse) and the Born-Engelberg Anticline (where recharge, at least in part, is through the Molasse and Malm aquifer).

Path lines simulated for the Hauptrogenstein aquifer are shown in Fig. 4-45. As in base case C3, recharge areas are mainly located close to the Jura Thrusts (at topographic high points) while discharge locations were mainly simulated along the Eppenbergl Flexure, in the Aare valley and just north of Lostorf. A few path lines also leave the model domain towards the east and west.

The forward path lines starting in the Muschelkalk aquifer are shown in Fig. 4-46. The path lines show virtually the same recharge (close to the Jura Thrusts) and discharge areas (out of the model domain at the eastern, southern and western boundary and along the Eppenbergl Flexure) as base case C3. The different hydraulic properties of the fault systems are apparent from path lines leaving the model boundary to the west. Where in base case C3, path lines in the western part of the model are partitioned by the impermeable fault planes constituting the Born-Engelberg Anticline, in base case C3a path lines simply cross these fault planes (as they are permeable) and leave the model domain in a much broader area.

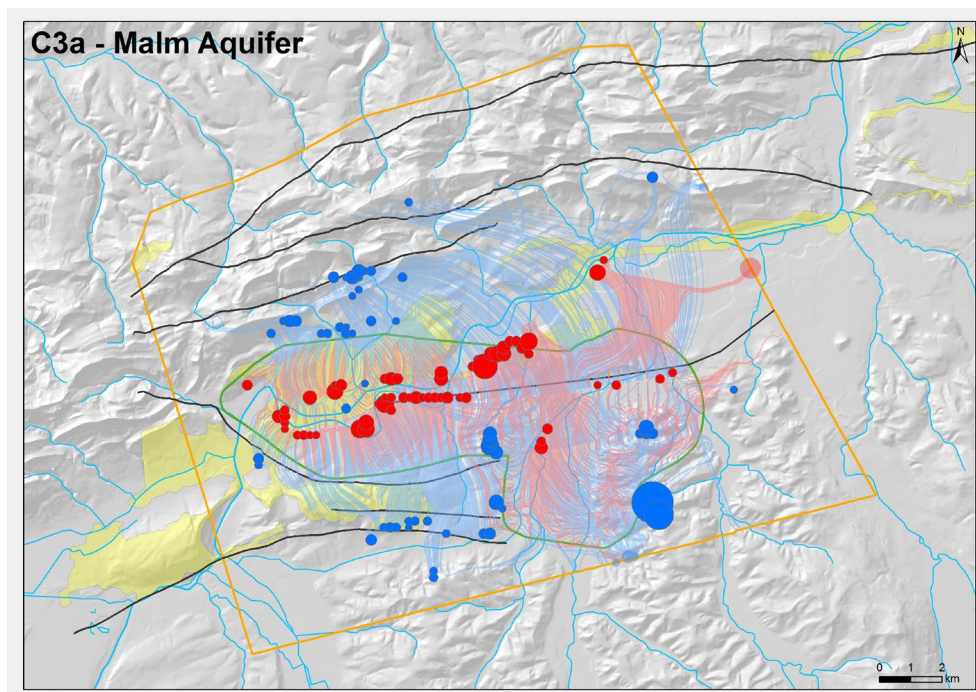


Fig. 4-44: Base case C3a – Calculated path lines starting from the Malm aquifer. (Blue: recharge path; red: discharge paths, green polygon depicts the siting region, strong colors indicate pathlines reaching the top of the model, pale colors indicate pathlines leaving the model along the lateral boundaries).

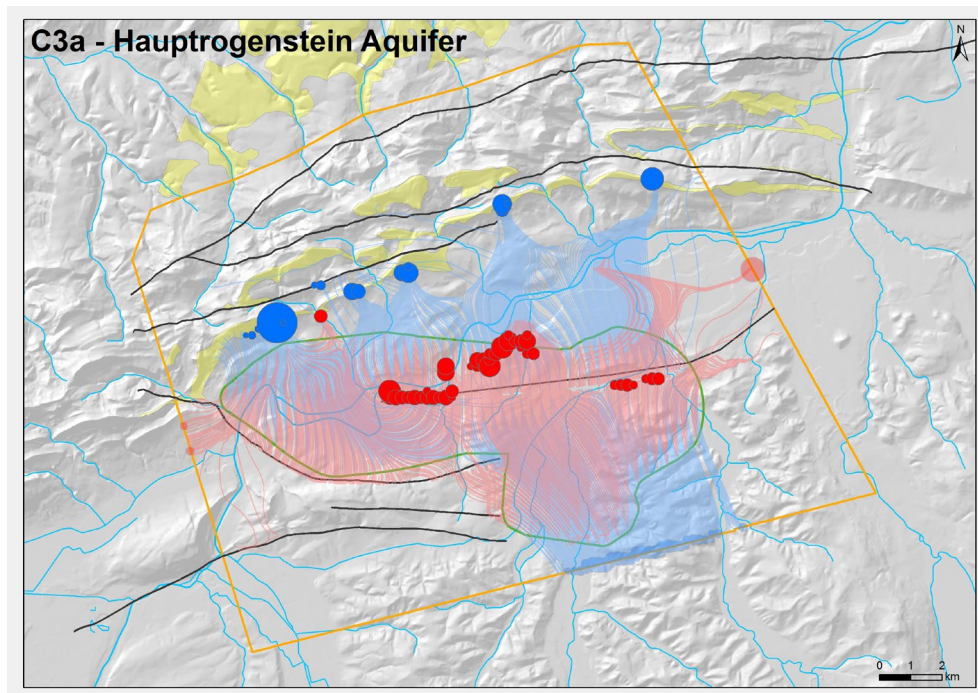


Fig. 4-45: Base case C3a – Calculated path lines starting from the Hauptrogenstein aquifer. (Blue: recharge path; red: discharge paths, green polygon depicts the siting region, strong colors indicate pathlines reaching the top of the model, pale colors indicate pathlines leaving the model along the lateral boundaries).

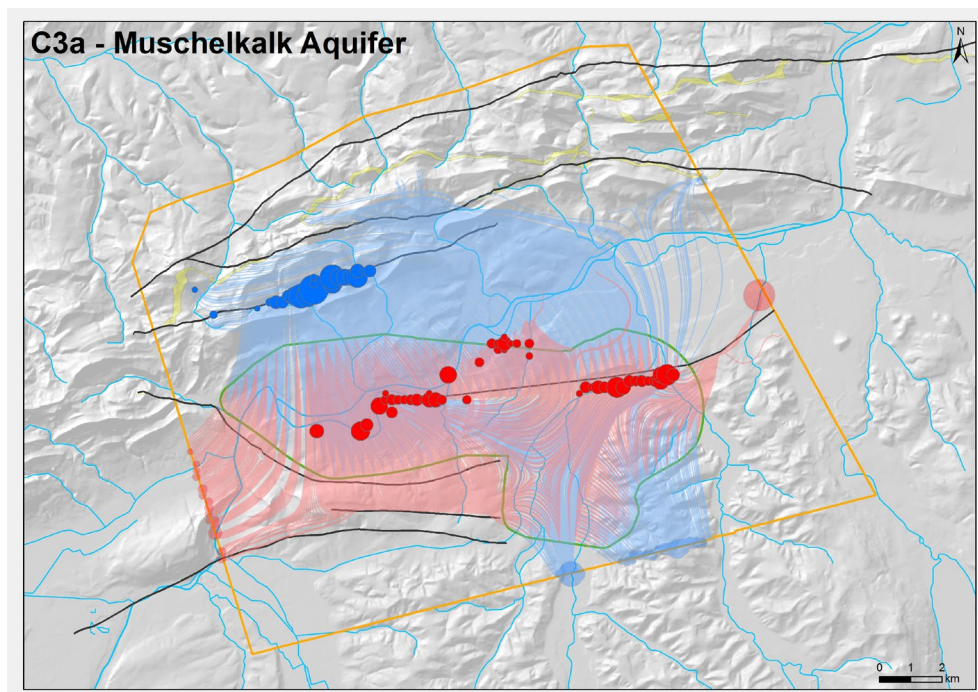


Fig. 4-46: Base case C3a – Calculated path lines starting from the Muschelkalk aquifer. (Blue: recharge path; red: discharge paths, green polygon depicts the siting region, strong colors indicate pathlines reaching the top of the model, pale colors indicate pathlines leaving the model along the lateral boundaries).

4.5.3 Comparison of results C3a and C3

As mentioned above, C3a differs from C3 by additionally allowing flow across the fault planes and the resulting flow fields are more or less comparable to those of base case C3.

Fig. 4-47 to Fig. 4-50 show the simulated head distributions of C3a in the Malm aquifer, RD2 (Hauptrogenstein aquifer), Keuper aquifer and Muschelkalk aquifer, with comparison to the corresponding head distributions of base case C3. The assumed additional flow across the fault planes makes the head distribution patterns of C3a more continuous and smooth in the vicinity of the fault zones and enhances groundwater interactions between the hydrogeological units. The major difference between these two base cases is that while in case C3, the impermeable (inner) fault layer channels the flow around the faults, in case C3a flow simply crosses the (permeable) faults. This is most obvious in the lower aquifers (Keuper aquifer and Muschelkalk aquifer).

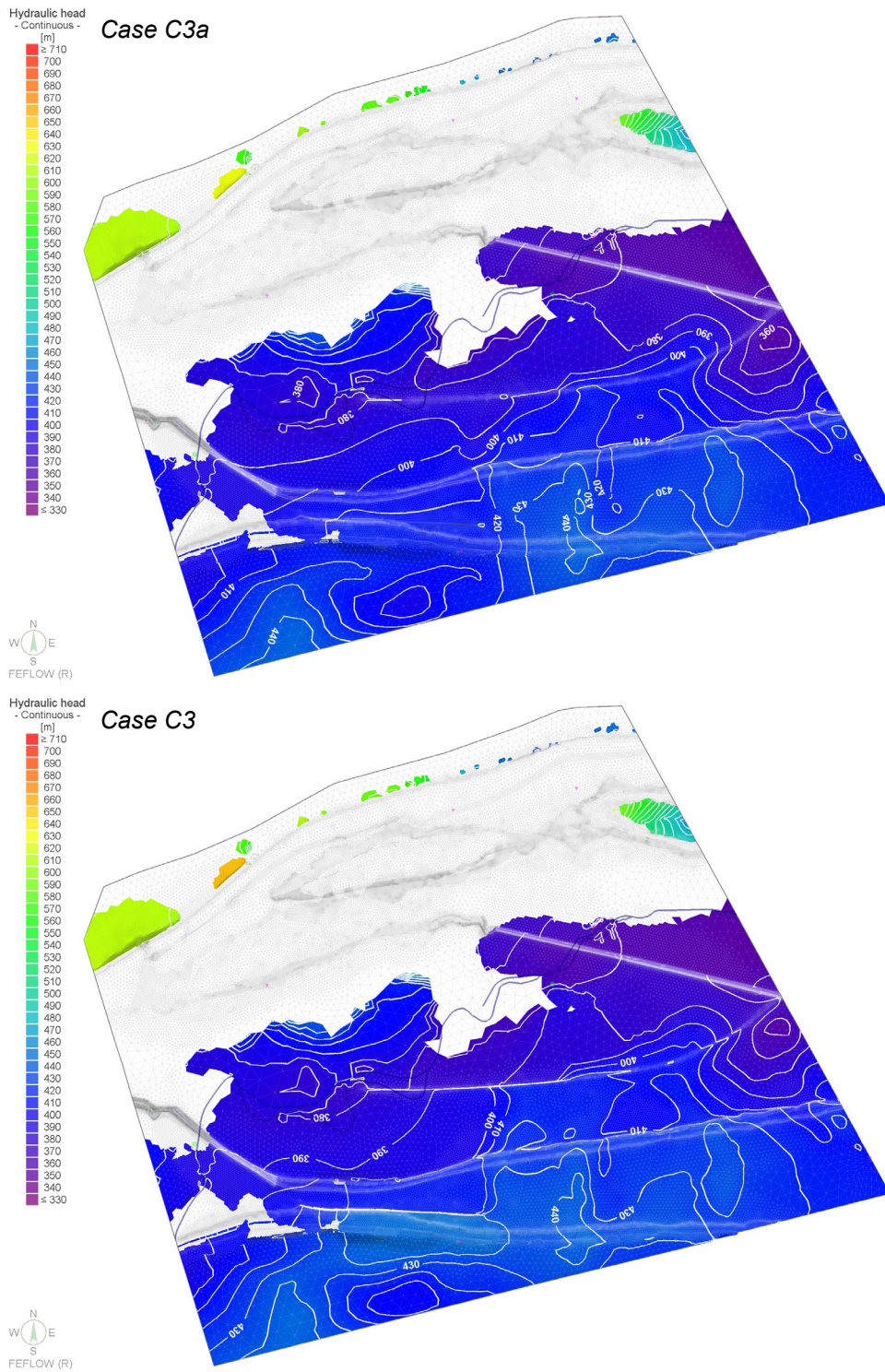


Fig. 4-47: Base case C3a – Simulated head field in the Malm aquifer compared to base case C3.

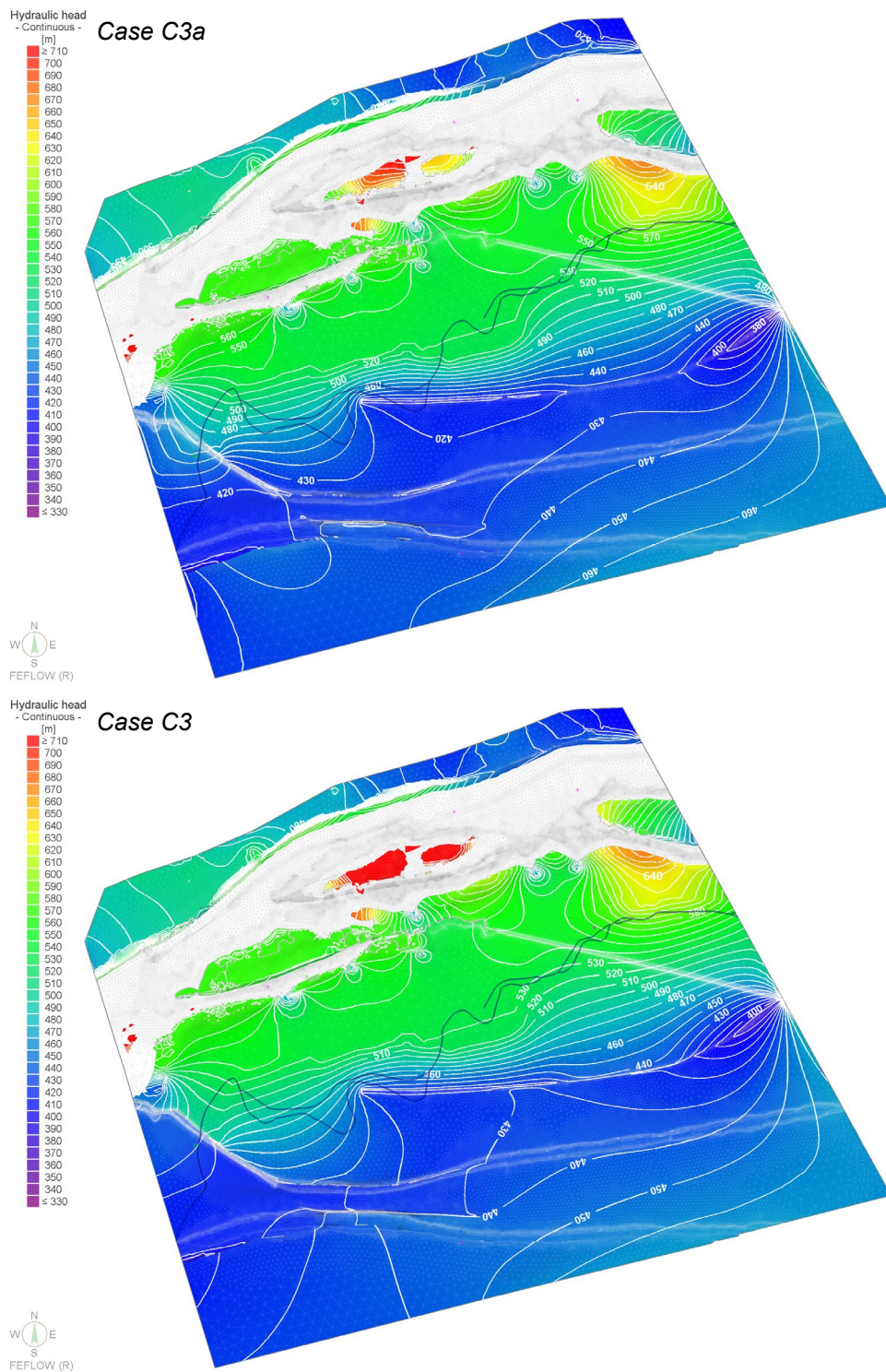


Fig. 4-48: Base case C3a – Simulated head field in RD2 (Hauptrogenstein) compared to base case C3.

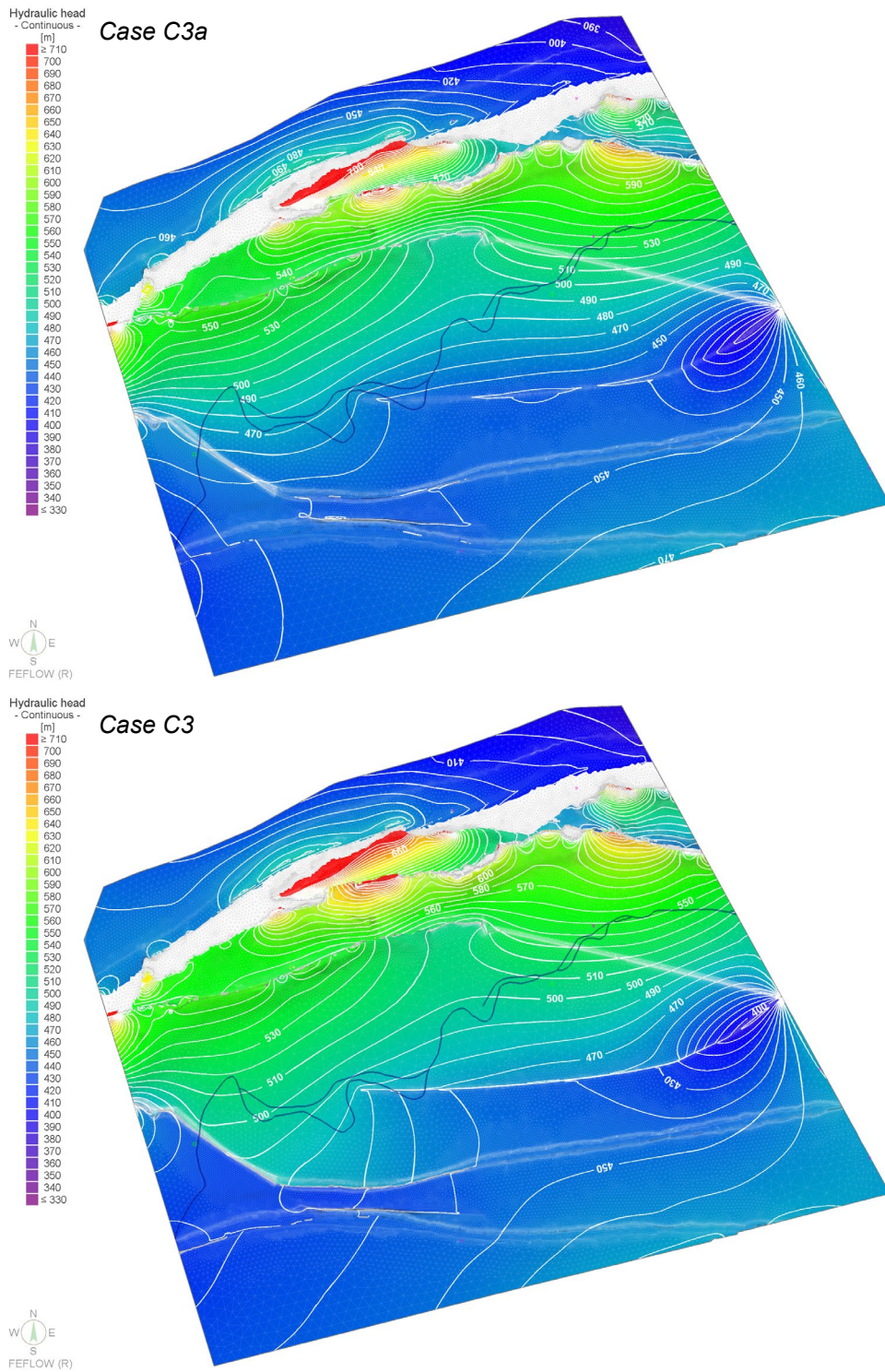


Fig. 4-49: Base case C3a – Simulated head field in the Keuper aquifer compared to base case C3.

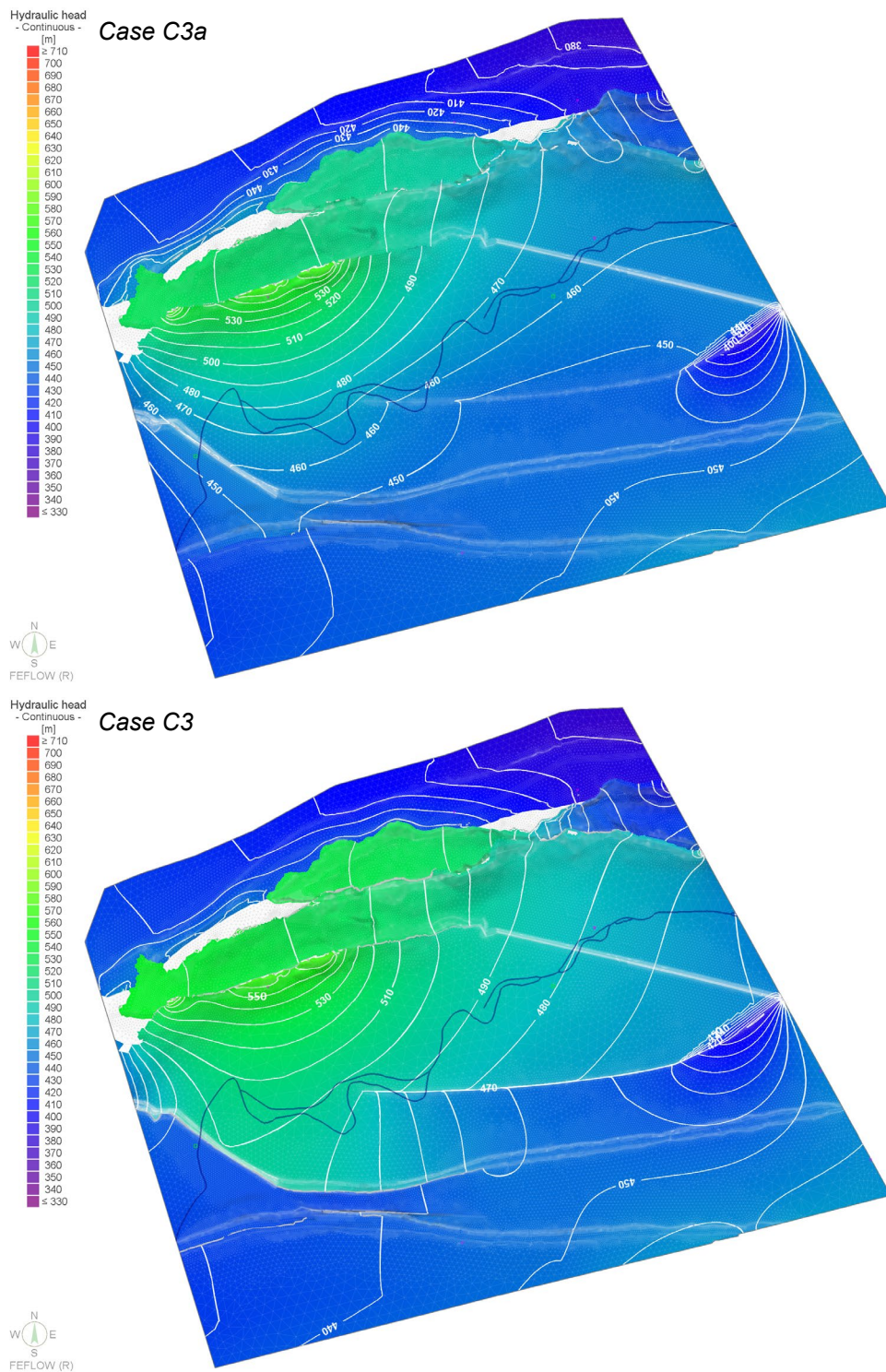


Fig. 4-50: Base case C3a – Simulated head field in the Muschelkalk aquifer compared to base case C3.

5 Discussion of results

Based on the implemented hydrogeological model, the corresponding hydraulic reference parameters and boundary conditions (see Chapter 3), four model hypotheses have been investigated to account for the general uncertainty related to the hydraulic behaviour of the modelled faults zones. In this context, four base cases have been modelled, namely:

- Base case C1 ("throw only"): Potential groundwater flow along and across the fault is suppressed unless aquifers are (sub-/horizontally) connected, i.e. the geological offset either is too small to offset the aquifer so that it abuts against an aquitard or the offset is large enough so that two different aquifers are directly connected
- Base case C2 ("sealing fault"): Any groundwater flow along and across the fault is suppressed
- Base case C3 ("connecting fault"): Groundwater flow can exclusively occur in the fault plane meaning that multiple-aquifer systems are (sub-/vertically) connected but flow across (i.e. perpendicular to the fault plane) is suppressed
- Base case C3a ("fully connecting fault"): Groundwater can flow along and across the fault

Comparison with existing hydraulic data bases

The number of measurements of hydraulic heads in the siting region Jura-Südfuss is limited to measurements from 5 boreholes (Schafisheim, Oftringen, Gösigen and Lostorf) and measurements from a borehole for the Wisenberg tunnel (see Fig. 5-1). Head measurements from the Keuper aquifer from the borehole Schafisheim showed negative values (-120 m), indicating abnormal formation pressure conditions (i.e. they cannot be explained by the local or regional discharge levels). This value is therefore not used for a direct comparison with the simulated values.

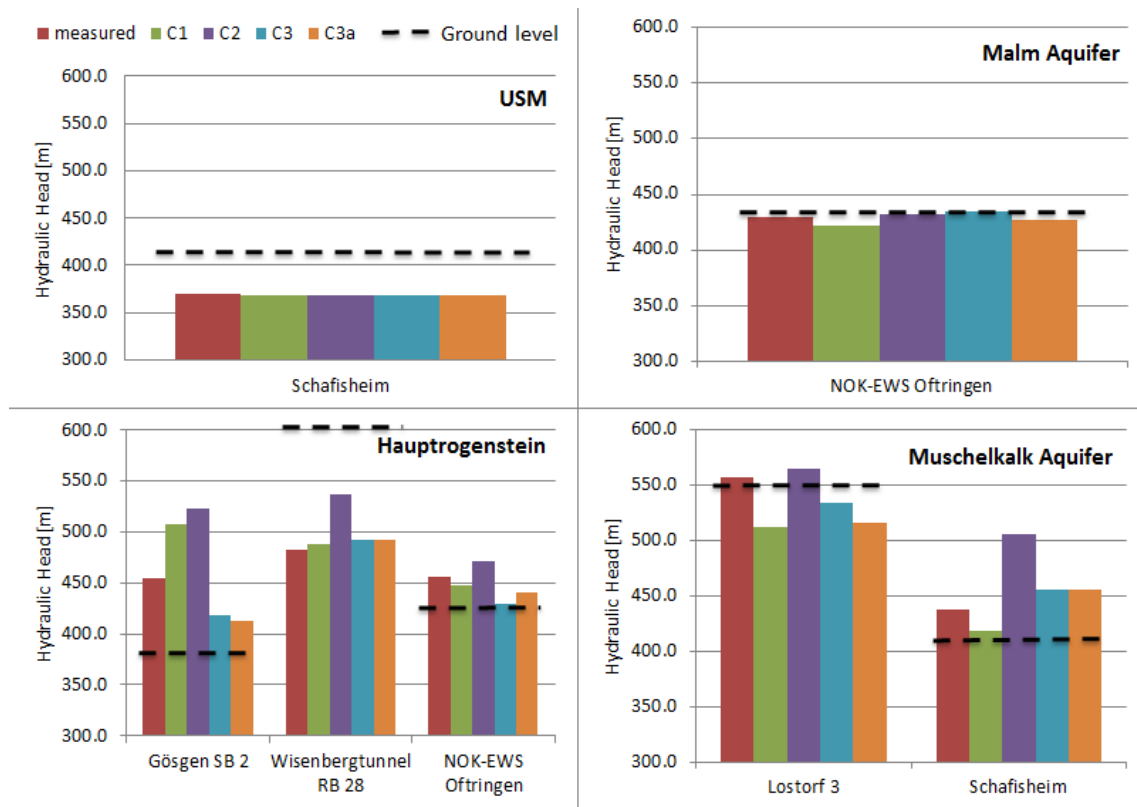


Fig. 5-1: Comparison of measured and simulated values for different aquifers and boreholes within the model domain.

The borehole Schafisheim is located right at the boundary of the model domain; simulated values here therefore may be more influenced by the boundary conditions taken from the regional model than by the simulations performed at the local scale. The borehole for the Wisenbergtunnel is located at the north-western corner of the model domain, north of the Jura Thrusts and hence indicates the hydraulic conditions in the northern-most block which is mostly neglected in this report (as this block is hydraulically decoupled from the rest of the model domain due to the low conductive Anhydritgruppe along the Jura Thrusts). However, most simulations account reasonable well for the corresponding measured values.

Measurements and simulations in the different boreholes clearly show the dependence of the measured (simulated) values on the local recharge/discharge areas (except the Keuper aquifer and Muschelkalk aquifer for which the discharge areas are mostly outside of the model domain). In summary, based on the comparison of measured and simulated values, no clear preference for one of the base cases C1 – C3a can be made, even though special features of local groundwater flow might be better represented by one or the other base case. The full spectrum of modelling results, comprising all base case simulations and the corresponding sensitivity cases need to be considered to define the range of expectations on ground water flow conditions in the siting region Jura-Südfuss.

Discussion

The comparison of simulated and measured hydraulic heads shows a reasonably good agreement throughout the model domain (see Fig. 5-1) so that it can be assumed that the boundary conditions are valid for the different modelling scenarios.

The groundwater system is mainly driven by surface water infiltrating through the outcrops and mountains and the implemented (regional) fault systems which, depending on their hydraulic properties, effectively channel groundwater flow.

The hydraulic head distribution in the Malm aquifer, as the uppermost regional aquifer in the model domain, shows the strongest influence by the topography with the lowest head values towards the Aare valley (Niederamt). An additional discharge area has been simulated by the regional model in the area of Wildegg. Recharge areas are located throughout the model domain, some of the simulated recharge areas indicate recharge through the Quaternary (northern part of the model) and through the Molasse (southern part of the model). Recharge and discharge areas are local and the hydraulic properties of the implemented fault systems only have a minor effect on the general discharge and recharge areas.

Though the Effingen Member (namely the unit EFF2, representative for the potentially transmissive Gerstenhübel-Schichten) has not explicitly been assigned with a higher conductivity as a sensitivity case, it is apparent that the flow direction would be comparable to the groundwater flow in the Hauptrogenstein aquifer (RD2). The Hauptrogenstein aquifer is stratigraphically located below EFF2, even the lowest potentially water conducting unit (Sissach Member, RD4) still shows a strong influence of the topography on the simulated hydraulic head distribution in the sensitivity cases (see below). It can therefore reasonably be assumed that recharge and discharge areas of the potentially water conducting unit EFF2 are comparable to the Hauptrogenstein aquifer. Since outcrops of the unit EFF2 are topographically slightly lower than for the Hauptrogenstein aquifer, hydraulic heads in EFF2 would most likely also be lower but still higher than in the Malm aquifer resulting in an upward directed flow across the unit EFF1.

The hydrogeological unit RD2 represents the Hauptrogenstein aquifer which, in the model domain, occurs as a fractured or karst aquifer with an average thickness of ~100m. Though the Hauptrogenstein aquifer covers the whole model domain, the large vertical offset along the Jura Thrusts in the north decouples the northern from the southern part. Comparable to the Malm aquifer, the topography dominates the simulated head distribution. The main recharge areas are located along the topographically high points close to the Jura Thrusts. These comparatively high local recharge areas are responsible for the artesian conditions simulated (and measured) in the Hauptrogenstein aquifer (compare Fig. 5-1). No recharge along the Born-Engelberg Anticline occurs since, in this area, no outcrops of the Hauptrogenstein aquifer have been mapped and the Hauptrogenstein aquifer is hydraulically decoupled from the Malm aquifer above by the low-conductive Effingen Member and the hydrogeological unit RD1, representing the clay-rich aquitards of the upper Dogger. Base case C1 mainly indicated discharge outside of the model domain with the exception of an area just north of Lostorf. In base case C2, the impermeable fault systems and the location of the main recharge areas channel groundwater flow between the Eppenbergr Flexure and the Born-Engelberg Anticline and towards the east. This leads to higher hydraulic heads on the northern side of the Eppenbergr Flexure than on the southern side. If the fault planes are (at least vertically) permeable (base cases C3 and C3a), a hydraulic depression develops along the Eppenbergr Flexure (especially in the area of Suhr and in the area of Niederamt) and marks possible discharge areas where water can flow along the fault plane into higher aquifers or towards the surface.

The Keuper aquifer is implemented as a local aquifer below the Opalinus Clay. According to the simulation of the different base cases, recharge occurs close to the Jura Thrusts within the model domain. In addition, high hydraulic heads occur along the western model border (and hence are, at least in part, caused by the fixed-head boundary conditions from the regional model) in base case C2. Flow generally is directed towards the south with a complex pattern of discharge locations (outside of the model domain), especially in base cases C1 and C2. The regional model simulated the main discharge areas close to the Reuss (area of Birmenstorf), the "Klus" of Aarburg and the area of Baden (Limmat valley). In base cases C3 and C3a the discharge areas are mainly influenced by the permeable fault planes. In these cases, the main discharge areas are located in the area of the Niederramt and in the groundwater depression along the Eppenberg Flexure within the model domain.

The Muschelkalk aquifer is the lowest aquifer in the simulations and covers the whole model domain. However, as for the higher hydrogeological units, the Jura Thrusts with their large vertical offset decouples the northern from the southern part of the model. The main recharge areas are located close to the Jura Thrusts in the topographic high areas. Discharge areas in base cases C1 and C2 are all located outside of the model domain. The regional model simulated the main discharge areas close to Birmenstorf in the Reuss valley (C1) and the Rhine valley close to Laufenburg (C2). In base cases C3 and C3a, where the faults allow vertical flow along the fault planes, discharge within the groundwater depression at the Eppenberg Flexure occurs in addition to discharge just outside of the model domain ("Klus" of Aarburg).

In general, the main recharge areas of the hydrogeological system are located within the model domain close to the Jura Thrusts. The hydraulic heads at these recharge locations are, according to the top boundary conditions, dominated by the topography. Locations of the discharge areas are strongly dependent on the hydraulic properties of the faults, especially the Eppenberg Flexure. If the faults allow vertical flow along the fault plane (base cases C3 and C3a), they represent preferred pathways where groundwater can flow upwards and the hydraulic heads in the groundwater systems are partially equilibrated. If the faults are impermeable (base case C2), the orientation of the Eppenberg Flexure (E-W) and the location of recharge areas (south of the Jura Main Fault) channel the flow between the Eppenberg Flexure and the Born-Engelberg Anticline. Since the Eppenberg Flexure has been implemented without any offset, the flow field in base case C1 is not influenced by this fault.

The sensitivity cases were simulated to evaluate cases where the Arietenkalk or the Sissach Member (RD4) is treated as a locally important transmissive unit. Both sensitivity cases show that the increased conductivity leads to higher hydraulic heads in the recharge areas. Since drainage is also enhanced in the locally transmissive unit, these high hydraulic heads quickly subside until only a negligible change compared to the base cases (where the respective unit is treated as an aquitard) remains. In discharge areas, the enhanced drainage due to the increased conductivities causes lower hydraulic heads (compared to the base cases).

Vertical gradients through the Opalinus Clay have also been calculated for the different base cases and the sensitivity cases (see appendix A). These calculations show that the distribution of upward or downward directed gradients within the siting region greatly depend on the hydraulic setting (including locally transmissive units, permeable faults etc.). Therefore, no preferred flow (upward or downward) in the siting region can be deduced, both flow directions (with varying intensities) are possible.

6 Conclusions

A hydrogeological model of the siting region Jura-Südfuss was elaborated, aimed at evaluating the local groundwater flow conditions for a variety of hypothesis regarding the hydraulic behaviour of faults and the role of local aquifers/potentially transmissive units. In the present study, the time of validity of the hydrogeological modelling results is inherently associated with the assumption that the topography remains largely unchanged, implying that the recharge and discharge conditions are subjected to moderate changes only.

The model analyses elaborated on the hydraulic state conditions in the proposed host rocks and the aquifer systems of the siting region, particularly including:

- The assessment of the Opalinus Clay and the Effingen Member as flow barriers, separating the groundwater flow systems of the regional aquifers Malm aquifer, Hauptrogenstein aquifer and Muschelkalk aquifer. Emphasis of the investigations has been on the direction (up/downward) and magnitude of hydraulic gradients in the two proposed host rocks. The impact of the regional fault systems has been analyzed by parametric studies.
- The detailed evaluation of groundwater flow in the hydrogeological units above and below the Opalinus Clay formation. The hydraulic significance of the Sissach Member, the Arietenkalk and the Keuper aquifer is addressed with particular focus on their potential role as a local aquifer or locally transmissive units. The impact of the Jura Thrusts, the Eppenbergr Flexure and the Born-Engelberg Anticline on groundwater flow on the regional Malm aquifer, Hauptrogenstein aquifer and Muschelkalk aquifer is analyzed in terms of prevailing flow direction and representative ranges of hydraulic gradients. Finally, the main discharge areas are inferred.

The host rock formations Opalinus Clay and Effingen Member

The Opalinus Clay formation in the siting region is, in the model, characterized by a typical (model) thickness of 85 m, a high clay content and a uniform lithology. The vertical hydraulic gradient in the Opalinus Clay is controlled by the hydraulic heads in the water conducting units above and below the host rock and the hydraulic properties of the fault systems. Therefore, a clear preference (i.e. a reference) for the vertical gradient cannot be deduced from the simulations.

The Effingen Member in the siting region Jura-Südfuss is composed of clay-rich and calcareous sequences, revealing an average thickness of 220 m (in the model). Vertical flow through the Effingen Member is controlled by the low hydraulic conductivity of the clay-rich sequences. Table 6-1 summarises the spectrum of expectations on vertical hydraulic gradients in the Effingen Member of the siting region Jura-Südfuss. In case the unit EFF2 would also be a water conducting layer, vertical gradients through the host rock would most likely be comparable to, but slightly lower than, the vertical gradient calculated from the heads of the Hauptrogenstein and Malm aquifers. Recharge areas of the unit EFF2 are topographically lower than for the Hauptrogenstein aquifer but higher than for the Malm aquifer, hence simulated hydraulic heads would also be higher than in the Malm aquifer, decreasing the head difference between the Hauptrogenstein aquifer and EFF2 or EFF2 and the Malm aquifer (compared to the difference from Hauptrogenstein aquifer and Malm aquifer).

In summary, the following conclusions can be drawn:

- The locally transmissive units/aquifers and regional aquifers in the siting region are partitioned by the main regional fault systems (Jura Thrusts and Born-Engelberg Anticline), resulting in lateral fragmentation of the groundwater flow systems. The head differences between the regional aquifer systems are mostly bracketed by the local recharge and discharge levels rather than by far-off recharge and discharge areas (e.g. Alpine region). Locally, the Eppenbergl Flexure also plays an important role in base cases C2, C3 and C3a (since the Eppenbergl Flexure has been implemented without vertical offset it does not influence the flow field in base case C1).
- The vertical gradient shows a complex pattern of upward and downward directed vertical gradients. Table 6-1 displays the spectrum of expectations on vertical hydraulic gradients in the Opalinus Clay and the Effingen Member.

Tab. 6-1: Hydrogeological characteristics of the Opalinus Clay and the Effingen Member in the siting region Jura-Südfuss. Note that since the orientation of the vertical gradient changes in most simulations within the siting region, the expected minimum and maximum gradients are given instead of reference values. POI means the point of interest.

RV: Reference value (best guess, defendable value).

AV: Alternative value (pessimistic value; complementary model assumption, definition of RV not possible).

Host rock	Parameter	RV	AV	Remarks
Opalinus Clay	Hydraulic head / mid of the formation [m]	*	-	RV: * Subhydrostatic conditions (defined by the ground level at the POI)
	Vertical gradient in the host rock [m/m]	-	0.5 0.5	AV1: Upflow AV2: Downflow
Host rock	Parameter	RV	AV	Remarks
Effingen Member	Hydraulic head / mid of the formation [m]	*	-	RV: * Subhydrostatic conditions (defined by the ground level at the POI)
	Vertical gradient in the host rock [m/m] - western part of the siting region	-	1 0.1	AV1: Upflow derived from pressure difference between Hauptrogenstein and Malm aquifer AV2: Possible downflow (in permeable faults)

Groundwater flow in the local and regional aquifer systems

The evaluation of groundwater flow in the aquifer systems above and below the host rocks is motivated by the safety assessment which requires a complete description of the composite radionuclide release path from the disposal system through the host rock and the aquifer systems, finally discharging into the biosphere. Since the present model was used to simulate "only" the local scale hydrogeological system, some of the recharge and discharge areas mentioned below are outside of the model domain of the local scale model. In that case, the respective information was taken from the hydrogeological regional model which is explained in detail in Gmünder et al. (2013b).

The following conclusions can be drawn with respect to the local and regional aquifer systems:

- The lateral continuity of the regional aquifers Muschelkalk aquifer, Hauptrogenstein aquifer and Malm aquifer is broken by the regional Jura Thrusts and Born-Engelberg Anticline. The resulting fragmentation governs the groundwater flow systems in the siting region. The regional faults may show a simple offset disrupting the continuity of the hydrogeological units (case C1). Otherwise they could act as sealing faults (case C2) or leaky faults (cases C3 and C3a). In most cases, the hydraulic heads in the regional aquifer systems are defined by the local recharge and discharge levels, giving rise to (sub)hydrostratic to slightly artesian conditions and low hydraulic horizontal gradients in the siting region.
- The expected discharge areas of the Muschelkalk aquifer, Keuper aquifer, Hauptrogenstein aquifer and Malm aquifer, together with the expected ranges of the horizontal hydraulic gradient in the aquifers, are given in Table 6-2.
- The Arietenkalk is represented as 15 m thick unit in the hydrogeological model Jura-Südfuss, located around 26 m above the Keuper aquifer and only approx. 3m below the Opalinus Clay. This unit has been treated as a locally transmissive unit in the sensitivity simulations where model analyses exhibit a similar head distribution as in the Keuper aquifer and consequently, similar discharge areas.
- The Sissach Member (RD4) is represented as a 8 m thick unit in the hydrogeological model Jura-Südfuss, located directly above the Opalinus Clay. In the sensitivity cases, where this units is treated as a potential, locally transmissive unit, model analyses exhibit a similar head distribution as in the Hauptrogenstein aquifer and, consequently, similar discharge areas.

Tab. 6-2: Hydrogeological characteristics of the regional and local aquifer systems/potentially transmissive units in the siting region Jura-Südfuss. Note that only the most prominent discharge areas are given in the table. In case that no clear preferred value can be deduced for a certain parameter, only alternative values are given.

RV: Reference value (best guess, defensible value).

AV: Alternative value (pessimistic value; complementary model assumption; no reference value definable).

Hydro-geological Unit	Parameter	RV	AV	Remarks
Muschelkalk aquifer (regional aquifer)	Hydraulic head / mid of the formation [m]	*	+50	RV: * Hydrostatic conditions AV: Artesian conditions
	Horizontal component of hydraulic gradient [m/m]	0.01	0.003	RV: Value deduced from case C1, C3 and C3a AV: Value deduced from case C2
	Discharge area	-	-	AV1: Niederamt AV2: Area of Hunzenschwill AV3: "Klus" of Aarburg AV4: Area of Birmenstorf AV5: Rhine valley (area of Laufenburg)
Keuper aquifer (local aquifer)	Hydraulic head / mid of the formation [m]	*	+30 m	RV: * Hydrostatic conditions AV: * Artesian conditions
	Horizontal component of hydraulic gradient [m/m]	0.02	0.1	RV: Value deduced from cases 1-3a AV: Pessimistic value
	Discharge area	-	-	AV1: Area of Hunzenschwill AV2: "Klus" of Aarburg AV3: Area of Birmenstorf AV4: Area of Baden
Hauptrogenstein (regional aquifer)	Hydraulic head / mid of the formation [m]	+50	*	RV: Artesian conditions AV: * Hydrostatic conditions
	Horizontal component of hydraulic gradient [m/m]	-	0.1 0.03	AV1: Value deduced from cases 3/3a AV2: Value deduced from cases 1/2
	Discharge area	-	-	AV1: Niederamt AV2: Area of Hunzenschwill AV3: "Klus" of Aarburg AV4: North of Lostorf AV5: Trimbach
Malm aquifer (regional aquifer)	Hydraulic head / mid of the formation [m]	*	+50	RV: * Hydrostatic conditions AV: Artesian conditions
	Horizontal component of hydraulic gradient [m/m]	0.05	0.1	RV: Value deduced from cases 1-3a AV: pessimistic value
	Discharge area	-	-	AV1: Niederamt AV2: Aare valley (Wildeggen) AV2: lower Suhre valley

7 References

- Bitterli-Dreher P. (2012): Die Ifenthal-Formation im nördlichen Jura.- Swiss Bulletin für angewandte Geologie 17 / 2, 93-117.
- Bläsi, H.R., Deplazes, G., Schnellmann, M. & Traber, D. (2013): Sedimentologie und Stratigraphie des 'Braunen Doggers' und seiner westlichen Äquivalente. Nagra Arbeitsbericht NAB 12-51. Nagra, Wettingen.
- Butler G.A., Cauffman T.L., Lolcama J.L., Longsine D.E., McNeish J.A. (1989): Interpretation of hydraulic testing at the Weiach borehole. Nagra Technischer Bericht NTB 87-20. Nagra, Baden.
- Deplazes, G., Bläsi, H.R., Schnellmann, M. & Traber, D. (2013): Sedimentologie und Stratigraphie der Effinger Schichten. Nagra Arbeitsbericht NAB 13-16. Nagra, Wettingen.
- DHI-WASY GmbH (2012): FEFLOW 6, User Manual.
- Gmünder, C., Jordan, P., Becker, J.K. (2013a): Documentation of the Nagra 3D Geological Model 2012. Nagra NAB 13-28. Nagra, Wettingen.
- Gmünder, C., Malaguerra, F., Nusch, S., Traber, D. (2013b): Regional hydrogeological model of northern Switzerland. NAB 13-23. Nagra, Wettingen.
- Isler, A., Pasquier, F. & Huber, M. (1984): Geologische Karte der zentralen Nordschweiz 1:100'000. Herausgegeben von der Nagra und der Schweiz. Geol. Komm.
- Madritsch H., Hammer P., Pestalozzi A. (2012): Characterisation of Cenozoic brittle deformation of potential geological siting regions for radioactive waste repositories in Northern Switzerland based on structural geological analysis of field outcrops: Update. NAB 12-41. Nagra, Wettingen.
- Müller W.H., Huber M., Isler A., Kleboth P. (1984): Erläuterungen zur 'Geologischen Karte der zentralen Nordschweiz, 1:100000'. Nagra Technischer Bericht NTB 84-25. Nagra, Baden.
- Nagra (1989): Technischer Bericht NTB 88-08: Sondierbohrung Weiach Untersuchungsbericht: Beilageband NTB 88-08 A & B. Nagra, Baden.
- Nagra (1997): Geosynthese Wellenberg 1996: Ergebnisse der Untersuchungsphasen I und II: Textband. NTB 96-01. Nagra, Wettingen. Laubscher, H. (1986): The eastern Jura: Relations between thin-skinned and basement tectonics, local and regional. Geologische Rundschau 75, 535-553, doi:10.1007/BF01820630.
- Nagra (2002): Technischer Bericht NTB 02-03: Projekt Opalinuston Synthese der geowissenschaftlichen Untersuchungsergebnisse - Entsorgungsnachweis für abgebrannte Brennelemente, verglaste hochaktive sowie langlebige mittelaktive Abfälle. Wettingen, Dez. 2002.
- Nagra (2008): Technischer Bericht NTB 08-04: Vorschlag geologischer Standortgebiete für das SMA- und das HAA-Lager, Nationale Genossenschaft für die Lagerung radioaktiver Abfälle. Wettingen, Okt. 2008.

- Nagra (2010): Technischer Bericht NTB 10-01: Beurteilung der geologischen Unterlagen für die provisorischen Sicherheitsanalysen in SGT Etappe 2, Nationale Genossenschaft für die Lagerung radioaktiver Abfälle. Wettingen, Okt. 2010.
- Nusch, S., Gmünder, C. and Traber, D. (2013): Hydrogeologisches Regionalmodell - Datenkompilation Hydrodaten. Nagra Arbeitsbericht NAB-13-43. Nagra, Wettingen.
- Reisdorf A.G.; Wetzel A.; Schlatter R.; Jordan P. (2011): The Staffelegg Formation: a new stratigraphic scheme for the Early Jurassic of northern Switzerland. *Swiss Journal of Geosciences* 104 / 1, 97-146.
- Sanford, W. (2002): Recharge and groundwater models: an overview. *Hydrogeology Journal*, Vol 10, 1 pp 110-120.
- Swiss Federal Office of Energy (SFOE) (2008): Sectoral Plan for Deep Geological Repositories, Conceptual Part. Swiss Federal Office of Energy, Bern, Switzerland.

Appendix 1: Vertical gradients

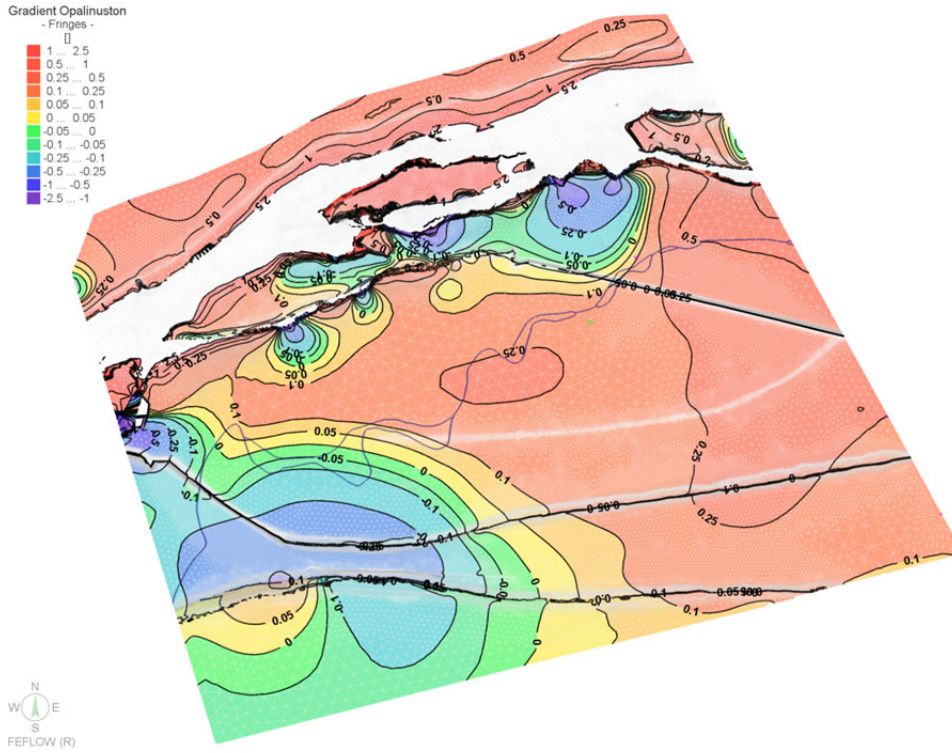


Fig. A-1: Vertical gradient in the Opalinus Clay in base case C1.

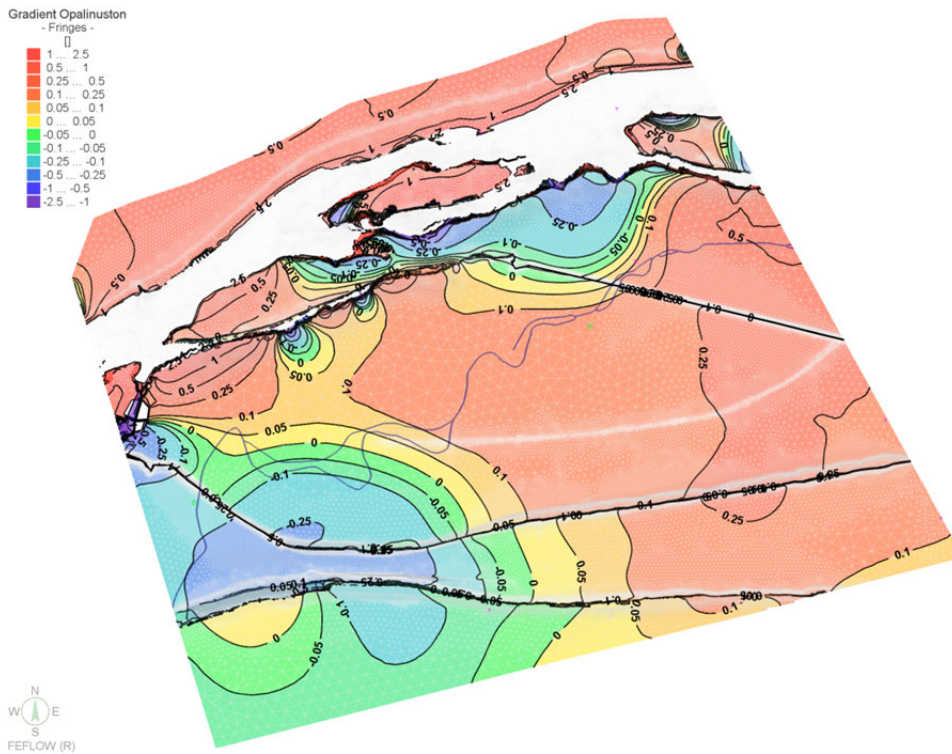


Fig. A-2: Vertical gradient in the Opalinus Clay in sensitivity case C1-RD4.

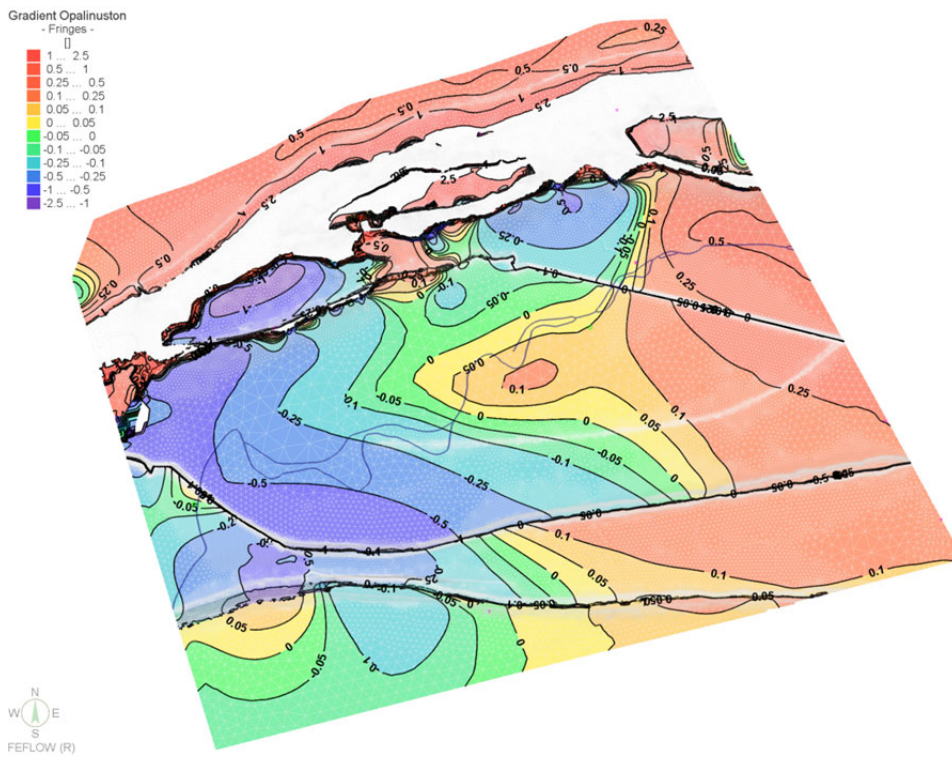


Fig. A-3: Vertical gradient in the Opalinus Clay in sensitivity case C1-AKA.

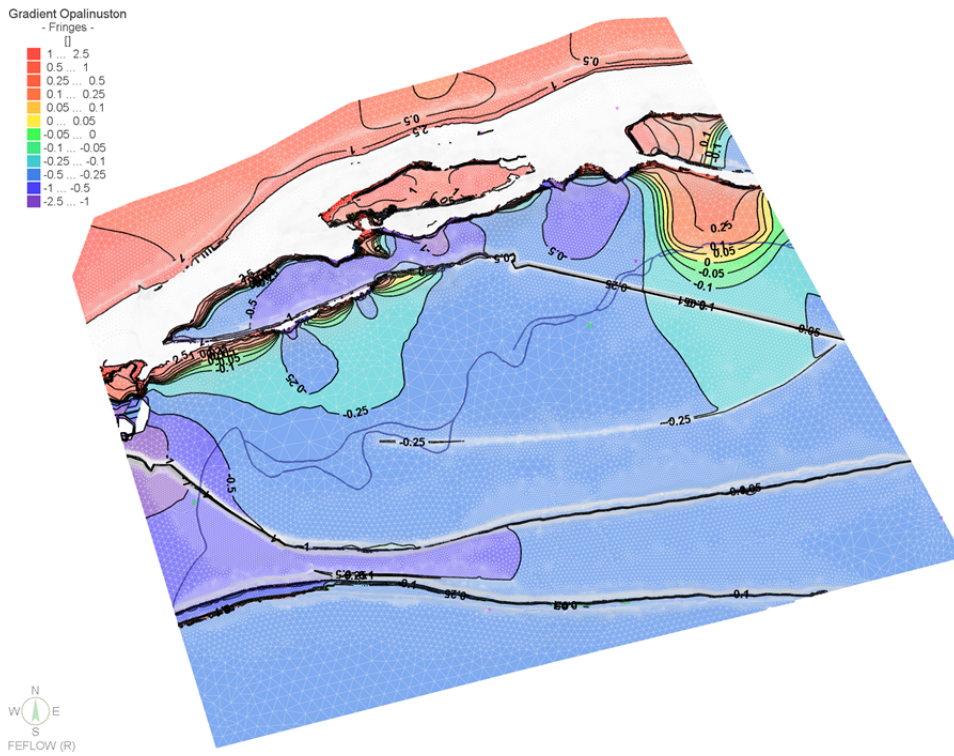


Fig. A-4: Vertical gradient in the Opalinus Clay in base case C2.

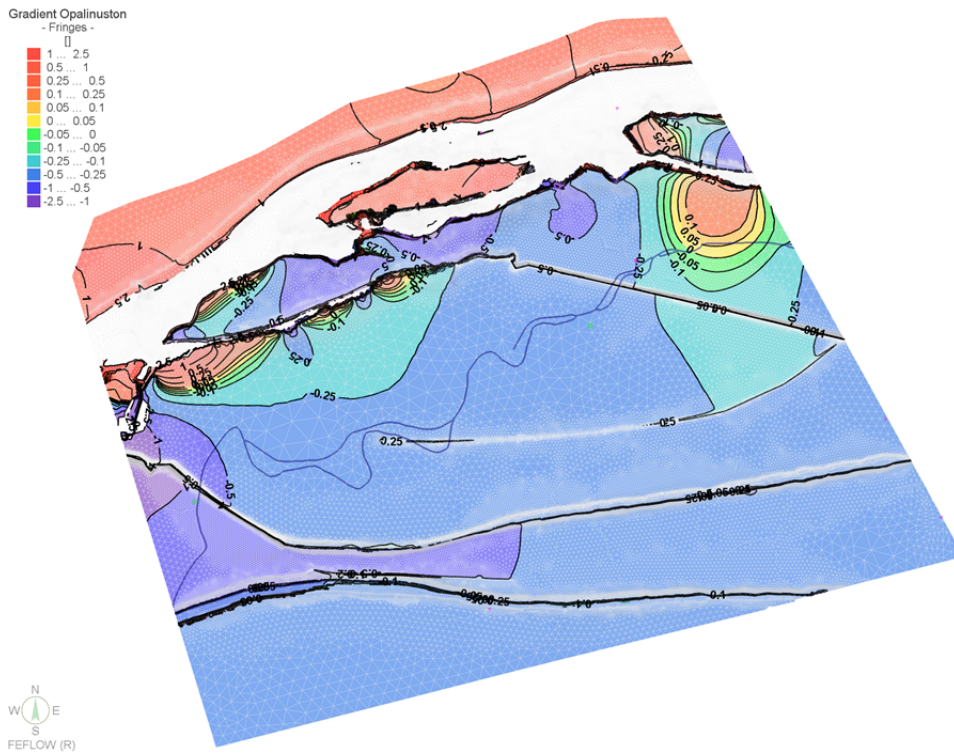


Fig. A-5: Vertical gradient in the Opalinus Clay in sensitivity case C2-RD4.

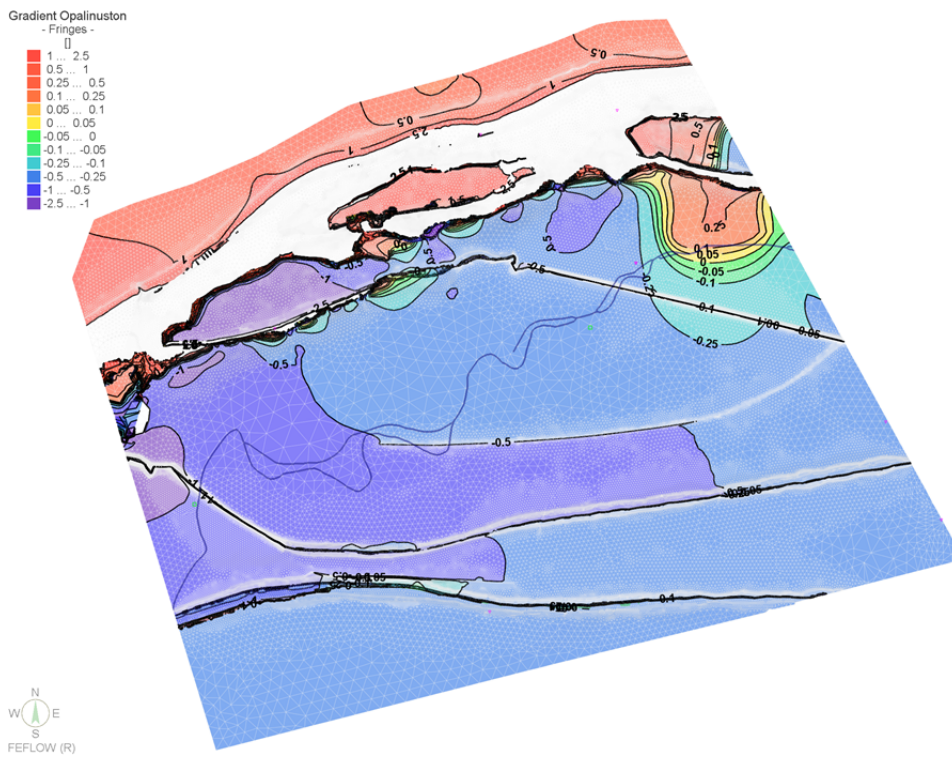


Fig. A-6: Vertical gradient in the Opalinus Clay in sensitivity case C2-AKA.

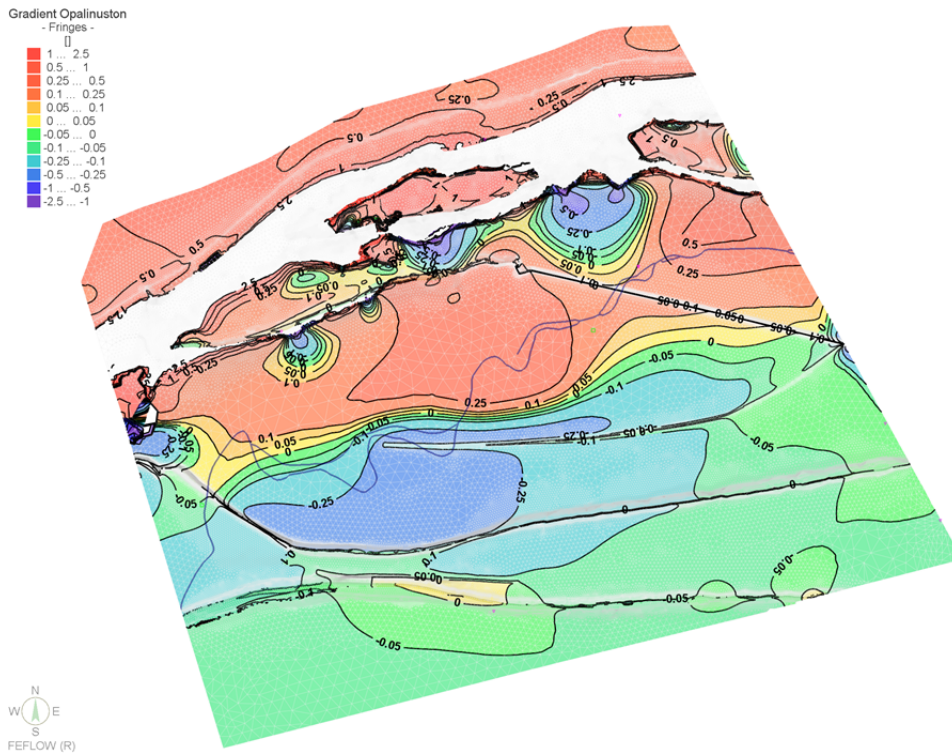


Fig. A-7: Vertical gradient in the Opalinus Clay in base case C3.

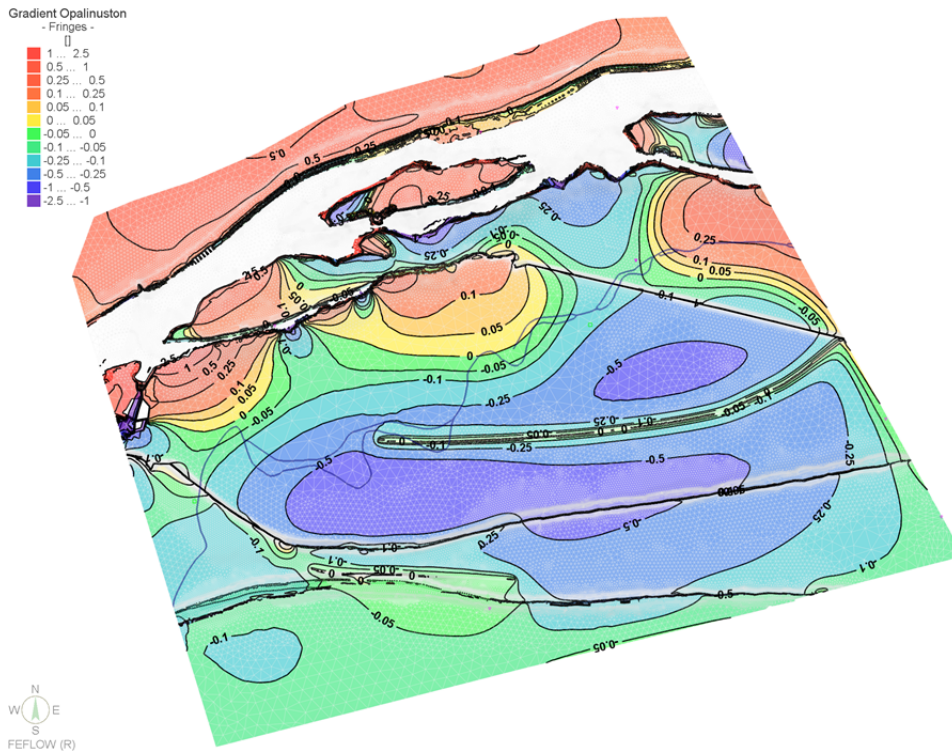


Fig. A-8: Vertical gradient in the Opalinus Clay in sensitivity case C3-RD4.

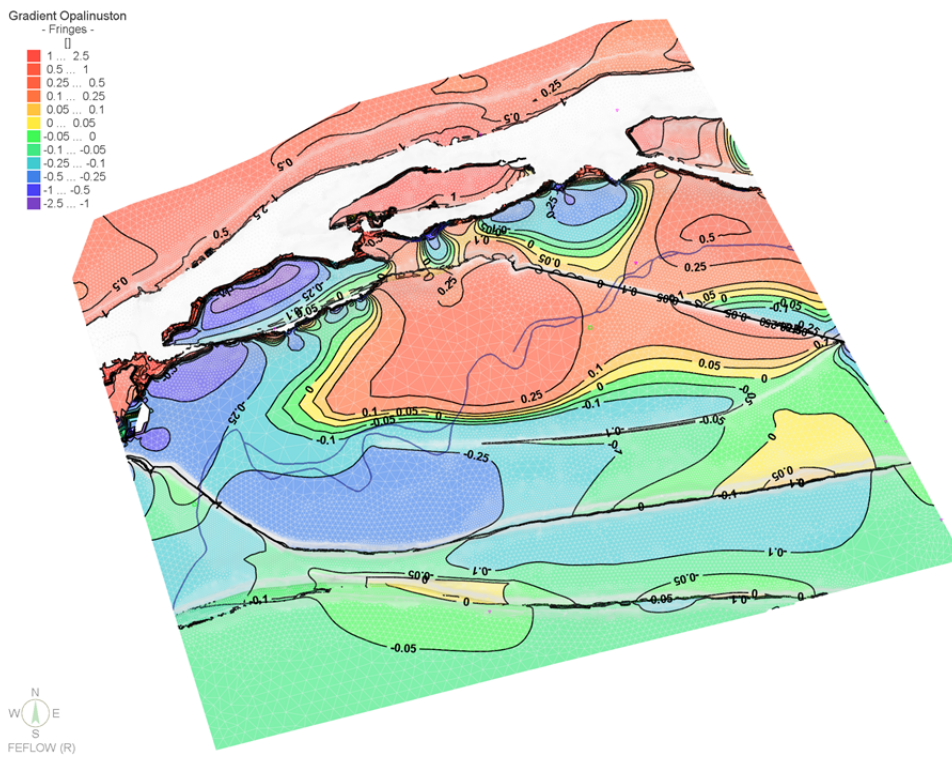


Fig. A-9: Vertical gradient in the Opalinus Clay in sensitivity case C3-AKA.

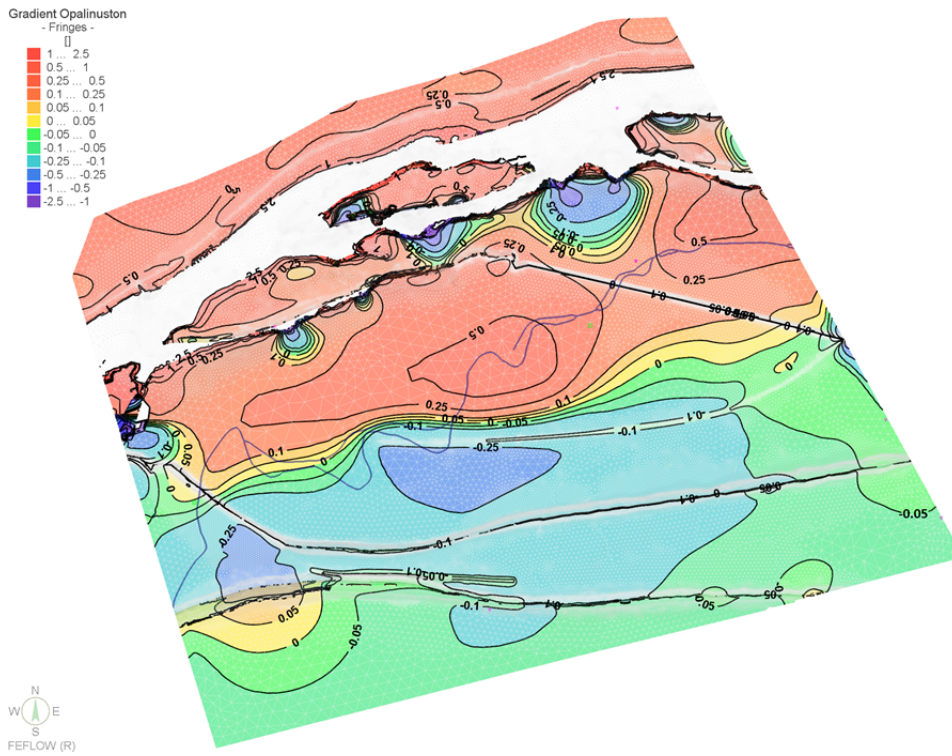


Fig. A-10: Vertical gradient in the Opalinus Clay in base case C3a.